THE FUNCTIONS AND ROLES OF THE COPPER CHAPERONE OF SUPEROXIDE DISMUTASE 1

by

Morgan S. Ullrich

APPROVED BY SUPERVISORY COMMITTEE:

_____

Dr. Duane D. Winkler, Chair

_____

Dr. Zachary Campbell

_____

Dr. Lee Bulla

_____

Dr. Gabriele Meloni

To the sympathetic ears of my mom and brother, which made this possible.

THE FUNCTIONS AND ROLES OF THE COPPER CHAPERONE OF SUPEROXIDE DISMUTASE 1

by

MORGAN S. ULLRICH, MS, BS

DISSERTATION

Presented to the Faculty of

The University of Texas at Dallas

in Partial Fulfillment

of the Requirements

for the Degree of

DOCTOR OF PHILOSOPHY IN

MOLECULAR AND CELLULAR BIOLOGY

THE UNIVERSITY OF TEXAS AT DALLAS

DECEMBER 2020

ACKNOWLEDGMENTS

Thanks to my friends and family, who have helped me through this monumental task. Also to my committee members who have all devoted time, energy, resources, and people to helping me complete my goals with this project. An extra big thank you to everyone in the Winkler lab, who have poured their own blood, sweat, and tears into this work right alongside me. I could not have done this without all of you.

November 2020

THE FUNCTIONS AND ROLES OF THE COPPER CHAPERONE OF SUPEROXIDE DISMUTASE 1

Morgan S. Ullrich, PhD
The University of Texas at Dallas, 2020

Supervising Professor: Duane D. Winkler

Superoxide dismutase 1 is a vital antioxidant that catalyzes the dismutation of radical oxygen to water and hydrogen peroxide. It is present in all known aerobic life, with a structural and functional homologue present in organisms as disparate as yeast and humans. Its high levels of expression and activity led to its early discovery and research, which has resulted in a vast body of literature available on its function. On top of its already significant antioxidant function, it is a regulator and signaling enzyme in many different cell systems, from immune response to cell division. Additionally, it is implicated to play a role in many diseases, notably amyotrophic lateral sclerosis (ALS), cancer, and Parkinson's disease. The importance of Sod1 to overall life cannot be understated.

Sod1 does not begin life with all these functions, however. It is first made in an immature state that lacks antioxidant activity and must undergo a maturation process to become functional. This process mainly consists of three posttranslational modifications (PTMs): addition of zinc, addition of copper, and formation of a disulfide bond. Sod1 is unable to gain these PTMs in vivo and needs the help of another protein, the copper chaperone for Sod1 (Ccs).

This thesis will cover the maturation of Sod1 by Ccs as completely as possible. We will begin with the potential copper sources for Ccs as copper availability is heavily restricted by the cell. Then, we will look at the mechanism of Sod1 activation in yeast and the role Ccs plays in the addition of all three PTMs. This will then be compared to the mechanism of activation in human cells, as yeast Sod1 and yeast Ccs are structural and functional homologues of human Sod1 and human Ccs. With the normal mechanism of maturation established, we can then explore how this breaks down in ALS with common ALS-causing mutations of Sod1. Finally, we will look at a recently-discovered mutation of Ccs that has been linked to ALS-like disease symptoms.

TABLE OF CONTENTS

LIST OF FIGURES

LIST OF TABLES

CHAPTER 1

COPPER SOURCES FOR SOD1 ACTIVATION

Stefanie D. Boyd, Morgan S. Ullrich, Amelie Skopp and Duane D. Winkler

The Department of Biological Sciences, BSB12

The University of Texas at Dallas

800 West Campbell Road

Richardson, Texas 75080-3021

Abstract

Copper ions (i.e., copper) are a critical part of several cellular processes, but tight regulation of copper levels and trafficking are required to keep the cell protected from this highly reactive transition metal. Cu, Zn superoxide dismutase (Sod1) protects the cell from the accumulation of radical oxygen species by way of the redox cycling activity of copper in its catalytic center. Multiple posttranslational modification events, including copper incorporation, are reliant on the copper chaperone for Sod1 (Ccs). The high-affinity copper uptake protein (Ctr1) is the main entry point of copper into eukaryotic cells and can directly supply copper to Ccs along with other known intracellular chaperones and trafficking molecules. This review explores the routes of copper delivery that are utilized to activate Sod1 and the usefulness and necessity of each.

Introduction

Numerous cellular processes cannot function without intracellular copper working in the active site of enzymes. The varied roles for enzyme-bound copper include, but are not limited to, energy production, signaling, and oxidative stress response [1–3]. Cu, Zn superoxide dismutase (Sod1) is an antioxidant enzyme that eliminates superoxide anions ($O2^{-}$) from within the cell as a method of heading off the production of the more dangerous hydroxyl radicals (·OH) [4,5]. Copper serves as the cofactor necessary for this reaction [6–8]. The key to copper's broad utility arises from its ability to cycle between two oxidative states: Cu(I) and Cu(II) [9]. This redox property of copper allows it to function as both an electron donor and recipient, however, this can also lead to the nonenzymatic production of hydroxyl radicals from the breakdown of hydrogen peroxide (H_2O_2) [2,9,10]. Sod1 homologues exist in all eukaryotic aerobes ranging from single-celled yeast

to humans. With few exceptions, forms of Sod1 can be substituted between species without any phenotypic change to the organisms [11–14].

In order to prevent deleterious copper interactions, the cell utilizes a class of proteins, termed copper chaperones, to secure and deliver the necessary copper to cellular targets [9]. These proteins are known to locate the copper importers at the plasma membrane, acquire the copper as it is dispensed into the cytosol, and distribute it to specific enzymes or copper-binding proteins, thus sequestering the copper from other cellular components. There are many copper chaperones in the cell, including antioxidant 1 (Atox1) that provides copper to the transporters ATP7a and ATP7b, Cox17, which supplies copper to cytochrome c oxidase, and the copper chaperone for Sod1 (Ccs) which delivers copper exclusively to Sod1 [15–18]. Copper chaperones have been thoroughly studied for decades, however, the mode(s) of copper acquisition by these proteins remains somewhat ambiguous [19,20]. Reported copper sources for these chaperones are transporters that move copper into the various cellular compartments, copper sinks that store excess copper in the cell and other copper chaperones [21–25] (**Figure 1.1**).

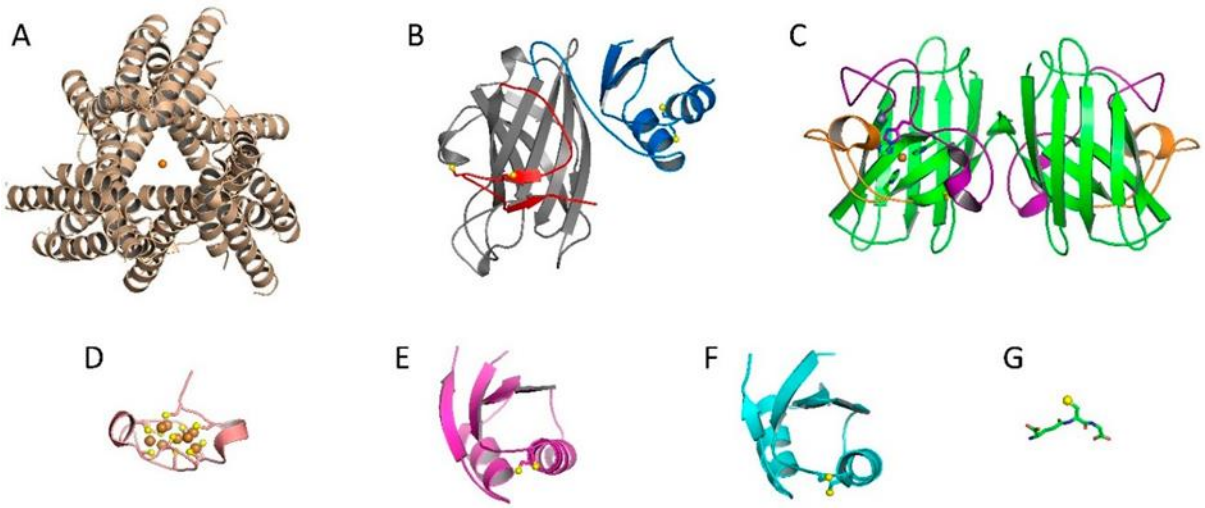

Figure 1.1. A collection of copper-binding molecules relevant to copper acquisition, regulation, and distribution to Sod1. (A) The copper importer Ctr1 with copper (orange sphere) bound in the

channel (PDB: 6M98). (B) The structure of yeast Ccs, complete with D1 (blue), D2 (gray), and D3 (red). Copper binding cysteines are shown as yellow spheres (PDB: 5U9M). (C) Mature Sod1 dimer with the β-barrel shown in green and critical loop elements in purple (zinc loop) and orange (electrostatic loop). Active site bound copper is displayed as an orange sphere and the adjacent zinc shown in grey (PDB: 1PU0). (D) Copper bound MT3 domain with the coppers as orange spheres and the coordinating cysteines as yellow spheres (PDB: 1RJU). (E) The copper chaperone Atox1 (monomer) with the MTCxxC cysteines shown as yellow spheres (PDB: 5F0W). (F) A copper-binding domain (repeat 2) of the transport protein ATP7B, again with the conserved MTCxxC cysteines shown as yellow spheres (PDB: 2LQB). Notice the structural similarities between Ccs D1, Atox1, and ATP7B. (G) The structure of the glutathione tri-peptide, with the cysteine shown as a yellow sphere (PDB: 1AQW).

The majority of copper enters the cytosol through the high-affinity copper uptake protein (Ctr1) [26,27]. This transmembrane import protein acquires extracellular Cu(II) from ceruloplasmin [28,29], which accounts for about 90% of copper in the blood [28], and albumin [30,31] and imports it as Cu(I). Copper reduction is likely to be facilitated by metalloreductases at the cell surface [32,33]. Studies have shown that Ccs can secure Cu(I) held by the cytosolic C-terminal domain of Ctr1 and deliver it to Sod1 [34,35]. Additionally, evidence exists that both Atox1 and Cox17 can acquire copper by way of Ctr1 [36,37] (**Figure 1.1**).

Other important cytosolic copper-binding molecules include the metallothionein superfamily of proteins (MT) and the reduced form of glutathione (GSH). MT proteins are ubiquitously expressed, highly conserved, and important for both copper and zinc homeostasis [38,39]. MT genes are upregulated, similar to those coding for Sod1, during times of oxidative stress [40]. GSH is an abundant antioxidant tripeptide present within the cytosol that, amongst other functions, can bind Cu(I) and has even been shown to deliver this cargo to Sod1 [22,41] (**Figure 1.1**). This review will focus on the known and proposed copper transport pathways for Sod1. The movement of Cu(I) from Ctr1 to Ccs to Sod1 seems simple, yet cooperation among and

transfer between copper coordinating molecules creates potential branch points and alternative routes for this pathway that are not yet fully explored [4,6,15,42,43]. Our goal is to provide new insight into the totality of copper transport pathways benefitting Sod1, and to highlight opportunities for new and exciting research in this arena.

Discussion

Cu, Zn Superoxide Dismutase (Sod1) and Copper Chaperone for Sod1 (Ccs1)

In 1969, McCord and Fridovich discovered an enzyme, termed erythrocuprein, which has since been renamed Sod1 [5]. It is a ubiquitously expressed antioxidant enzyme that protects the cell from the buildup of radical oxygen species through the disproportionation of superoxide to oxygen and hydrogen peroxide ($2O_2^- + 2H + \rightarrow O_2 + H_2O_2$) [5]. The fully mature homodimeric form of Sod1 (**Figure 1.1**) is highly efficient, catalyzing the above reaction at or near the diffusion limit [44]. An inherent "electrostatic guidance system" composed of positively charged sites within the electrostatic loop region of Sod1 contributes to the enzyme's catalytic efficiency (**Figure 1.1**) [4]. An arginine residue at position 143 forms the backside of the active site and is critical for both substrate attraction and nonsubstrate exclusion. Mutations at this site eliminate Sod1 activity [45]. Zinc ion (i.e., zinc or Zn(II)) binding at an adjacent site and an intra-subunit disulfide bond are also critical for both protein stability and enzymatic function (as more fully described below) [4,41].

Sod1 is abundant in the cell, found mostly in the cytoplasm, and is predominantly found in an immature state where it lacks the necessary posttranslational modifications (PTMs) required for antioxidant activity [46]. Sod1 requires three PTMs during the maturation process: (1) zinc binding at a site connected to the active site, (2) direct insertion of the catalytic copper to the active site,

and (3) disulfide bond oxidation that promotes a stable homodimeric conformation [4,47–50]. Zinc is bound at a conserved loop region (i.e., zinc loop) by three histidines and an aspartic acid (H63, H71, H80, and D83). Sod1-bound copper will switch between two oxidation states during the disproportionation of superoxide (i.e., Cu(I) and Cu(II)) [5]. In the reduced form, copper is coordinated by three histidines (H46, H48, and H120) in a trigonal planar conformation [51,52]. The oxidized form of copper is coordinated by an additional histidine (H63) in a distorted square planar conformation (**Figure 1.1**) [53]. As noted above, H63 also facilitates zinc binding and is known as the "primary bridge" that links the copper and zinc sites of Sod1 [4]. A critical intra-subunit disulfide bond between C57 and C146 within each Sod1 monomer secures the loops regions making up the metal-binding sites of Sod1, which effectively excludes unwanted reactants from the active site [54,55]. Stable disulfide bonds are rare in the reducing environment of the cytosol and, when found, usually play a functional role [4].

The copper chaperone for Sod1 (Ccs) was first identified by the Culotta lab in 1997 as a protein essential for Sod1 activation in yeast [15]. The far majority of Ccs molecules across species consist of three structurally distinct domains (D1, D2, and D3) [56]. Domain 1 contains a MxCxxC copper binding motif and its fold resembles that of the copper chaperone Atox1 [48]. Proposed roles for D1 include copper acquisition from the copper importer Ctr1, copper scavenging under copper-limiting conditions and direct copper delivery to Sod1 [43]. The roles of this domain are still under debate and are likely varied between species. Ccs D2 shares both sequence and structural homology with Sod1, likely indicating that this is the main Sod1 interaction platform and a number of Sod1·Ccs crystal structures have confirmed this notion [57]. All forms of Ccs D2 lack the copper-binding site, but mammalian Ccs molecules have retained the zinc-binding site, disulfide

bond, and loop elements [58]. Domain 3 is a relatively short, unstructured, yet highly conserved domain that contains a CxC copper binding motif [59]. The available evidence seems to point towards a role in copper delivery and/or formation of the disulfide bond in Sod1 [6,60]. In recent publications, we and others have demonstrated that Ccs domain 3 can form a stable β-hairpin [41,43]. Our structure shows the conserved CxC motif located near the disulfide residues and active site of Sod1, inferring a molecular mechanism for copper delivery and disulfide bond formation [41]. More recent work has revealed that Ccs prefers a completely immature form of Sod1 (E,E-Sod1^{SH}) and each step of maturation decreases the affinity of the Sod1·Ccs interaction [61]. In addition to delivering copper for Sod1, Ccs binding increases the affinity and zinc occupancy of Sod1, of which D3 is required [60]. Ccs-Mediated Sod1 Maturation

The traditional understanding of Ccs-mediated Sod1 maturation highlights the well-established roles for copper delivery and disulfide bond formation in Sod1 [47]. We and others have expanded upon this mechanism to include roles for Ccs that include: Sod1 folding, facilitated site-specific zinc acquisition and the formation of a copper drop-off point or "entry-site" upon Sod1 binding [41,60,62]. These additional properties separate Ccs from all other known copper chaperones, and thus, Ccs is better characterized as a multifunctional chaperoning molecule with roles in each level of Sod1 maturation.

Our "entry-site" model for Ccs-mediated copper delivery proposes that Cu(I) is delivered from the CxC copper-binding motif in Ccs D3 to site formed near the Sod1·Ccs heterodimeric interface [41]. Observation of the Sod1-Ccs crystal structure published previously by our lab reveals a strong interaction between Sod1 and a B-hairpin formed by Ccs D3 [4]. Further spectroscopic analysis of the purified protein complex showed that a copper atom was coordinated

at this entry site [36]. This interaction was also biochemically analyzed with in vitro functional and mutational assays, which suggest that the site is formed via residues in both Sod1 (H120 and C57) and Ccs (C231, yeast sequence). Intercalation of the Ccs D3 β-hairpin under the Sod1 disulfide loop exposes an electropositive path that likely attracts a superoxide or hydroxide molecule to the coordinated copper and accelerates sulfenylation of the adjacent C146 on Sod1. The existence of the sulfenyl intermediate was confirmed by Western blot with an antibody specific to sulfenyl modified cysteines [36]. Key disulfide exchange reactions promoted by the sulfenic acid group on C146 ends with the formation of the critical C57-C146 Sod1 disulfide bond and releases of the copper into the active site. Disulfide bond formation in Sod1 terminates interaction with Ccs and promotes its own homodimerization, where the mature enzyme can now perform its normal antioxidant functions [4,41].

An alternative model has been proposed by the laboratory of Lucia Banci. Here, Ccs D1 is primarily responsible for copper acquisition and delivery to the Sod1 active site [6], though, the structural details of this proposed conformational switch are currently undefined. The singular role for Ccs D3 is the transfer of a preformed disulfide bond to Sod1. As opposed to the "entry-site" model, this version is a distinct two-step process where copper delivery and disulfide bond formation are separate, though closely related, functions of Ccs. This model is based on experimental evidence obtained using in-cell NMR to measure metal transfer.

Until very recently, the role, if any, Ccs plays in Sod1 zinc acquisition had been essentially ignored. New evidence, from our lab and others, has illustrated multifunctional or molecular chaperoning roles for Ccs [60,63]. We have highlighted that Ccs functions in both copper delivery and facilitating high-affinity Zn(II)-binding of Sod1 [60]. Data show that Ccs binding to Sod1

increases both affinity and occupancy of zinc at the zinc-binding site in Sod1. This is likely due to Ccs stabilizing a beneficial conformation of the zinc loop; an extension of the disulfide loop that makes up a section of the interaction interface between Sod1 and Ccs (**Figure 1.1**). Interestingly, it has also been shown that Ccs binding alone (i.e., without copper delivery) can resolve mis-metalation events where zinc is initially found in the active site. However, some pathogenic Sod1 mutants that cause an inherited form of amyotrophic lateral sclerosis (fALS) seemingly counteract these processes [62].

Ccs-Independent Sod1 Maturation

While highly conserved across all eukaryotic organisms, there are some divergencies among the group of Sod1 molecules [64]. One important distinction is the existence of an additional pathway for Sod1 maturation; the Ccs-independent pathway is necessitated by a simple amino acid change (e.g., proline substitution) between mammals and other lower eukaryotes [65,66]. Indeed, human Sod1 expressed in ΔCcs/ΔCcs mice retains ~25% activity, thus indicating a pathway for Sod1 maturation liberated from Ccs [7]. Another interesting anomaly is Caenorhabditis elegans, where no Ccs exists, yet the population of Sod1 molecules are found to have their complete assortment of posttranslational modifications and are fully active [67]. For most other eukaryotes, including yeast, Sod1 maturation requires Ccs [19].

Potential copper sources for the Ccs-independent Sod1 maturation pathway have been proposed that include, but are not limited to, the reduced form of glutathione (GSH), metallothioneins (MTs) and other known copper chaperones [65,68,69]. Nevertheless, there lacks solid evidence to indicate a clear mechanism for this pathway. GSH seems one of the most likely sources as it has been shown to acquire copper from the Ctr1 importer and is present in large

quantities within the cytosol [65]. The mechanism of a potential GSH-mediated Sod1 maturation event is unclear, to say the least.

Leitch et al. have found that the kinetics of Sod1 activation and the copper source is identical despite the differing roles for Ccs (e.g., completely dependent, independent, or partially dependent on Ccs) [66]. In contrast, the mechanism of disulfide bond formation for Sod1 is strikingly different and contingent upon the role that Ccs plays in its activation. Ccs dependent disulfide bond formation relies on available oxygen species, yet, inexplicably, the Ccs-independent pathway does not [42,65,66]. Ensuing sections will delve into the current literature and preliminary models for these pathways.

Copper Acquisition by Ccs via Ctr1

The mechanism of Ccs-mediated Sod1 maturation has been studied extensively, as evidenced by the dense literature and multiple models for Ccs action [4]. On the other hand, the source(s) of copper for this process and connections to other copper delivery pathways have not been fully explored. The major port of entry for all copper trafficking is the copper importer Ctr1 [34]. From this point, it is proposed that the intracellular trafficking molecules acquire and then depart towards target delivery. Is there a pecking order among the trafficking molecules? Are their intermediaries in the acquisition or delivery processes? How about during times of stress or copper variability? We hope to address these unresolved questions while centering our discussion around the routes of copper delivery to Sod1.

The Ctr-family is a functionally, but not structurally, conserved group of transmembrane copper transporters present across eukaryotic organisms, of which Ctr1 is the most prevalent [70–76]. Ctr proteins import copper from the extracellular environment into the cytosol. For humans

and other select species, more than one copper transporter has been identified [25,77–79]. Ctr2 functions alongside Ctr1 as a low-affinity copper transporter, a regulator of micropinocytosis, and modulator of Ctr1 positioning within the plasma membrane. Ctr2 influences Ctr1 membrane location by promoting a truncated form of Ctr1 that is a target of the endo-lysosomal pathway [24,33,80].

The human form of Ctr1 is comprised of a large extracellular domain, three transmembrane helices, and a short C-terminal cytosolic tail that harbors the intracellular copper-binding HCH motif [26,81–83]. The functioning transporter is a trimeric conical channel; a 9 Å opening faces the extracellular milieu that widens towards the cytosol (22 Å) [32,84,85]. The N-terminal ecto-domain is glycosylated (both N- and O-linked) and these modifications likely impact Ctr1 stability and plasma membrane localization [27,86,87]. While the exact mechanism of copper transfer is not fully understood, ATP-driven transport of the metal has been excluded due to the lack of an ATP-hydrolyzing domain [88]. Histidine residues lining the inside of the transmembrane domain regulate Cu(I) import, which is roughly 80% of all copper brought into the cell [32,81]. While fungal copper transporters work in conjunction with copper reductases, little evidence exists for a similar setup in mammalian systems [89,90]. Further research is needed to elucidate the mechanism of copper reduction prior to Ctr1-mediated copper import.

A C-terminal HCH motif on Ctr1 acts as a sink for Cu(I) ions and is suggested to be the site of hand-off for copper chaperones and other copper binding molecules [21,91]. Docking studies between Atox1 and the C-terminal domain of Ctr1 (Ctr1c) show that Cu(I) can be donated directly from Ctr1 to Atox1 [68]. Related work by the Unger group suggests that Ccs1 and Atox1 can associate with the plasma membrane, thus providing a means for targeted interaction between

transporter and chaperone [21,92]. Relatedly, Kaplan and colleagues demonstrated that Ctr1 could hand copper to the reduced form of glutathione (GSH), which is present in high concentrations within the cytosol and can act as a copper reservoir [92].

Our lab has recently shown that the Cu(I)-bound form of Ctr1c can form a stable complex with Ccs [34]. Only the addition of immature Sod1 (i.e., copper-free and disulfide reduced) to this complex can separate the copper-mediated Ctr1c·Ccs complex. The reaction produces a mature Sod1 molecule (i.e., copper-bound and disulfide oxidized) that is fully active. When a C146A mutation is introduced to Sod1 that prevents both copper delivery and disulfide bond formation, a stable Ctr1c·Ccs·Sod1 trimeric complex is observed. These results help to confirm that copper mediates a stable interaction between Ctr1 and Ccs and that localized activation of Sod1 terminates all interactions [34]. Interestingly, Ctr1 is not obligatory for Sod1 to access copper [93]. Thus, what are other potential routes of copper delivery for Ccs-mediated and Ccs-independent Sod1 maturation?

Involvement of other Chaperones and Metalloproteins

Atox1

Atox1 delivers copper to the secretory pathway and was one of the first members of the copper chaperone family [94]. Atox1 comprises a small single-domain with a ferredoxin-like fold and a conserved MTCxxC copper binding motif, which it shares with its targets ATP7A and ATP7B [2,95,96]. ATP7A/B are P-type ATPase copper transporters that remove excess copper from the cytosol, thus protecting the cell from elevated copper levels [1]. Atox1 also provides the

copper essential for metalation of secreted proteins such as ceruloplasmin, a copper-carrying ferroxidase in the blood [97].

As stated previously, both Ccs and Atox1 are capable of interacting with lipid bilayers and this may facilitate interaction with Ctr1 [35,98]. Localization of the plasma membrane may also enable copper exchange between the two chaperones. Ccs D1 and Atox1 share both structural and sequence homology, which allots similar copper-binding affinities [99]. Despite their similarities, Atox1 cannot fulfill the role of Ccs in the cell [100]. Wittung-Stafhede and colleagues have shown that Ccs can retrieve Cu(I) from Atox1 by coupled size-exclusion chromatography and copper transfer assays [68]. While Atox1 can access copper though Ctr1, its additional role in removing excess copper from the cytosol and its ability to transfer copper to Ccs provides another likely route for copper in Ccs-mediated Sod1 maturation [16]. These findings show the cross-reactivity and interconnectedness of the cellular copper transfer machinery [68].

MTs

The metallothionein family encompasses a group of small cysteine-rich proteins involved in metal homeostasis and detoxification [39]. Most MTs buffer zinc, however, their thiolate clusters can act as a copper sink if cellular copper concentrations are high [23,101]. Though all isoforms bind copper, when MT1 and MT2 are isolated from cells, each is bound solely to zinc [39,102]. MT3 mostly occupies the central nervous system and is isolated with both zinc and copper bound, likely because of its complex biological roles in these cells [40]. There lacks extensive research concerning copper transfer between MTs and Sod1 or Ccs. However, MTs have been shown to influence zinc binding by Sod1 [103]. MTs bind copper with a high affinity (average 10^{-19} M), thus a potential mechanism for hand-off to copper chaperones, carriers, or enzymes is

not obvious, but could involve oxidation of the coordinating cysteines by molecules such as superoxide [40]. Crosstalk between these classes of molecules is quite likely as ever-changing cellular conditions require the activity of specific target proteins, including Sod1 [69,104].

Glutathione

One major copper recipient from Ctr1 is the reduced form of glutathione (GSH), which is present within the cell at low millimolar concentrations in order to maintain the redox status of the cytosol while also functioning as an intracellular copper sink. A number of independent groups have shown that GSH can supply copper to chaperones such as Ccs [22,92,105]. GSH likely serves as a general copper reservoir for cytosolic copper-binding proteins. The relatively low copper affinity emphasizes the role of GSH as an upstream hub for copper delivery to multiple downstream targets. In accordance, when monitoring copper uptake via Ctr1, only GSH depletion impaired cellular copper uptake, while knock out of copper chaperones such as Atox1 or Ccs did not have a pronounced effect [92].

In mammals, it has been demonstrated that Sod1 can be activated in a Ccs-independent manner and that GSH plays an essential, if not well defined, role in this pathway [22]. For lower eukaryotes (e.g., yeast), GSH cannot unilaterally activate Sod1, but GSH has shown the ability to provide copper for activation in the presence of Ccs [34,41]. Here, Cu(I)-GSH was added to a pre-made Sod1cotCcs complex, where the complex was void of copper and resulted in copper transfer and complete maturation of Sod1. It was noteworthy that the copper acquisition role of Ccs D1 was essentially bypassed as the process works with a mutant version of Ccs where the MxCxxC copper binding motif cysteines were changed to alanines. Additionally, the removal of Ccs D3 prohibited the Sod1 maturation process. We have proposed that Ccs D3 forms a copper “entry-

site" or drop off point along with the disulfide cysteines of Sod1 near the interaction interface. Without this site, copper delivery to Sod1 and disulfide bond formation cannot occur [41].

Conclusions and Perspectives

Copper is tightly regulated due to the vital roles it plays within the cell, but also because of its potential for adverse redox activity [2]. To maintain homeostasis, cells have evolved an intricate copper distribution center to efficiently direct copper delivery [3]. For the vast majority, copper's journey in the mammalian cell begins when it is imported by Ctr1 [26]. This transporter moves copper across the plasma membrane and uses its cytosolic C-terminal tail (Ctr1c) to hold the copper until it can be picked up by a chaperoning protein, such as Atox1, Ccs or a sequestering molecule such as GSH or MT protein (**Figure 1.2**) [21,27]. It is very likely that these copper carriers participate in extensive crosstalk and regulation, which maintains copper homeostasis and allows for quick response to cellular changes [104].

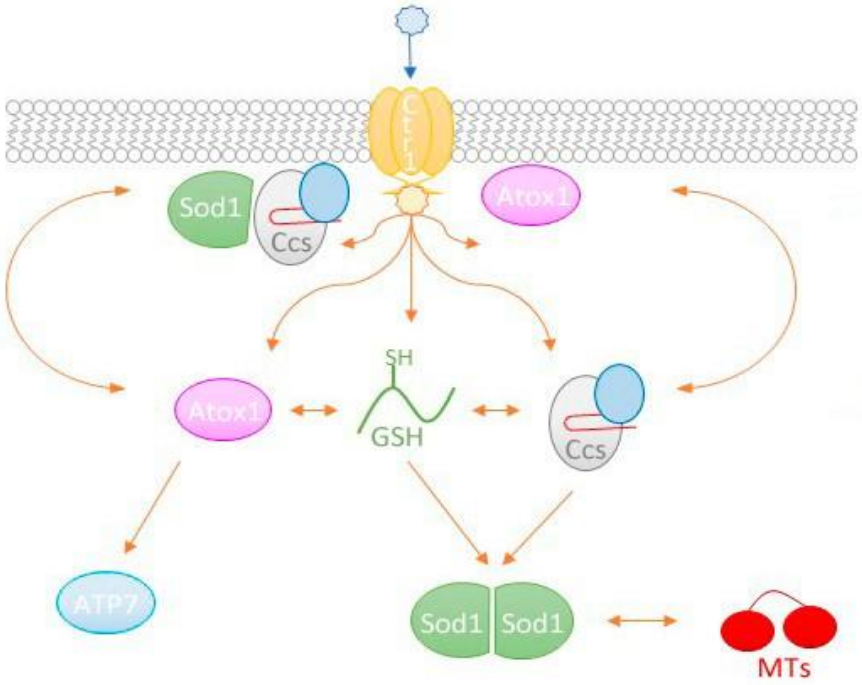

Figure 1.2. Potential routes of delivery between the copper importer Ctr1 and Sod1. Extracellular copper is commonly carried as Cu(II) (blue star) and must be reduced to Cu(I) (yellow star) for import by Ctr1. From here, the copper has numerous paths that can be taken based upon cellular conditions and availability of carrier molecules (orange arrows). Both Ccs and Atox1 have shown the propensity to associate with lipid bilayers, which may facilitate copper acquisition from Ctr1. Additionally, Atox1 and Ccs have been demonstrated to directly exchange copper with each other before delivery to their targets (ATP7A/B and Sod1, respectively). Past work in the field has also shown that the reduced form of glutathione (GSH) can act as a copper acceptor from Ctr1, exchange that copper with other copper chaperones while also delivering its copper cargo directly to immature Sod1. Further evidence has suggested that metallothioneins (MTs) may be able to exchange copper(s) with other copper-binding proteins, like Sod1, likely under conditions of oxidative stress. The colors of molecules and domains in this figure attempt to mimic those in **Figure 1.1.**

For years, accumulating evidence has indicated that copper-dysregulation plays a significant role in the development of several neurodegenerative diseases [3]. As previously described, the import of copper by Ctr1 plays a pivotal role in the copper supplementation of intracellular and secreted molecules [32]. Both Menkes and Wilson's Disease are caused by a disruption in copper homeostasis due to mutations in the transmembrane copper pumps ATP7A and ATP7B, respectively [3]. A diverse set of mutations in Sod1 causes an inherited form of the

fatal neurodegenerative disease fALS [106,107]. A role for Ccs in Sod1-linked fALS is gaining momentum as immature forms of the Sod1 protein make up a large proportion of the aggregates found in the motor neurons of mice expressing pathogenic forms of Sod1 and from the autopsies of ALS patients [108].

Given that copper regulation is important to cellular function and that dysfunction often leads to disease, therapeutics targeting copper maintenance could be useful in treatment [3,9]. For instance, diacetylbis(N(4)-methylthiosemicarbazonato)-copper(II) (Cu(II)-ATSM) is currently used for imaging tumor hypoxia, but a recent discovery indicates that Cu(II)-ATSM could be a potential therapeutic agent in the treatment of ALS [109]. Potential future treatments will rely on our understanding of copper trafficking and homeostasis. Insights gained from the thorough understanding of metal transfer between Ccs and Sod1 provide a framework for future studies.

Intracellular copper transport has been studied extensively for many years. However, key elements of copper trafficking are still unknown. Ctr1 has been investigated for nearly 30 years [110], but its mode of copper import, initial copper acquisition and reduction to Cu(I), and possible interactions with copper carriers has not been fully elucidated. Upon transfer from Ctr1 to designated copper coordinating molecule, the complex interplay between these key players of intracellular copper delivery still harbors unresolved questions. Do chaperones directly retrieve copper from Ctr1, or do they acquire copper from a Cu(I)-GSH intermediary? Does chaperone scaffolding with the plasma membrane support copper acquisition and/or possible delivery to the target? Does the availability of copper influence the mode of copper acquisition by chaperones, carriers and their target enzymes? More investigation, including biophysical, biochemical, and

cellular approaches, is required to map out this intricate intracellular copper network to improve our understanding of these elaborate copper delivery mechanisms and, ultimately human health.

Author Contributions: Writing—original draft preparation, S.D.B., M.S.U., and A.S.; writing—review and editing, S.D.B., M.S.U., and D.D.W. All authors have read and agreed to the published version of the manuscript.

Funding: This research was supported in part by R01 GM120252 from the National Institutes of Health awarded to D.D.W. and by funds from the University of Texas at Dallas. The content is solely the responsibility of the authors and does not necessarily represent the official views of the National Institutes of Health.

Conflicts of Interest: The authors declare that they have no conflicts of interest with the contents of this article.

References

1. Nevitt, T.; Ohrvik, H.; Thiele, D.J. Charting the travels of copper in eukaryotes from yeast to mammals. Biochim. et Biophys. Acta (BBA) Bioenerg. 2012, 1823, 1580–1593. [CrossRef]

2. Boal, A.K.; Rosenzweig, A.C. Structural Biology of Copper Trafficking. Chem. Rev. 2009, 109, 4760–4779. [CrossRef]

3. Cox, D.W. Disorders of copper transport. Br. Med. Bull. 1999, 55, 544–555. [CrossRef] [PubMed]

4. Fetherolf, M.M.; Boyd, S.D.; Winkler, D.D.; Winge, D.R. Oxygen-dependent activation of Cu,Zn-superoxide dismutase-1. Metallomics 2017, 9, 1047–1059. [CrossRef]

5. Mccord, J.M.; Fridovich, I. Superoxide dismutase. An enzymic function for erythrocuprein (hemocuprein).J. Boil. Chem. 1969, 244, 6049–6055.

6. Banci, L.; Bertini, I.; Cantini, F.; Kozyreva, T.; Massagni, C.; Palumaa, P.; Rubino, J.T.; Zovo, K. Human superoxide dismutase 1 (hSOD1) maturation through interaction with human copper chaperone for SOD1 (hCCS). Proc. Natl. Acad. Sci. USA 2012, 109, 13555–13560. [CrossRef] [PubMed]

7. Wong, P.C.; Waggoner, D.; Subramaniam, J.R.; Tessarollo, L.; Bartnikas, T.B.; Culotta, V.C.; Price, N.L.; Rothstein, J.; Gitlin, J.D. Copper chaperone for superoxide dismutase is essential to activate mammalian Cu/Zn superoxide dismutase. Proc. Natl. Acad. Sci. USA 2000, 97, 2886–2891. [CrossRef] [PubMed]

8. Culotta, V.C.; Yang, M.; O'Halloran, T.V. Activation of superoxide dismutases: Putting the metal to the pedal. Biochim. et Biophys. Acta (BBA) Bioenerg. 2006, 1763, 747–758. [CrossRef]

9. Harrison, M.; Jones, C.E.; Dameron, C.T. Copper chaperones: Function, structure and copper-binding properties. JBIC J. Boil. Inorg. Chem. 1999, 4, 145–153. [CrossRef]

10. Stadtman, E.R.; Berlett, B.S. Fenton chemistry. Amino acid oxidation. J. Boil. Chem. 1991, 266, 17201–17211.

11. Okado-Matsumoto, A.; Fridovich, I. Subcellular Distribution of Superoxide Dismutases (SOD) in Rat Liver: Cu, Zn-SOD In Mitochondria. J. Boil. Chem. 2001, 276, 38388–38393. [CrossRef]

12. Sturtz, L.A.; Diekert, K.; Jensen, L.T.; Lill, R.; Culotta, V.C. A fraction of yeast Cu,Zn-superoxide dismutase and its metallochaperone, CCS, localize to the intermembrane space of mitochondria. A physiological role for SOD1 in guarding against mitochondrial oxidative damage. J. Boil. Chem. 2001, 276, 38084–38089.

13. Gleason, J.E.; Galaleldeen, A.; Peterson, R.L.; Taylor, A.B.; Holloway, S.P.; Waninger-Saroni, J.; Cormack, B.P.; Cabelli, D.E.; Hart, P.J.; Culotta, V.C. Candida albicans SOD5 represents the prototype of an unprecedented class of Cu-only superoxide dismutases required for pathogen defense. Proc. Natl. Acad. Sci. USA 2014, 111, 5866–5871. [CrossRef] [PubMed]

14. Gunther, M.R.; Vangilder, R.; Fang, J.; Beattie, D.S. Expression of a familial amyotrophic lateral sclerosis-associated mutant human superoxide dismutase in yeast leads to decreased mitochondrial electron transport. Arch. Biochem. Biophys. 2004, 431, 207–214. [CrossRef] [PubMed]

15. Culotta, V.C.; Klomp, L.W.J.; Strain, J.; Casareno, R.L.B.; Krems, B.; Gitlin, J.D. The Copper Chaperone for Superoxide Dismutase. J. Boil. Chem. 1997, 272, 23469–23472. [CrossRef] [PubMed]

16. Hamza, I.; Prohaska, J.; Gitlin, J.D. Essential role for Atox1 in the copper-mediated intracellular trafficking of the Menkes ATPase. Proc. Natl. Acad. Sci. USA 2003, 100, 1215–1220. [CrossRef]

17. Banci, L.; Bertini, I.; Ciofi-Baffoni, S.; Hadjiloi, T.; Martinelli, M.; Palumaa, P. Mitochondrial copper(I) transfer from Cox17 to Sco1 is coupled to electron transfer. Proc. Natl. Acad. Sci. USA 2008, 105, 6803–6808. [CrossRef]

18. Horng, Y.-C.; Cobine, P.A.; Maxfield, A.B.; Carr, H.S.; Winge, D.R. Specific Copper Transfer from the Cox17 Metallochaperone to Both Sco1 and Cox11 in the Assembly of Yeast Cytochrome c Oxidase. J. Boil. Chem. 2004, 279, 35334–35340. [CrossRef] [PubMed]

19. Rae, T.D. Undetectable Intracellular Free Copper: The Requirement of a Copper Chaperone for Superoxide Dismutase. Science 1999, 284, 805–808. [CrossRef] [PubMed]

20. Kawamata, H.; Manfredi, G. Import, Maturation, and Function of SOD1 and Its Copper Chaperone CCS in the Mitochondrial Intermembrane Space. Antioxid. Redox Signal. 2010, 13, 1375–1384. [CrossRef] [PubMed]

21. Xiao, Z.; Wedd, A.G. A C-terminal domain of the membrane copper pump Ctr1 exchanges copper(I) with the copper chaperone Atx1. Chem. Commun. 2002, 2002, 588–589. [CrossRef] [PubMed]

22. Freedman, J.H.; Ciriolo, M.R.; Peisach, J. The role of glutathione in copper metabolism and toxicity. J. Boil. Chem.1989, 264, 5598–5605.

23. Presta, A. Incorporation of copper into the yeast saccharomyces cerevisiae. Identification of Cu(I)-metallothionein in intact yeast cells. J. Inorg. Biochem. 1997, 66, 231–240. [CrossRef]

24. Blair, B.G.; Larson, C.A.; Adams, P.L.; Abada, P.B.; Pesce, C.E.; Safaei, R.; Howell, S.B. Copper transporter 2 regulates endocytosis and controls tumor growth and sensitivity to cisplatin in vivo. Mol. Pharmacol. 2010, 79, 157–166. [CrossRef]

25. Knight, S.; Labbé, S.; Kwon, L.F.; Kosman, D.J.; Thiele, D.J. A widespread transposable element masks expression of a yeast copper transport gene. Genome Res. 1996, 10, 1917–1929. [CrossRef] [PubMed]

26. Eisses, J.F.; Kaplan, J. Molecular Characterization of hCTR1, the Human Copper Uptake Protein. J. Boil. Chem. 2002, 277, 29162–29171. [CrossRef] [PubMed]

27. Klomp, A.E.M.; Tops, B.; Van DenBerg, I.E.T.; Berger, R.; Klomp, L.W.J. Biochemical characterization and subcellular localization of human copper transporter 1 (hCTR1). Biochem. J. 2002, 364, 497–505. [CrossRef]

28. Lee, J.; Peña, M.M.O.; Nose, Y.; Thiele, D.J. Biochemical Characterization of the Human Copper Transporter Ctr1. J. Boil. Chem. 2001, 277, 4380–4387. [CrossRef]

29. Ramos, D.; Mar, D.; Ishida, M.; Vargas, R.; Gaite, M.; Montgomery, A.; Linder, M.C. Mechanism of Copper Uptake from Blood Plasma Ceruloplasmin by Mammalian Cells. PLoS ONE 2016, 11, e0149516. [CrossRef]

30. Shenberger, Y.; Shimshi, A.; Ruthstein, S. EPR Spectroscopy Shows that the Blood Carrier Protein, Human Serum Albumin, Closely Interacts with the N-Terminal Domain of the Copper Transporter, Ctr1. J. Phys. Chem. B 2015, 119, 4824–4830. [CrossRef]

31. Stefaniak, E.; Płonka, D.; Drew, S.C.; Bossak-Ahmad, K.; Haas, K.L.; Pushie, M.J.; Faller, P.; Wezynfeld, N.E.; Bal, W. The N-terminal 14-mer model peptide of human Ctr1 can collect Cu(ii) from albumin. Implications for copper uptake by Ctr1. Metallomics 2018, 10, 1723–1727. [CrossRef]

32. De Feo, C.J.; Aller, S.G.; Siluvai, G.S.; Blackburn, N.J.; Unger, V.M. Three-dimensional structure of the human copper transporter hCTR1. Proc. Natl. Acad. Sci. USA 2009, 106, 4237–4242. [CrossRef] [PubMed]

33. Ohrvik, H.; Thiele, D.J. How copper traverses cellular membranes through the mammalian copper transporter 1, Ctr1. Ann. N. Y. Acad. Sci. 2014, 1314, 32–41. [CrossRef] [PubMed]

34. Skopp, A.; Boyd, S.D.; Ullrich, M.S.; Liu, L.; Winkler, D.D. Copper–zinc superoxide dismutase (Sod1) activation terminates interaction between its copper chaperone (Ccs) and the cytosolic metal-binding domain of the copper importer Ctr1. BioMetals 2019, 32, 695–705. [CrossRef] [PubMed]

35. Pope, C.R.; De Feo, C.J.; Unger, V.M. Cellular distribution of copper to superoxide dismutase involves scaffolding by membranes. Proc. Natl. Acad. Sci. USA 2013, 110, 20491–20496. [CrossRef] [PubMed]

36. Linz, R.; Lutsenko, S. Copper-transporting ATPases ATP7A and ATP7B: Cousins, not twins. J. Bioenerg. Biomembr. 2007, 39, 403–407. [CrossRef]

37. La Fontaine, S.; Mercer, J.F. Trafficking of the copper-ATPases, ATP7A and ATP7B: Role in copper homeostasis. Arch. Biochem. Biophys. 2007, 463, 149–167. [CrossRef]

38. Hamer, D.H. Metallothionein. Ann. Rev. Biochem. 1986, 55, 913–951. [CrossRef]

39. Vašák, M.; Meloni, G. Chemistry and biology of mammalian metallothioneins. JBIC J. Boil. Inorg. Chem. 2011, 16, 1067–1078. [CrossRef]

40. Calvo, J.S.; Lopez, V.M.; Meloni, G. Non-coordinative metal selectivity bias in human metallothioneins metal-thiolate clusters. Metallomics 2018, 10, 1777–1791. [CrossRef]

41. Fetherolf, M.M.; Boyd, S.D.; Taylor, A.B.; Kim, H.J.; Wohlschlegel, J.A.; Blackburn, N.J.; Hart, P.J.; Winge, D.R.; Winkler, D.D. Copper-zinc superoxide dismutase is activated through a sulfenic acid intermediate at a copper ion entry site. J. Boil. Chem. 2017, 292, 12025–12040. [CrossRef]

42. Furukawa, Y.; Torres, A.S.; O'Halloran, T.V. Oxygen-induced maturation of SOD1: A key role for disulfide formation by the copper chaperone CCS. EMBO J. 2004, 23, 2872–2881. [CrossRef] [PubMed]

43. Fukuoka, M.; Tokuda, E.; Nakagome, K.; Wu, Z.; Nagano, I.; Furukawa, Y. An essential role of N-terminal domain of copper chaperone in the enzymatic activation of Cu/Zn-superoxide dismutase. J. Inorg. Biochem. 2017, 175, 208–216. [CrossRef] [PubMed]

44. Keele, B.B.; Mccord, J.M.; Fridovich, I. Further characterization of bovine superoxide dismutase and its isolation from bovine heart. J. Boil. Chem. 1971, 246, 2875–2880.

45. Fisher, C.L.; Cabelli, D.E.; Tainer, J.; Hallewell, R.A.; Getzoff, E.D. The role of arginine 143 in the electrostatics and

mechanism of Cu, Zn superoxide dismutase: Computational and experimental evaluation by mutational analysis. Proteins Struct. Funct. Bioinform. 1994, 19, 24–34. [CrossRef] [PubMed]

46. Luchinat, E.; Barbieri, L.; Rubino, J.T.; Kozyreva, T.; Cantini, F.; Banci, L. In-cell NMR reveals potential precursor of toxic species from SOD1 fALS mutants. Nat. Commun. 2014, 5, 5502. [CrossRef] [PubMed]

47. Leitch, J.M.; Yick, P.J.; Culotta, V.C. The Right to Choose: Multiple Pathways for Activating Copper, Zinc Superoxide Dismutase. J. Boil. Chem. 2009, 284, 24679–24683. [CrossRef]

48. Lamb, A.L.; Wernimont, A.K.; Pufahl, R.A.; O'Halloran, T.V.; Rosenzweig, A.C. Crystal Structure of the Second Domain of the Human Copper Chaperone for Superoxide Dismutase. Biochemistry 2000, 39, 1589–1595. [CrossRef]

49. Rosenzweig, A. Structure and chemistry of the copper chaperone proteins. Curr. Opin. Chem. Boil. 2000, 4, 140–147. [CrossRef]

50. Furukawa, Y.; O'Halloran, T.V. Posttranslational Modifications in Cu,Zn-Superoxide Dismutase and Mutations Associated with Amyotrophic Lateral Sclerosis. Antioxid. Redox Signal. 2006, 8, 847–867. [CrossRef]

51. Ogihara, N.L.; Parge, H.E.; Hart, P.J.; Weiss, M.S.; Goto, J.J.; Crane, B.R.; Tsang, J.; Slater, K.; Roe, J.A.; Valentine, J.S.; et al. Unusual Trigonal-Planar Copper Configuration Revealed in the Atomic Structure of Yeast Copper−Zinc Superoxide Dismutase. Biochemistry 1996, 35, 2316–2321. [CrossRef] [PubMed]

52. Hart, P.J.; Balbirnie, M.M.; Ogihara, N.L.; Nersissian, A.M.; Weiss, M.S.; Valentine, J.S.; Eisenberg, D. A Structure-Based Mechanism for Copper−Zinc Superoxide Dismutase. Biochemistry 1999, 38, 2167–2178. [CrossRef] [PubMed]

53. Tainer, J.; Getzoff, E.D.; Richardson, J.S.; Richardson, D.C. Structure and mechanism of copper, zinc superoxide dismutase. Nature 1983, 306, 284–287. [CrossRef] [PubMed]

54. Cudd, A.; Fridovich, I. Electrostatic interactions in the reaction mechanism of bovine erythrocyte superoxide dismutase. J. Biol. Chem. 1982, 257, 11443–11447.

55. Klug, D.; Rabani, J.; Fridovich, I. A direct demonstration of the catalytic action of superoxide dismutase through the use of pulse radiolysis. J. Boil. Chem. 1972, 247, 4839–4842.

56. Schmidt, P.J.; Ramos-Gomez, M.; Culotta, V.C. A Gain of Superoxide Dismutase (SOD) Activity Obtained with CCS, the Copper Metallochaperone for SOD1. J. Boil. Chem. 1999, 274, 36952–36956. [CrossRef] [PubMed]

57. Casareno, R.L.B.; Waggoner, D.; Gitlin, J.D. The copper chaperone CCS directly interacts with copper/zinc superoxide dismutase. J. Boil. Chem. 1998, 273, 23625–23628. [CrossRef]

58. Rae, T.D.; Torres, A.S.; Pufahl, R.A.; O'Halloran, T.V. Mechanism of Cu,Zn-Superoxide Dismutase Activation by the Human Metallochaperone hCCS. J. Boil. Chem. 2000, 276, 5166–5176. [CrossRef]

59. Wright, G.S.A.; Hasnain, S.S.; Grossmann, J.G. The structural plasticity of the human copper chaperone for SOD1: Insights from combined size-exclusion chromatographic and solution X-ray scattering studies. Biochem. J. 2011, 439, 39–44. [CrossRef]

60. Boyd, S.D.; Calvo, J.S.; Liu, L.; Ullrich, M.S.; Skopp, A.; Meloni, G.; Winkler, D.D. The yeast copper chaperone for copper-zinc superoxide dismutase (CCS1) is a multifunctional chaperone promoting all levels of SOD1 maturation. J. Boil. Chem. 2018, 294, 1956–1966. [CrossRef]

61. Boyd, S.D.; Liu, L.; Bulla, L.; Winkler, D.D. Quantifying the Interaction between Copper-Zinc Superoxide Dismutase (Sod1) and its Copper Chaperone (Ccs1). J. Proteom. Bioinform. 2018, 11, 1–5. [CrossRef] [PubMed]

62. Boyd, S.; Ullrich, M.; Calvo, J.S.; Behnia, F.; Meloni, G.; Winkler, D.D. Mutations in Superoxide Dismutase 1 (Sod1) Linked to Familial Amyotrophic Lateral Sclerosis Can Disrupt High-Affinity Zinc-Binding Promoted by the Copper Chaperone for Sod1 (Ccs). Molecules 2020, 25, 1086. [CrossRef] [PubMed]

63. Luchinat, E.; Barbieri, L.; Banci, L. A molecular chaperone activity of CCS restores the maturation of SOD1 fALS mutants. Sci. Rep. 2017, 7, 17433. [CrossRef] [PubMed]

64. Rothstein, J.D.; Dykes-Hoberg, M.; Corson, L.B.; Becker, M.; Cleveland, D.W.; Price, N.L.; Culotta, V.C.; Wong, P.C. The copper chaperone CCS is abundant in neurons and astrocytes in human and rodent brain. J. Neurochem. 1999, 72, 422–429. [CrossRef] [PubMed]

65. Carroll, M.C.; Girouard, J.B.; Ulloa, J.L.; Subramaniam, J.R.; Wong, P.C.; Valentine, J.S.; Culotta, V.C. Mechanisms for activating Cu- and Zn-containing superoxide dismutase in the absence of the CCS Cu chaperone. Proc. Natl. Acad. Sci. USA 2004, 101, 5964–5969. [CrossRef]

66. Leitch, J.M.; Jensen, L.T.; Bouldin, S.D.; Outten, C.E.; Hart, P.J.; Culotta, V.C. Activation of Cu,Zn-Superoxide Dismutase in the Absence of Oxygen and the Copper Chaperone CCS. J. Boil. Chem. 2009, 284, 21863–21871. [CrossRef]

67. Jensen, L.T.; Culotta, V.C. Activation of CuZn Superoxide Dismutases from Caenorhabditis elegans Does Not Require the Copper Chaperone CCS. J. Boil. Chem. 2005, 280, 41373–41379. [CrossRef]

68. Petzoldt, S.; Kahra, D.; Kovermann, M.; Dingeldein, A.P.G.; Niemiec, M.S.; Ådén, J.; Wittung-Stafshede, P. Human cytoplasmic copper chaperones Atox1 and CCS exchange copper ions in vitro. Biometals 2015, 28, 577–585. [CrossRef]

69. Miyayama, T.; Ishizuka, Y.; Iijima, T.; Hiraoka, D.; Ogra, Y. Roles of copper chaperone for superoxide dismutase 1 and metallothionein in copper homeostasis. Metallomics 2011, 3, 693. [CrossRef] [PubMed]

70. Zhou, H.; Thiele, D.J. Identification of a Novel High Affinity Copper Transport Complex in the Fission YeastSchizosaccharomyces pombe. J. Boil. Chem. 2001, 276, 20529–20535. [CrossRef]

71. Sancenón, V.; Puig, S.; Mira, H.; Thiele, D.J.; Peñarrubia, L. Identification of a copper transporter family in Arabidopsis thaliana. Plant Mol. Boil. 2003, 51, 577–587. [CrossRef]

72. Kampfenkel, K.; Kushnir, S.; Babiychuk, E.; Inzé, D.; Van Montagu, M. Molecular characterization of a putative Arabidopsis thaliana copper transporter and its yeast homologue. J. Boil. Chem. 1995, 270, 28479–28486.

73. MacKenzie, N.C.; Brito, M.; Reyes, A.E.; Allende, M.L. Cloning, expression pattern and essentiality of the high-affinity copper transporter 1 (ctr1) gene in zebrafish. Gene 2004, 328, 113–120. [CrossRef]

74. Haremaki, T.; Weinstein, D. Xmc mediates Xctr1-independent morphogenesis inXenopus laevis. Dev. Dyn. 2009, 238, 2382–2387. [CrossRef] [PubMed]

75. Riggio, M.; Lee, J.; Scudiero, R.; Parisi, E.; Thiele, D.J.; Filosa, S. High affinity copper transport protein in the lizard Podarcis sicula: Molecular cloning, functional characterization and expression in somatic tissues, follicular oocytes and eggs. Biochim. Biophys. Acta (BBA) Gene Struct. Expr. 2002, 1576, 127–135. [CrossRef]

76. Lee, J.; Prohaska, J.R.; Dagenais, S.L.; Glover, T.W.; Thiele, D.J. Isolation of a murine copper transporter gene, tissue specific expression and functional complementation of a yeast copper transport mutant. Gene 2000, 254, 87–96. [CrossRef]

77. Dancis, A.; Haile, D.; Yuan, D.S.; Klausner, R.D. The Saccharomyces cerevisiae copper transport protein (Ctr1p). Biochemical characterization, regulation by copper, and physiologic role in copper uptake. J. Boil. Chem. 1994, 269, 25660–25667.

78. Waterman, S.R.; Hacham, M.; Hu, G.; Zhu, X.; Park, Y.; Shin, S.; Panepinto, J.; Valyi-Nagy, T.; Beam, C.; Husain, S.; et al. Role of a CUF1/CTR4 copper regulatory axis in the virulence of Cryptococcus neoformans. J. Clin. Investig. 2007, 117, 794–802. [CrossRef]

79. Ding, C.; Yin, J.; Tovar, E.M.M.; Fitzpatrick, D.A.; Higgins, D.; Thiele, D.J. The copper regulon of the human fungal pathogen Cryptococcus neoformans H99. Mol. Microbiol. 2011, 81, 1560–1576. [CrossRef]

80. Bertinato, J.; Swist, E.; Plouffe, L.J.; Brooks, S.P.; L'Abbé, M.R. Ctr2 is partially localized to the plasma membrane and stimulates copper uptake in COS-7 cells. Biochem. J. 2008, 409, 731–740. [CrossRef]

81. Puig, S.; Lee, J.; Lau, M.; Thiele, D.J. Biochemical and Genetic Analyses of Yeast and Human High Affinity Copper Transporters Suggest a Conserved Mechanism for Copper Uptake. J. Boil. Chem. 2002, 277, 26021–26030. [CrossRef]

82. Klomp, A.E.M.; Juijn, J.A.; Van Der Gun, L.T.M.; Berg, I.E.T.V.D.; Berger, R.; Klomp, L.W.J. The N-terminus of the human copper transporter 1 (hCTR1) is localized extracellularly, and interacts with itself. Biochem. J. 2003, 370, 881–889. [CrossRef] [PubMed]

83. Guo, Y.; Smith, K.; Lee, J.; Thiele, D.J.; Petris, M.J. Identification of Methionine-rich Clusters That Regulate Copper-stimulated Endocytosis of the Human Ctr1 Copper Transporter. J. Boil. Chem. 2004, 279, 17428–17433. [CrossRef]

84. Aller, S.G.; Eng, E.T.; De Feo, C.J.; Unger, V.M. Eukaryotic CTR Copper Uptake Transporters Require Two Faces of the Third Transmembrane Domain for Helix Packing, Oligomerization, and Function. J. Boil. Chem. 2004, 279, 53435–53441. [CrossRef] [PubMed]

85. De Feo, C.J.; Mootien, S.; Unger, V.M. Tryptophan Scanning Analysis of the Membrane Domain of CTR-Copper Transporters. J. Membr. Boil. 2010, 234, 113–123. [CrossRef] [PubMed]

86. Nose, Y.; Wood, L.K.; Kim, B.-E.; Prohaska, J.R.; Fry, R.S.; Spears, J.W.; Thiele, D.J. Ctr1 Is an Apical Copper Transporter in Mammalian Intestinal Epithelial Cells in Vivo That Is Controlled at the Level of Protein Stability. J. Boil. Chem. 2010, 285, 32385–32392. [CrossRef] [PubMed]

87. Maryon, E.B.; Molloy, S.A.; Kaplan, J. O-Linked Glycosylation at Threonine 27 Protects the Copper Transporter hCTR1 from Proteolytic Cleavage in Mammalian Cells. J. Boil. Chem. 2007, 282, 20376–20387. [CrossRef]

88. Eisses, J.F.; Kaplan, J.H. The Mechanism of Copper Uptake Mediated by Human CTR1 a Mutational Analysis. J. Biol. Chem. 2005, 280, 37159–37168. [CrossRef]

89. Hassett, R.; Kosman, D.J. Evidence for Cu(II) Reduction as a Component of Copper Uptake bySaccharomyces cerevisiae. J. Boil. Chem. 1995, 270, 128–134. [CrossRef]

90. Georgatsou, E.; Mavrogiannis, L.A.; Fragiadakis, G.S.; Alexandraki, D. The Yeast Fre1p/Fre2p Cupric Reductases

Facilitate Copper Uptake and Are Regulated by the Copper-modulated Mac1p Activator. J. Boil. Chem. 1997, 272, 13786–13792. [CrossRef]

91. Kahra, D.; Kovermann, M.; Wittung-Stafshede, P. The C-Terminus of Human Copper Importer Ctr1 Acts as a Binding Site and Transfers Copper to Atox1. Biophys. J. 2016, 110, 95–102. [CrossRef] [PubMed]

92. Maryon, E.B.; Molloy, S.A.; Kaplan, J. Cellular glutathione plays a key role in copper uptake mediated by human copper transporter 1. Am. J. Physiol. 2013, 304, C768–C779. [CrossRef] [PubMed]

93. Lee, J.; Petris, M.J.; Thiele, D.J. Characterization of Mouse Embryonic Cells Deficient in the Ctr1 High Affinity Copper Transporter. J. Boil. Chem. 2002, 277, 40253–40259. [CrossRef] [PubMed]

94. Simon, I.; Schaefer, M.; Reichert, J.; Stremmel, W. Analysis of the human Atox 1 homologue in Wilson patients. World J. Gastroenterol. 2008, 14, 2383–2387. [CrossRef]

95. Huffman, D.L.; O'Halloran, T.V. Function, Structure, and Mechanism of Intracellular Copper Trafficking Proteins. Annu. Rev. Biochem. 2001, 70, 677–701. [CrossRef]

96. Arnesano, F.; Banci, L.; Bertini, I.; Ciofi-Baffoni, S.; Molteni, E.; Huffman, D.L.; O'Halloran, T.V. Metallochaperones and Metal-Transporting ATPases: A Comparative Analysis of Sequences and Structures. Genome Res. 2002, 12, 255–271. [CrossRef]

97. Hellman, N.E.; Gitlin, J.D. Ceruloplasmin metabolism and function. Annu. Rev. Nutr. 2002, 22, 439–458. [CrossRef]

98. Flores, A.G.; Unger, V.M. Atox1 contains positive residues that mediate membrane association and aid subsequent copper loading. J. Membr. Boil. 2013, 246, 903–913. [CrossRef]

99. Xiao, Z.; Brose, J.; Schimo, S.; Ackland, S.M.; La Fontaine, S.; Wedd, A.G. Unification of the Copper(I) Binding Affinities of the Metallo-chaperones Atx1, Atox1, and Related Proteins. J. Boil. Chem. 2011, 286, 11047–11055. [CrossRef]

100. Puig, S.; Thiele, D.J. Molecular mechanisms of copper uptake and distribution. Curr. Opin. Chem. Boil. 2002, 6, 171–180. [CrossRef]

101. Salgado, M.T.; Stillman, M.J. Cu+ distribution in metallothionein fragments. Biochem. Biophys. Res. Commun. 2004, 318, 73–80. [CrossRef] [PubMed]

102. Kre˛z˙el, A.; Hao, Q.; Maret, W. The zinc/thiolate redox biochemistry of metallothionein and the control of zinc ion fluctuations in cell signaling. Arch. Biochem. Biophys. 2007, 463, 188–200. [CrossRef] [PubMed]

103. Suzuki, K.T.; Kuroda, T. Transfer of copper and zinc from ionic and metallothionein-bound forms to Cu, Zn—Superoxide dismutase. Res. Commun. Mol. Pathol. Pharmacol. 1995, 87, 287–296. [PubMed]

104. Lutsenko, S. Human copper homeostasis: A network of interconnected pathways. Curr. Opin. Chem. Boil. 2010, 14, 211–217. [CrossRef]

105. Brouwer, M.; Brouwer-Hoexum, T. Glutathione-mediated transfer of copper (I) into American lobster apohemocyanin. Biochemistry 1992, 31, 4096–4102. [CrossRef]

106. Deng, H.-X.; Hentati, A.; Tainer, J.; Iqbal, Z.; Cayabyab, A.; Hung, W.; Getzoff, E.; Hu, P.; Herzfeldt, B.; Roos, R.; et al. Amyotrophic lateral sclerosis and structural defects in Cu, Zn superoxide dismutase. Science 1993, 261, 1047–1051. [CrossRef]

107. Gurney, M.; Pu, H.; Chiu, A.; Canto, M.D.; Polchow, C.; Alexander, D.; Caliendo, J.; Hentati, A.; Kwon, Y.; Deng, H.-X.; et al. Motor neuron degeneration in mice that express a human Cu,Zn superoxide dismutase mutation. Science 1994, 264, 1772–1775. [CrossRef]

108. Watanabe, M.; Dykes-Hoberg, M.; Culotta, V.C.; Price, D.L.; Wong, P.C.; Rothstein, J.D. Histological Evidence of Protein Aggregationin Mutant SOD1 Transgenic Mice and inAmyotrophic Lateral Sclerosis Neural Tissues. Neurobiol. Dis. 2001, 8, 933–941. [CrossRef]

109. Kuo, M.T.; Beckman, J.S.; Shaw, C.A. Neuroprotective effect of CuATSM on neurotoxin-induced motor neuron loss in an ALS mouse model. Neurobiol. Dis. 2019, 130, 104495. [CrossRef]

110. Kaplan, J.; Maryon, E.B. How Mammalian Cells Acquire Copper: An Essential but Potentially Toxic Metal. Biophys. J. 2016, 110, 7–13. [CrossRef]

CHAPTER 2

COPPER–ZINC SUPEROXIDE DISMUTASE (SOD1) ACTIVATION TERMINATES INTERACTION BETWEEN ITS COPPER CHAPERONE (CCS) AND THE CYTOSOLIC METAL-BINDING DOMAIN OF THE COPPER IMPORTER CTR1

Amelie Skopp, Stefanie D. Boyd, Morgan S. Ullrich, Li Liu, and Duane D. Winkler

The Department of Biological Sciences, BSB12

The University of Texas at Dallas

800 West Campbell Road

Richardson, Texas 75080-3021

ABSTRACT

Copper–zinc superoxide dismutase (Sod1) is a critical antioxidant enzyme that rids the cell of reactive oxygen through the redox cycling of a catalytic copper ion provided by its copper chaperone (Ccs). Ccs must first acquire this copper ion, directly or indirectly, from the influx copper transporter, Ctr1. The three proteins of this transport pathway ensure careful trafficking of copper ions from cell entry to target delivery, but the intricacies remain undefined. Biochemical examination of each step in the pathway determined that the activation of the target (Sod1) regulates the Ccs·Ctr1 interaction. Ccs stably interacts with the cytosolic C-terminal tail of Ctr1 (Ctr1c) in a copper-dependent manner. This interaction becomes tripartite upon the addition of an engineered immature form of Sod1 creating a stable Cu(I)-Ctr1c·Ccs·Sod1 heterotrimer in solution. This heterotrimer can also be made by the addition of a preformed Sod1·Ccs heterodimer to Cu(I)-Ctr1c, suggestive of multiple routes to the same destination. Only complete Sod1 activation (i.e. active site copper delivery and intra-subunit disulfide bond formation) breaks the Sod1·Ccs·Ctr1c complex. The results provide a new and extended view of the Sod1 activation pathway(s) originating at cellular copper import.

Introduction

Copper is a critical cofactor for many enzymes that take advantage of its redox activity to catalyze a wide range of chemical reactions. Proper levels of copper are required throughout the cell for processes such as respiration, enzymatic catalysis, and neurotransmitter synthesis (Bremner 1998). Unregulated copper-based reactions are detrimental to the cell by generating free radical oxygen species (Halliwell and Gutteridge 1990; Pena et al. 1999). Therefore, aerobic organisms have evolved a tightly controlled network of copper trafficking molecules for import,

shuttling, and delivery to specific targets across the cellular land- scape (reviewed in Rosenzweig and O'Halloran 2000; Rosenzweig 2001; Robinson and Winge 2010).

Copper ion import is facilitated by the Ctr family of integral membrane transporters that bring copper into the cytoplasm in an ATP-independent fashion (Dancis and Haile 1994; Lee et al. 2002; Kim et al. 2008). Members of the Ctr-family, of which Ctr1 is the most prominent, are small transmembrane proteins consist-ing of a conserved extracellular N-terminal domain (ecto/NTD), three transmembrane domains (TMDs), and a short C-terminal tail (Ctr1c), which is the only domain that fully extends into the cytosol (Eisses and Kaplan 2002; Puig et al. 2002; Klomp et al. 2003). Trimerization of Ctr1 monomers forms a pore through which Cu(I) (i.e. reduced/cuprous copper) is trans- ported into the cell (De Feo et al. 2009). Cu(I) is then simultaneously coordinated by three Ctr1c tails, each containing an HCH copper binding motif. Binding of Cu(I) to a single HCH at one tail is possible, however normal Cu(I)-binding motifs involve two or three cysteine residues coordinating Cu(I). (Pickering et al. 1993) By holding the Cu(I) between multiple tails, Ctr1 can mimic the more favorable Cu(I) coordinating motifs. The Cu(I) is then offered to cytosolic copper traffickers (Kahra et al. 2016). Two ATP-dependent pumps ATP7A and ATP7B that reside in the membranes of the trans-Golgi network, handle copper ion export (Lutsenko et al. 2002; Voskoboinik and Camakaris 2002).

A diverse family of intracellular copper binding proteins termed ‘‘copper chaperones’’ transport cytosolic copper ions to dedicated protein targets (O'Halloran and Culotta 2000; Kahra et al. 2016; Kaplan and Maryon 2016). One such molecule is the copper chaperone for Sod1 (Ccs) that has been shown to be critical for efficient activation of the ubiquitous anti-oxidant enzyme copper–zinc superoxide dismu- tase (Sod1) (Culotta et al. 1997; Schmidt et al. 2000; Wong et al.

2000; Fetherolf et al. 2017a, b). Ccs proteins consist of three conserved domains that are essential for target recognition and copper ion delivery (reviewed in Fetherolf et al. 2017a, b). Unlike other copper chaperones, Ccs also plays a crucial role in the formation of an intra-subunit disulfide bond within Sod1 (reviewed in Fetherolf et al. 2017a, b). The N-terminal domain (D1) contains a MxCxxC copper- binding motif and is structurally similar to another copper chaperone that guides copper to the aforementioned secretory pathway (Atx1/Atox1) (Xiao and Wedd 2002; Hussain et al. 2008; Rodri- guez-Granillo and Wittung-Stafshede 2008; Hussain et al. 2009; Rodriguez-Granillo and Wittung-Staf- shede 2009; Rodriguez-Granillo et al. 2010). The second domain (D2) is analogous to Sod1 in both sequence and structure (Lamb et al. 1999) and plays a key role in Sod1 binding (Lamb et al. 2000, 2001; Winkler et al. 2009; Fetherolf et al. 2017a, b). The C-terminal domain (D3) possesses an invariant CxC motif known to bind copper and is essential for complete Sod1 activation in vivo (Schmidt et al. 1999). Though multiple three-dimensional structures of Ccs (Lamb et al. 1999, 2000; Banci et al. 2013) and complete Ccs·Sod1 complexes have been determined (Lamb et al. 2001; Fetherolf et al. 2017a, b; Sala et al. 2019) a complete molecular mechanism for Ccs- mediated Sod1 activation is tenuous and remains under debate.

Even less understood is how, where, or when copper chaperones, including Ccs, acquire their copper cargo from the cell (Flores and Unger 2013). Indeed, the passage of Cu(I) from the cytosolic Ctr1c domain to Ccs still requires clarity, while related work implies that the reduced form of glutathione (GSH) may play an intermediary role (Maryon et al. 2013; Pope et al. 2013). Although Ctr1 has been studied extensively for years, an initial model for Ctr1- mediated Cu(I) import is only beginning to emerge (reviewed in Ohrvik and Thiele 2014).

Here, we demonstrate a direct Cu(I)-dependent interaction between human Ctr1c and Ccs. Unexpectedly, immediate copper transfer and dissolution of the Cu(I)-Ctr1c·Ccs complex did not occur. Furthermore, a stable Cu(I)-Ctr1c·Ccs·Sod1 heterotrimeric complex is observed when copper delivery and/or disulfide bond formation in Sod1 (i.e. Sod1 activation) is stalled. Cu(I)-Ctr1c will readily bind either Ccs or a pre-formed Ccs·Sod1 complex, which backs related data showing that the copper binding status of Ccs does not affect its affinity for immature Sod1 (Luchinat 2017; Boyd et al. 2018). Complete Sod1 activation (i.e. zinc and copper binding along with disulfide oxidation (Cu,Zn-Sod1^{SS})) dissociates the heterotrimeric complex into a mixture of its own parts (Banci et al. 2012; Wright et al. 2016). The data presented here builds a comprehensive molecular mechanism for the direct Ctr1-to-Ccs-to-Sod1 copper influx pathway and suggests that the entire pathway can proceed within a single macromolecular complex.

Materials and methods

Materials

The C-terminal 13 amino acids of the human Ctr1 Cu(I)-transporter (Ctr1c), KKAVVVDITEHCH, were custom-ordered as a lyophilized peptide from Sigma. DTT (dithiotreitol), TCEP-HCl (tris(2-car- boxyethyl)phosphine), and IPTG (isopropyl 1-thio-b-D-galactopyranoside) were purchased from GoldBio. Tris-base, mono- and di-basic sodium phosphate, sodium acetate, ammonium persulfate (APS), EDTA, b-mercaptoethanol (BME), and sodium chloride were acquired from Fisher. Nitroblue terazolium and bathocuproinedisulfonic acid (BCS) were purchased from

Alfa Aesar. Primers for site-directed mutagenesis and zinc sulfate heptahydrate were bought from Sigma. Maleimide-polyethyleneglycol 2000 was purchased from nanocs. Tetramethylethylenediamine (TEMED) was purchased from Thermo Scientific, while riboflavin was acquired from Acros Organics. Alexa-488-succinimidyl ester was purchased from Life Technologies. Cu(I)-(CH3CN4)PF6 was purchased from Strem Chemicals. His-Trap Nickel affinity columns, SQ (anion exchange) columns, and gel filtration columns were purchased from GE LifeSciences.

Ccs1 and Sod1 cloning, mutagenesis, expression, and purification

Human wild-type (WT) Ccs1 (UniProtKB—O14618) was cloned into a pAG8H vector containing an inducible lacZ site, N-terminal His8-tag, and an internal tobacco etch virus (TEV) cleavage site using NarI and SalI restriction sites. Sod1 WT (Uni- ProtKB—P00441) was cloned using NarI and HindIII sites into the same vector. Mutations in Ccs and Sod1 were generated using the Thermo Scientific site- directed mutagenesis kit according to the provided protocol. Escherichia coli BL21 DE3 PLysS cells (purchased from Promega) were transformed and grown at 37 °C in 2xYT medium to an A600nm of 0.6–0.9 and induced with 3–5 mM IPTG. After an additional 4 h of growth cells were harvested and purified using a His-Trap HP Ni^{2+} affinity column by GE Healthcare. The His8-tag was removed from the purified protein by digestion at room temperature overnight with TEV protease engineered to contain a non-cleavable His8-tag. The resulting cleaved His8-tag as well as the TEV protease were removed from Ccs1 by another Ni^{2+} affinity purification.

Protein metallation

Sod1 was stripped of metals by incubation in Sod1 stripping buffer 1 (50 mM NaOAc pH 3.5, 10 mM EDTA, 10 mM DTT) for 4 h at room temperature and then transferred to metal-free buffer 2 (50 mM NaOAc pH 5.5, 10 mM DTT) overnight at 4 °C. The metal free protein was buffer exchanged into 50 mM Tris pH8. Ccs1 was stripped of metals by incubation in Ccs1 stripping buffer (20 mM Tris pH 8, 10 mM EDTA, 10 mM DTT) overnight at 4 °C. The metal-free protein was buffer exchanged into either metal free 50 mM Tris pH. All proteins were Cu(I) loaded anaerobically using Cu–PF6. Metal loading was con- firmed by induced coupled plasma mass spectrometry (ICP-MS) using the Agilent 7900 facility here at UTD. Samples for ICP-MS were digested with 1% HNO3 for analysis and performed in triplicate. The buffer in these experiments was measured for baseline metal content. Sod1 activity assays were performed as described previously (Fetherolf et al. 2017a, b).

Cu(I)-loaded Ctr1c production

Apo-Ctr1c was quantified by amino acid analysis by AAA Service Laboratory, Inc. Absorbance was measured from 200 to 360 nm using a Cary300 UV–Vis spectrophotometer by Agilent and the extinction coefficient was calculated. The Ctr1c-peptide was Cu(I)-loaded anaerobically in equimolar ratio with Cu(I)-(CH3CN4)PF6 for 2 h and excess unbound Cu(I) was removed by size-exclusion chromatography using a BioRad P2 column in spectroscopy buffer or by dialysis. ICP-MS results indicated that one Cu(I) ion was coordinated by 3 Ctr1c peptides, similar to what is seen in full-length Ctr1 (De Feo et al. 2009). Even when copper was added in 3–5-fold excess of peptide, the resulting copper bound remained consistent.

Amine-specific labeling of Ctr1c

Apo and Cu(I)-Ctr1c were incubated with equimolar amounts of Alexa-488 succinimidyl ester by Fisher at room temperature in pH 7.4 buffer for 1 h. The labeling reaction was quenched with 1 M Tris pH 8 was then dialyzed overnight at 4 °C to remove excess dye and its metal status was confirmed by assaying its ability to provide Cu(I) to Sod1.

Nickel pulldown assay

His8-tagged WT and mutant Ccs1 and Sod1 variants were expressed and purified by Ni-affinity chromatography. 5uM bait protein was incubated with 40 µL Ni- NTA agarose bead slurry in 20 mM Tris pH 7.5, 150 mM NaCl, 2 mM TCEP-HCl, and 200 µM BCS for 1 h at room temperature. 15uM Cu(I)-Ctr1c488 was incubated with the bait proteins at room temperature for 1 h and washed three times with 500 µL 20 mM Tris pH 7.5, 150 mM NaCl, 2 mM TCEP-HCl, and 100 mM imidazole. Proteins for SDS-PAGE analysis were eluted by the addition of 2X Laemmli dye with BME and boiling. Reactions were visualized on a BioRad 4–20% pre-cast SDS-PAGE stain-free gel using the BioRad ChemiDoc stain-free protocol or fluorescently using the Typhoon 9500 by Thermo. For 384-well plate analysis, proteins were treated as above, then eluted with 40 µL 20 mM Tris pH7.5, 150 mM NaCl, 2 mM TCEP-HCl, and 1 M Imidazole. 15 µL of each fraction were loaded onto a 384-well clear-bottom microtiter plate and visualized on the Typhoon 9500. Samples from these fractions were also analyzed for metal content by ICP-MS.

Sod1, Ccs1, and Cu(I)-Ctr1c-Ccs1 affinity determination

H46R/H48Q/C146S Sod1 was fluorescently labeled with Alexa-546-C-maleimide and the reaction was quenched with DTT. Excess unbound dye was removed by gel filtration using a GE Sepharose S200 increase gel filtration column. Final Sod1-probe concentration in all assays was 10 nM. Ccs1 was titrated into reactions in increasing concentrations. We followed the HI-FI

method to determine dissociation constants (KD) as outlined in previous publications (Winkler et al. 2012). Fluorescence quenching was visualized and KD and binding curves were determined with the GraphPad Prism software suite.

Results

Ctr1c stably binds Ccs through a Cu(I) intermediate

To focus upon the intracellular copper transfer between Ctr1 and Ccs, we utilized the cytosolic copper delivery domain of Ctr1 (Ctr1c) (Kahra et al. 2016). Ctr1c is a short 13 amino acid peptide that is difficult to visualize/quantitate biochemically, so a fluorescent label (Alexa 488) was conjugated to the N-terminus. Labeled peptide (Ctr1c488) was purified and then visualized on Native-PAGE to confirm that non-native oligomerization did not occur (**Fig. S2.1**). Fluoro-labeling did not affect copper binding, as both labeled and unlabeled Ctr1c peptides bound Cu(I) equivalently as determined by ICP-MS analysis (**Table 2.1**).

Table 2.1. ICP-MS results shown as the percentage of copper- bound protein

ICP-MS results		Protein:Cu(I) ratio
Ctr1c	22.6% ± 1.4	3–4:1
$Ctr1c_{488}$	23.9% ± 1.7	3–4:1
WT Ccs	87.4% ± 2.6	1:1
MXAXXA	85.2% ± 0.4	1:1
AXA	82.0% ± 1.2	1:1

The percentage of Cu(I) bound to Ctr1c indicates that multiple Ctr1c peptides bind a single copper at their HCH motifs, likely in a 3:1–4:1 stoichiometry (**Fig. 2.1a**). We suggest that the 3:1 ratio is more likely as Cu(I) prefers to bind 2 or 3 ligands. Trimeric binding of Ctr1c to copper also occurs in full- length Ctr1. To determine if Ctr1c and Ccs would stably interact, both apo and Cu(I)-loaded Ctr1c488 were incubated with Ccs and visualized fluorescently on Native-

PAGE. Apo-Ctr1c488 did not bind to Ccs, but Cu(I)-Ctr1c488 formed a stable complex that ran as a clear band on the gel (**Fig. 2.1b, Lanes 1 and 2**). However, Ctr1c could not form a similar interaction with Ccs' target (metal-free, disulfide reduced Sod1 (E,E-Sod1^{SH})). Incubation of Cu(I)-Ctr1c488 with E,E- Sod1^{SH} did not result in stable complex formation (**Fig. 2.1b, Lane 3**). Furthermore, the Sod1 from this reaction was subsequently analyzed for metal content by ICP-MS, and no direct copper transfer occurred between Ctr1c and Sod1.

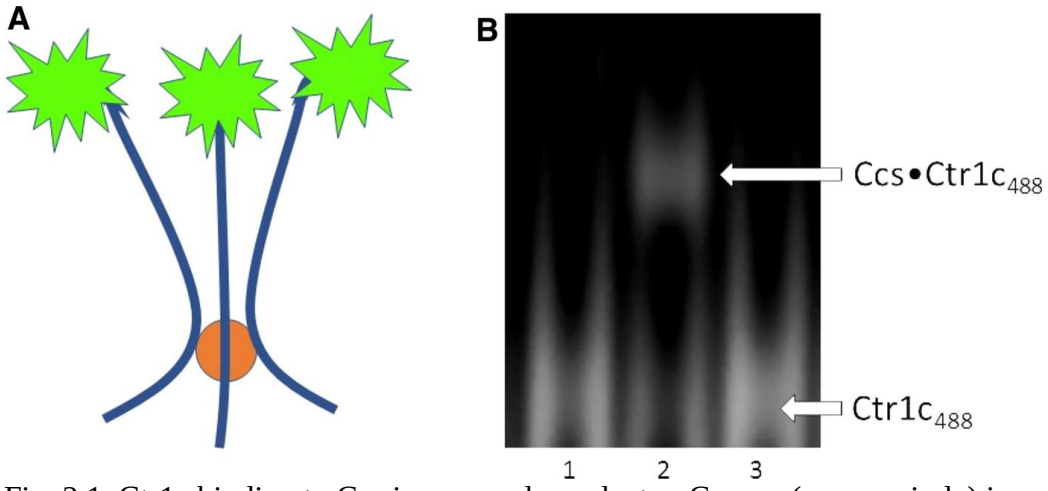

Fig. 2.1. Ctr1c binding to Ccs is copper dependent. **a** Copper (orange circle) is coordinated by three Ctr1c488 peptides at their C-terminal HCH motifs. The Alexa 488 dye is conjugated to the N-terminus using a succinimidyl ester linkage. ICP-MS determined that Ctr1c488 bound Cu(I) in a 3:1 stoichiometry, similar to full-length Ctr1. **b** Native PAGE gel imaged fluorescently for Alexa 488. Lane 1: Ctr1c488 + Ccs. Lane 2: Cu(I) - Ctr1c488 + Ccs. Lane 3: Cu(I) - Ctr1c488 + E,E-Sod1^{SH}. (Color figure online)

Stable Ctr1c·Ccs interaction can form at either copper binding motif of Ccs

We use a high-throughput experimental setup that takes advantage of clear-bottom microplates for fluorescent-based visualization and quantification of pull-down results (detailed in the ''Materials and Methods'' section). **Figure 2.2a** shows an example of the pull-down assays performed to examine the role of the copper binding motifs in Ccs in coordinating Ctr1c. His-

tagged wild-type Ccs or Ccs variants with Cu(I)-Ctr1c488 (top row) were assayed and then normalized against a copper-null variant of Ccs that was also incubated with Cu(I)-Ctr1c488 (bottom row). Three experimental replicates were performed and quantified to determine relative binding propensity (**Fig. 2.2b**). There does not appear to be a strong preference for either copper binding site in Ccs (D1–MxCxxC or D3–CxC). The copper-mediated interaction between Ctr1c and Ccs occurs as long as copper is bound by at least one of these sites. Similar Cu(I) content was observed in all three samples by ICP-MS (**Table 2.1**). Incubating with 15 μM Cu(I) Ctr1c488 consistently resulted in the recovery of > 4 μM copper-bound Ccs, supporting the binding of copper by peptide in a 3:1 ratio. If the peptide to copper ratio was 4:1 the maximum amount of copper transferred to Ccs would be 3.75 μM. In vitro Sod1 activation assays performed using the Cu(I)-Ctr1c488·Ccs containing samples showed that the complexes are functional and although Cu(I)-Ctr1c488 will coordinate with both copper-binding motifs in Ccs, only the CxC motif in Ccs D3 is critical for full activation of immature Sod1 under these conditions (**Fig. 2.2c**).

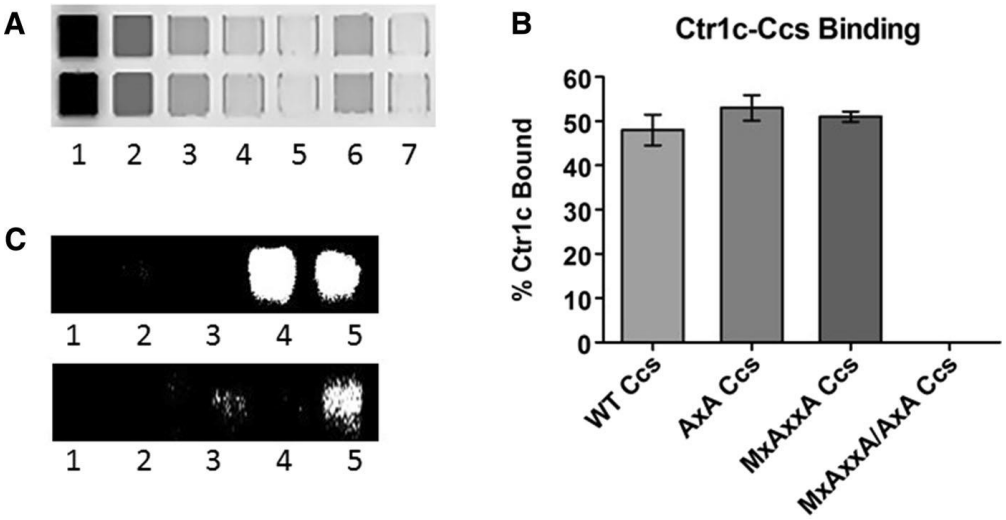

Fig. 2.2. Ctr1c can bind both copper binding domains of Ccs. **a** Nickel pulldown assays were loaded into a clear-bottom 384-well plate and visualized fluorescently using the Typhoon 9500. Lane 1: Input, Lane 2: Flow-through, Lanes 3-5: Washes, Lane 6: Elution, Lane 7: Buffer blank. **b** This graph of fluorescence intensity is normalized to mutant Ccs lacking copper binding motifs. (**c, Top**) Lane 1: Sod1 stripped of metals, Lane 2: Sod1 with Cu(I) - Ctr1c, Lane 3: Sod1 with apo-

MxAxxA Ccs, Lane 4: Sod1 with apo-MxAxxA Ccs and Cu(I)- Ctr1c, Lane 5: Sod1 with Cu(1)-WT Ccs. (**C, Bottom**) Lane 1: Sod1 stripped of metals, Lane 2: Sod1 with Cu(I)-Ctr1c, Lane 3: Sod1 with apo-AxA Ccs, Lane 4: Sod1 with apo-AxA Ccs and Cu(I)-Ctr1c, Lane 5: Sod1 with Cu(1)-WT Ccs.

Copper-loaded Ctr1c associates stably with a Ccs·Sod1 complex

To characterize possible Ctr1c·Ccs interactions with Sod1, similar pull-down assays utilizing a His-tagged Ccs in complex with Cu(I)-Ctr1c$_{488}$ were conducted (**Fig. 2.3**). Immediate copper transfer and dissociation does not occur and a stable Cu(I)-Ctr1c$_{488}$·Ccs complex is formed, as previously demonstrated (**Fig. 2.1**). The Sod1 molecule used in this assay is an engineered immature form of Sod1 that cannot bind copper at the active site or form its intra-subunit disulfide bond (X,Zn-Sod1X), which is commonly used to form ‘‘stalled’’ Ccs·Sod1 complexes (Lamb et al. 2000, 2001; Winkler et al. 2009). Direct interaction between Cu(I)-Ctr1c$_{488}$ and X,Zn-Sod1X is not detected under any conditions tested (**Figs. 2.1b, 2.2c**). In addition, we show that a stable Cu(I)-Ctr1c$_{488}$ Ccs complex can recognize and bind to X,Zn-Sod1X in a similar manner to that of Ccs alone (**Fig. 2.4b**). Strikingly, Cu(I)-Ctr1c$_{488}$ also interacts stably with a pre- formed Ccs·X,Zn-Sod1X heterodimeric complex (**Fig. 2.3, lane 12**). The Ctr1c molecule does not dissociate upon Ccs binding to Sod1 and forms a Cu(I)-Ctr1c$_{488}$·Ccs·X,Zn-Sod1X heterotrimeric complex, supporting multiple delivery options arising from the Ctr1 transporter.

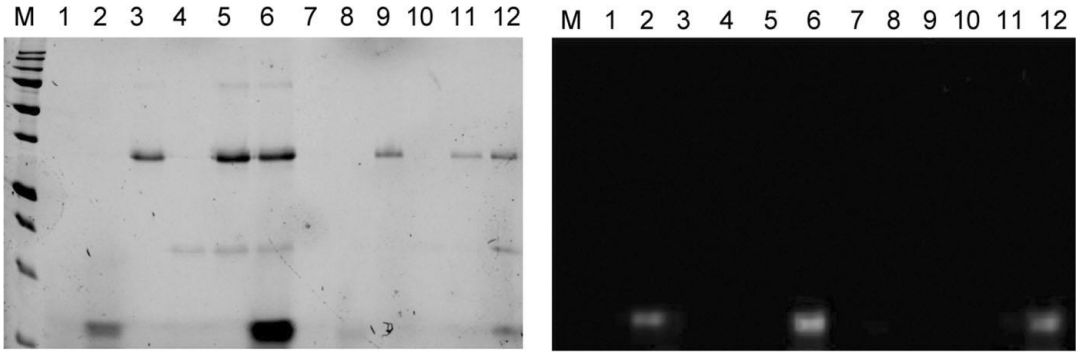

Fig. 2.3. Immature Sod1 can form a stable Sod1•Ccs•Ctr1c heterotrimeric complex. Lane 1: beads supernatant, Lane 2: Cu(I)-Ctr1c$_{488}$ supernatant, Lane 3: His8-Ccs supernatant, Lane 4: Sod1 supernatant, Lane 5: His8-Ccs•Sod1 supernatant, Lane 6: His8-Ccs•Sod1 and Cu(I)-Ctr1c$_{488}$ supernatant, Lane 7: beads elution, Lane 8: Cu(I)-Ctr1c$_{488}$ elution, Lane 9: His8-Ccs elution, Lane 10: Sod1 elution, Lane 11: His8-Ccs•Sod1 elution, Lane 12: His8-Ccs•Sod1 and Cu(I)-Ctr1c$_{488}$ elution. The right image is the same gel as the left (stain-free) but visualized fluorescently.

Ccs association with Ctr1c does NOT affect its affinity for Sod1

The assumed order of operation for Sod1 activation starts with the metalation of Ccs, which then finds/ binds an immature Sod1 molecule to activate (see reviews Culotta, Lin et al. 1999; Rosenzweig 2001; Furukawa and O'Halloran 2006; Leitch et al. 2009; Robinson and Winge 2010;Fetherolf et al. 2017a, b). Much like the yeast Ccs·Sod1 interaction (Boyd et al. 2018), human Ccs favors binding to completely immature Sod1 (E,E-Sod1^{SH}) (**Fig. 2.4a**).

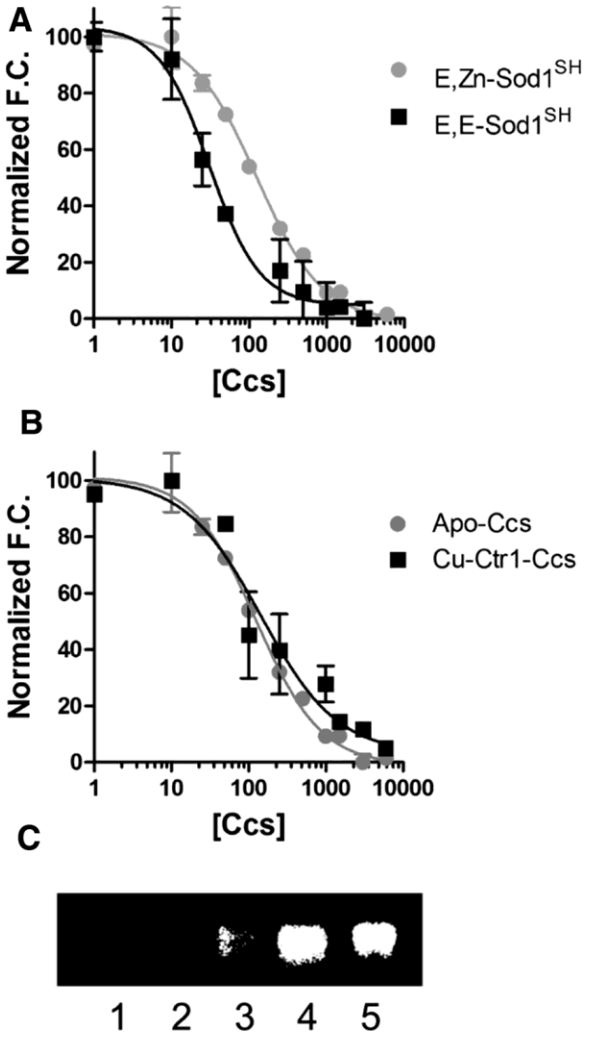

Fig. 2.4. Cu(I)-Ctr1c binding to Ccs does not affect its Sod1 binding affinity. The concentration of Ccs1 is nanomolar. The curves have been normalized for comparison for panels **a** and **b**. **a** apo-Ccs binding to completely immature Sod1 (89 nM ± 11) and Zn-bound Sod1 (22 nM ± 6). **b** Comparison of binding affinities for apo-Ccs (89 nM ± 11) and Cu(I)-Ctr1c complexed Ccs to Sod1 (120 nM ± 27). c Sod1 activity assay. Lane 1: Sod1 stripped of metals, Lane 2: Sod1 with Cu(I)-Ctr1c, Lane 3: Sod1 with apo-Ccs, Lane 4: Sod1 with Cu(I)-Ctr1c complexed Ccs, Lane 5: Sod1 with Cu(I)-Wt Ccs.

The copper occupancy of Ccs has a negligible role in Sod1 binding affinity, as the copper-loaded form of Ccs binds to E,E-Sod1^{SH} in a nearly indistinguishable fashion. Additionally, a pre-made Cu(I)-Ctr1c Ccs complex binds E,E-Sod1^{SH} with a similar affinity to both apo and copper-

bound Ccs (**Fig. 2.4b**). Again, we also wanted to ensure that the Cu(I)-Ctr1c·Ccs complex assembled is functional and can fully activate immature Sod1. *In vitro* Sod1 activation assays reveal that Cu(I)-Ctr1c cannot directly activate Sod1, alone, but requires the Cu(I)-Ctr1c·Ccs complex (**Fig. 2.4c, Lanes 4 and 2**, respectively). Control gels of the reactions were visualized by multiple approaches to confirm equal loading (**Fig. S2.2**). Our results continue to support the idea that an entire copper-trafficking pathway can, but is not necessitated to occur within a single complex, yet the question arises as to what finally triggers eventual dissociation.

Complete Sod1 activation terminates the Sod1·Ccs·Ctr1c association

To study dissociation of the Cu(I)-Ctr1c·Ccs·Sod1 complex, we performed pulldowns now using immature Sod1 (E,Zn-Sod1^{SH}) (**Fig. 2.5a**). When E,Zn- Sod1^{SH} was added to a pre-formed Cu(I)-Ctr1c488·Ccs complex, immediate and complete dissociation of the complex resulted (**Fig. 2.5a, Lane 14**). Activation assays were performed on samples obtained from the pull- downs and the E,Zn-Sod1^{SH} that had been allowed to interact with Cu(I)-Ctr1c Ccs complex was analyzed and had activity comparable to that of E,Zn-Sod1^{SH} incubated with Cu(I)-Ccs, alone (i.e. the Sod1 is now fully mature (Cu,Zn-Sod1^{SS})). E,Zn-Sod1^{SH} incubated with Cu(I)-Ctr1c alone did not have activity, nor did the immaturely-trapped X,Zn-Sod1X mutant that was complexed with Cu(I)-Ctr1c·Ccs (**Fig. 5b**). This clearly indicates that the Cu(I)-Ccs·Ctr1c complex can activate immature Sod1 in a way that Cu(I)- Ctr1c cannot accomplish (**Fig. 4c, Lanes 4 and 2, respectively**). Only complete Sod1 activation triggers dissociation of the stable Cu(I)-Ctr1c·Ccs·Sod1 complex, suggesting that the portion of Sod1 activated through this direct Ctr1-to-Ccs-to-Sod1 pathway occurs while tethered to the cell membrane via the complete Ctr1 Cu-transporter.

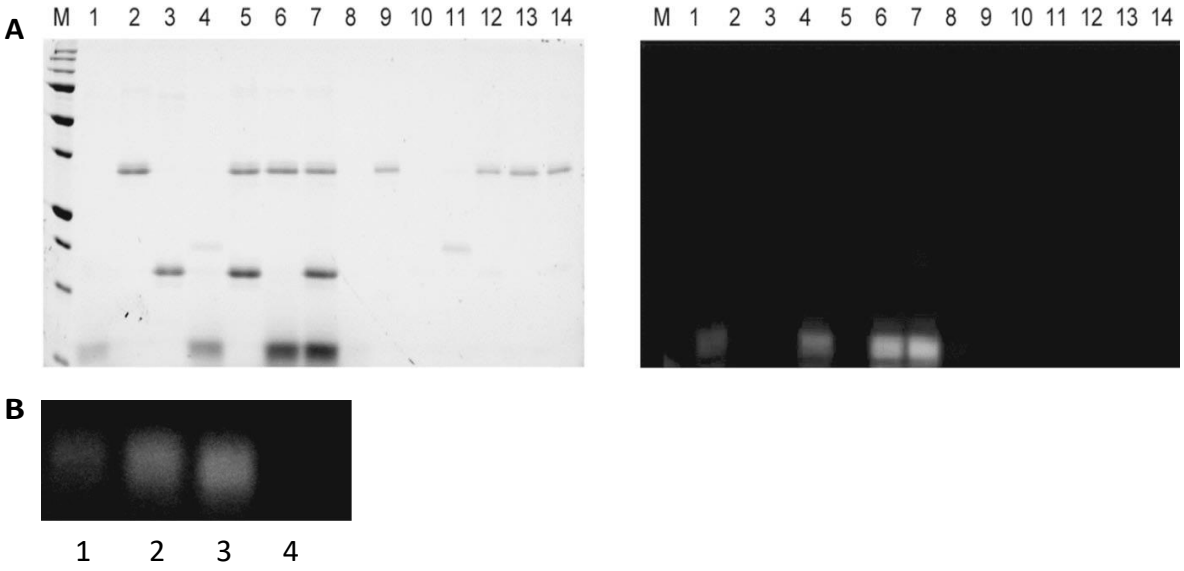

Fig. 2.5. **a** Sod1 maturation disassociates the Sod1•Ccs•Cu(I)-Ctr1c complex. Lane 1: Cu(I)-Ctr1c$_{488}$ supernatant, Lane 2:His8-Ccs supernatant, Lane 3: Sod1 supernatant, Lane 4: His8-Sod1 with Cu(I)-Ctr1c$_{488}$ supernatant, Lane 5: His8-Ccs•Sod1 supernatant, Lane 6: His8-Ccs with Cu(I)-Ctr1c$_{488}$ supernatant, Lane 7: His8-Ccs•Sod1 with Cu(I)-Ctr1c$_{488}$ supernatant, Lane 8: Cu(I)-Ctr1c$_{488}$ elution, Lane 9: His8-Ccs elution, Lane 10: Sod1 elution, Lane 11: His8-Sod1 with Cu(I)-Ctr1c$_{488}$ elution, Lane 12: His8-Ccs•Sod1 elution, Lane 13: His8-Ccs with Cu(I)-Ctr1c$_{488}$ elution, Lane 14: His8-Ccs•Sod1 with Cu(I)-Ctr1c$_{488}$ elution. The right image is the same gel as the left (stain free), but visualized fluorescently. **b** Lane 1: Cu(I)-loaded Ctr1c488 + WT Sod1 from a, Lane 4. Lane 2: Cu(I)-loaded WT His8-Ccs + WT Sod1 set up separately as a positive control. Lane 3: WT His8-Ccs + WT Sod1 + Cu(I)-Ctr1c$_{488}$ from a, Lane 7. Lane 4: WT His8-Ccs + immature Sod1 + Cu(I)-Ctr1c$_{488}$ from Fig. 3, Lane 12

Discussion

Up until now, a considerable amount of work has been completed on the Ccs-mediated Sod1 activation process (reviewed in Seetharaman et al. 2009), yet details of copper transfer to Ccs were still unclear. Our data shows that the intracellular C-terminal tail of the influx transporter Ctr1 (Ctr1c) forms a stable copper-mediated interaction with Ccs, as complete copper transfer does not immediately follow first contact. The introduction of an engineered Sod1 variant that cannot bind copper or form its conserved intra-subunit disulfide bond (X, Zn-Sod1X) generates a heterotrimeric Cu(I)-Ctr1c·Ccs·Sod1 complex. Only complete Sod1 activation severs the ties

between transporter, chaperone, and target. Together, the results presented above provide clear evidence for a complete copper delivery pathway held within a singular 3-part complex.

The Unger laboratory was the first to show that yeast Ccs1 interacts directly with Ctr1 (Pope et al. 2013). Their work highlighted that yCcs1 can engage with lipid bilayers and suggested that recruitment to the plasma membrane is an essential step in Ccs-mediated Sod1 activation (Pope et al. 2013). The authors of that study submit mechanistic ambiguities in the proposed process and how further investigation would be needed to ‘‘unravel’’ these details. In the present study, we have taken a much narrower focus upon the intracellular C-terminal domain of Ctr1 (Ctr1c). This domain is known to be important for the coordination and eventual distribution of copper to trafficking molecules within the cytosol (Xiao and Wedd 2002; Kahra et al. 2016). We show that this domain alone is enough to interact with Ccs or a Ccs·Sod1 complex, and the interactions are entirely copper dependent (**Figs. 2.1, 2.4**), much like for the complete Ctr1 transporter (Pope et al. 2013). Similar results have been demonstrated for Ctr1c and the copper chaperone Atx1 (Xiao and Wedd 2002), which shares similarity with D1 of Ccs.

Numerous groups, including our own, have previously shown that Ccs recognizes and binds immature forms of Sod1 (Banci et al. 2012; Wright et al. 2016; Fetherolf et al. 2017a, b; Luchinat et al. 2017; Boyd et al. 2018). The Sod1-like D2 of Ccs directs this interaction with D3 contributing to high-affinity binding and full activation (Boyd et al. 2018). More recently, we have demonstrated that copper binding by Ccs does not significantly affect the Sod1 interaction (Boyd et al. 2018). The question then arose as to whether the Cu(I)-Ctr1c·Ccs interaction alters Ccs recognition and binding to Sod1. Upon examination, Ccs can recognize and bind immature Sod1 while still coordinating copper with Ctr1c. In fact, a stable high-affinity Cu(I)-Ctr1c·Ccs·Sod1

complex is observed (**Figs. 2.2, 2.3, 2.4**). The next logical steps were to test if this heterotrimeric complex results in activation of Sod1. Ccs-mediated Sod1 activation is an intricate process involving fold-induced zinc binding by Sod1 that is followed by disulfide bond driven copper delivery (Culotta et al. 1997, 2006). Multiple lines of evidence suggest that cellular conditions may necessitate the role(s) for Ccs and that ancillary molecules like reduced glutathione (GSH) may facilitate the activation process (Maryon et al. 2013). In fact, GSH has been shown to promote an entirely Ccs-independent Sod1 activation pathway in mammals (Leitch et al. 2009). The Cu(I)-Ctr1c construct will not donate Cu(I) to Sod1 directly, but a preformed Cu(I)- Ctr1c·Ccs complex can fully activate immature Sod1 in vitro (**Fig. 2.5b**). This excludes a Ccs-independent mechanism of Sod1 activation catalyzed directly by Ctr1c.

It is quite intriguing that the Cu(I)-Ctr1c·Ccs·Sod1 complex is not transiently associated. This suggests that a simple Cu(I) hand-off between Ctr1c and Ccs is not occurring; so, what induces eventual dissociation? The Ccs·Sod1 interaction, without Ctr1c, has also been shown to be remarkably stable as long as copper cannot be delivered to the Sod1 active site (Fetherolf et al. 2017a, b). This can be ensured in two ways: (1) copper is not provided to the complex or (2) the active site is modified so that the bound copper cannot be delivered to that site (Fetherolf et al. 2017a, b). We have previously shown that Ccs delivers copper to an ‘‘entry-site’’ near the Sod1·Ccs interface (Fetherolf et al. 2017a, b). Oxygen dependent disulfide bond formation eliminates this site, promotes copper shuttling to the nearby active site, and terminates interaction with Ccs (Fetherolf et al. 2017a, b). Copper must be present to form the Cu(I)-Ctr1c·Ccs·Sod1 heterotrimer, but the Sod1 active site must be ablated or the complex readily activates Sod1 and the complex promptly dissolves. This likely indicates that Ctr1c is co-coordinating the copper ion

up until disulfide bond formation in Sod1 disperses the complex producing Cu,Zn-Sod1SS that can now homodimerize along with copper-free forms of both Ccs and Ctr1c that no longer have any affinity for each other (**Fig. 2.6**).

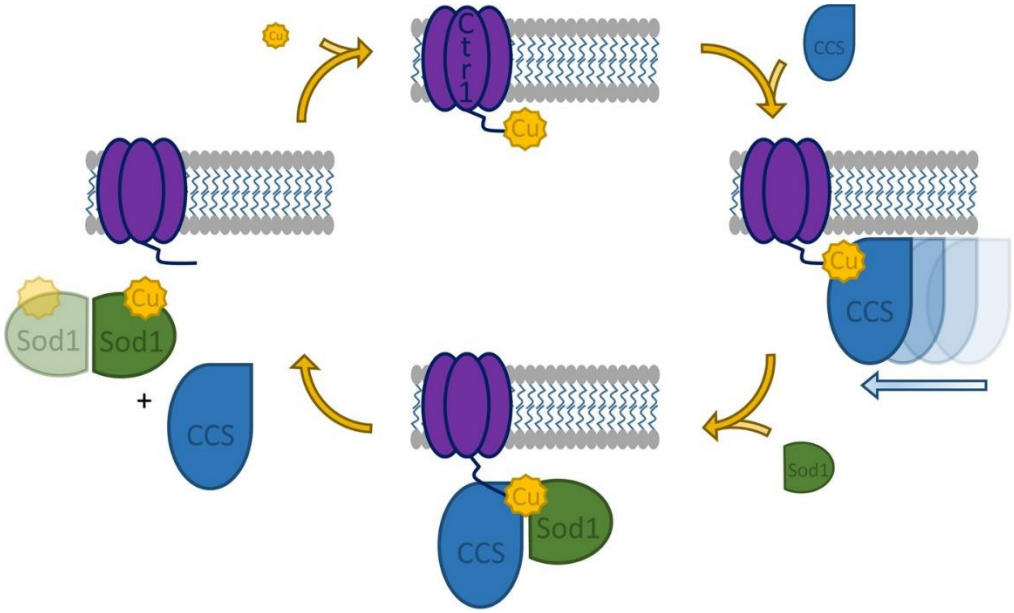

Fig. 2.6. Model of Ccs copper acquisition from Ctr1 and complex disassembly by Sod1 maturation. Ctr1 (purple) transports copper (yellow) into the cytosol. Ccs (blue) scans the membrane and associates with the copper-bound Ctr1 C-terminal domain. Sod1 (green) interacts with the Cu(I)-Ctr1-Ccs complex. Sod1 maturation terminates the ternary complex. Ccs is allowed to cycle through the copper-acquisition process again. The Sod1 homodimer is fully active. (Color figure online)

Noteworthy is that Pope et al. showed that yeast Ccs1 strongly associates with lipid bilayers, but that the yCcs1·ySod1 heterodimer reduced this propensity most likely due to a critical positively charged patch on yCcs1 that is not present on ySod1 (Pope et al. 2013). This observation may explain how Ccs first comes into contact with Cu(I)-Ctr1, and how the products of this reaction (e.g. activated Sod1 and apo- Ccs) are provided release from the membrane to freely access other cellular locations. Together, this present study establishes an all-inclusive design for

Ctr1-to-Ccs-to-Sod1 copper delivery and provides new evidence for a singular heterotrimeric complex forming the foundation for the pathway.

Acknowledgements: This research was supported in part by R01 GM120252 from the National Institutes of Health awarded to D.D.W. The content is solely the responsibility of the authors and does not necessarily represent the official views of the National Institutes of Health.

Compliance with ethical standards

Conflicts of interest: The authors declare that they have no conflicts of interest with the contents of this article.

References

Banci L, Bertini I, Cantini F, Kozyreva T, Massagni C, Palumaa P, Rubino JT, Zovo K (2012) Human superoxide dismutase 1 (hSOD1) maturation through interaction with human copper chaperone for SOD1 (hCCS). Proc Natl Acad Sci USA 109:13555–13560

Banci L, Cantini F et al (2013) Mechanistic aspects of hSOD1 maturation from the solution structure of Cu(I)-loaded hCCS domain 1 and analysis of disulfide-free hSOD1 mutants. ChemBioChem 14(14):1839–1844

Boyd SD, Liu L et al (2018) Quantifying the interaction between copper-zinc superoxide dismutase (Sod1) and its copper chaperone (Ccs1). J Proteom Bioinform 11(4):473

Bremner I (1998) Manifestations of copper excess. Am J Clin Nutr 67(5 Suppl):1069S–1073S

Culotta VC, Klomp LW et al (1997) The copper chaperone for superoxide dismutase. J Biol Chem 272(38):23469–23472 Culotta VC, Lin SJ et al (1999) Intracellular pathways of copper trafficking in yeast and humans. Adv Exp Med Biol

448:247–254

Culotta VC, Yang M et al (2006) Activation of superoxide dismutases: putting the metal to the pedal. Biochim Bio- phys Acta 1763(7):747–758

Dancis A, Haile D et al (1994) The Saccharomyces cerevisiae copper transport protein (Ctr1p). Biochemical characteri- zation, regulation by copper, and physiologic role in copper uptake. J Biol Chem 269(41):25660–25667

De Feo CJ, Aller SG et al (2009) Three-dimensional structure of the human copper transporter hCTR1. Proc Natl Acad Sci USA 106(11):4237–4242

Eisses JF, Kaplan JH (2002) Molecular characterization of hCTR1, the human copper uptake protein. J Biol Chem 277(32):29162–29171

Fetherolf MM, Boyd SD et al (2017a) Copper-zinc superoxide dismutase is activated through a sulfenic acid intermediate at a copper ion entry site. J Biol Chem 292(29):12025–12040

Fetherolf MM, Boyd SD et al (2017b) Oxygen-dependent acti- vation of Cu, Zn-superoxide dismutase-1. Metallomics 9(8):1047–1059

Flores AG, Unger VM (2013) Atox1 contains positive residues that mediate membrane association and aid subsequent copper loading. J Membr Biol 246(12):903–913

Furukawa Y, O'Halloran TV (2006) Posttranslational modifi- cations in Cu, Zn-superoxide dismutase and mutations associated with amyotrophic lateral sclerosis. Antioxid Redox Signal 8(5–6):847–867

Halliwell B, Gutteridge JM (1990) Role of free radicals and catalytic metal ions in human disease: an overview. Methods Enzymol 186:1–85

Hussain F, Olson JS et al (2008) Conserved residues modulate copper release in human copper chaperone Atox1. Proc Natl Acad Sci USA 105(32):11158–11163

Hussain F, Rodriguez-Granillo A et al (2009) Lysine-60 in copper chaperone Atox1 plays an essential role in adduct formation with a target Wilson disease domain. J Am Chem Soc 131(45):16371–16373

Kahra D, Kovermann M et al (2016) The C-terminus of human copper importer Ctr1 acts as a binding site and transfers copper to Atox1. Biophys J 110(1):95–102

Kaplan JH, Maryon EB (2016) How mammalian cells acquire copper: an essential but potentially toxic metal. Biophys J 110(1):7–13

Kim BE, Nevitt T et al (2008) Mechanisms for copper acqui- sition, distribution and regulation. Nat Chem Biol 4(3):176–185

Klomp AE, Juijn JA et al (2003) The N-terminus of the human copper transporter 1 (hCTR1) is localized extracellularly, and interacts with itself. Biochem J 370(Pt 3):881–889

Lamb AL, Wernimont AK et al (1999) Crystal structure of the copper chaperone for superoxide dismutase. Nat Struct Biol 6(8):724–729

Lamb AL, Torres AS et al (2000a) Heterodimer formation between superoxide dismutase and its copper chaperone. Biochemistry 39(48):14720–14727

Lamb AL, Wernimont AK et al (2000b) Crystal structure of the second domain of the human copper chaperone for super- oxide dismutase. Biochemistry 39(7):1589–1595

Lamb AL, Torres AS et al (2001) Heterodimeric structure of superoxide dismutase in complex with its metallochaper- one. Nat Struct Biol 8(9):751–755

Lee J, Pena MM et al (2002) Biochemical characterization of the human copper transporter Ctr1. J Biol Chem 277(6):4380–4387

Leitch JM, Yick PJ et al (2009) The right to choose: multiple pathways for activating copper, zinc superoxide dismutase. J Biol Chem 284(37):24679–24683

Luchinat E, Barbieri L, Banci L (2017) A molecular chaperone activity of CCS restores the maturation of SOD1 fALS mutants. Sci Rep 7:17433

Lutsenko S, Efremov RG et al (2002) Human copper-trans- porting ATPase ATP7B (the Wilson's disease protein): biochemical properties and regulation. J Bioenerg Bio- membr 34(5):351–362

Maryon EB, Molloy SA et al (2013) Cellular glutathione plays a key role in copper uptake mediated by human copper transporter 1. Am J Physiol Cell Physiol 304(8):C768– C779

O'Halloran TV, Culotta VC (2000) Metallochaperones, an intracellular shuttle service for metal ions. J Biol Chem 275(33):25057–25060

Ohrvik H, Thiele DJ (2014) How copper traverses cellular membranes through the mammalian copper transporter 1, Ctr1. Ann NY Acad Sci 1314:32–41

Pena MM, Lee J et al (1999) A delicate balance: homeostatic control of copper uptake and distribution. J Nutr 129(7):1251–1260

Pickering IJ, George GN, Dameron CT, Kurz B, Winge DR, Dance IG (1993) X-ray absorption spectroscopy of cuprous-thiolate clusters in proteins and model systems. J Am Chem Soc 115:9498–9505

Pope CR, De Feo CJ et al (2013) Cellular distribution of copper to superoxide dismutase involves scaffolding by mem- branes. Proc Natl Acad Sci USA 110(51):20491–20496

Puig S, Lee J et al (2002) Biochemical and genetic analyses of yeast and human high affinity copper transporters suggest a conserved mechanism for copper uptake. J Biol Chem 277(29):26021–26030

Robinson NJ, Winge DR (2010) Copper metallochaperones.

Annu Rev Biochem 79:537–562

Rodriguez-Granillo A, Wittung-Stafshede P (2008) Structure and dynamics of Cu(I) binding in copper chaperones Atox1 and CopZ: a computer simulation study. J Phys Chem B 112(15):4583–4593

Rodriguez-Granillo A, Wittung-Stafshede P (2009) Differential roles of Met10, Thr11, and Lys60 in structural dynamics of human copper chaperone Atox1. Biochemistry 48(5):960–972

Rodriguez-Granillo A, Crespo A et al (2010) Copper-transfer mechanism from the human chaperone Atox1 to a metal- binding domain of Wilson disease protein. J Phys Chem B 114(10):3698–3706

Rosenzweig AC (2001) Copper delivery by metallochaperone proteins. Acc Chem Res 34(2):119–128

Rosenzweig AC, O'Halloran TV (2000) Structure and chem- istry of the copper chaperone proteins. Curr Opin Chem Biol 4(2):140–147 Sala FA, Antonyuk SV, Garratt RC, Hasnain SS (2019) Molecular recognition and maturation of SOD1 by its evolutionarily destabilised cognate chaperone hCCS. PLoS Biol 17(2):e3000141

Schmidt PJ, Rae TD et al (1999) Multiple protein domains contribute to the action of the copper chaperone for superoxide dismutase. J Biol Chem 274(34):23719–23725

Schmidt PJ, Kunst C et al (2000) Copper activation of super- oxide dismutase 1 (SOD1) in vivo. Role for protein-protein interactions with the copper chaperone for SOD1. J Biol Chem 275(43):33771–33776

Seetharaman SV, Prudencio M et al (2009) Immature copper- zinc superoxide dismutase and familial amyotrophic lateral sclerosis. Exp Biol Med (Maywood) 234(10):1140–1154

Voskoboinik I, Camakaris J (2002) Menkes copper-translocat- ing P-type ATPase (ATP7A): biochemical and cell biology properties, and role in Menkes disease. J Bioenerg Bio- membr 34(5):363–371

Winkler DD, Schuermann JP et al (2009) Structural and bio- physical properties of the pathogenic SOD1 variant H46R/ H48Q. Biochemistry 48(15):3436–3447

Winkler DD, Luger K et al (2012) Quantifying chromatin-as- sociated interactions: the HI-FI system. Methods Enzymol 512:243–274

Wong PC, Waggoner D et al (2000) Copper chaperone for superoxide dismutase is essential to activate mammalian Cu/Zn superoxide dismutase. Proc Natl Acad Sci USA 97(6):2886–2891

Wright GS, Antonyuk SV, Hasnain SS (2016) A faulty inter- action between SOD1 and hCCS in neurodegenerative disease. Sci Rep 6:27691

Xiao Z, Wedd AG (2002) A C-terminal domain of the mem- brane copper pump Ctr1 exchanges copper(I) with the copper chaperone Atx1. Chem Commun (Camb) 6:588–589

CHAPTER 3

THE YEAST COPPER CHAPERONE FOR COPPER-ZINC SUPEROXIDE DISMUTASE (CCS1) IS A MULTIFUNCTIONAL CHAPERONE PROMOTING ALL LEVELS OF SOD1 MATURATION

Stefanie D. Boyd, Jenifer S. Calvo, Li Liu, Morgan S. Ullrich, Amelie Skopp, Gabriele Meloni, and Duane D. Winkler

The Department of Biological Sciences, BSB12

The Department of Chemistry and Biochemistry, BSB13

The University of Texas at Dallas

800 West Campbell Road

Richardson, Texas 75080-3021

Abstract

Copper (Cu) is essential for the survival of aerobic organisms through its interaction with molecular oxygen (O_2). However, Cu's chemical properties also make it toxic, requiring specific cellular mechanisms for Cu uptake and handling, mediated by Cu chaperones. CCS1, the budding yeast (*S. cerevisiae*) Cu chaperone for Cu-zinc (Zn) superoxide dismutase (SOD1) activates by directly promoting both Cu delivery and disulfide formation in SOD1. The complete mechanistic details of this transaction along with recently proposed molecular chaperone-like functions for CCS1 remain undefined. Here, we present combined structural, spectroscopic, kinetic, and thermodynamic data that suggest multifunctional chaperoning role(s) for CCS1 during SOD1 activation. We observed that CCS1 preferentially binds a completely immature form of SOD1 and that the SOD1•CCS1 interaction promotes high-affinity Zn(II)-binding in SOD1. Conserved aromatic residues within the CCS1 C-terminal domain are integral in these processes. Previously, we have shown that CCS1 delivers Cu(I) to an entry site at the SOD1•CCS1 interface upon binding. We show here that Cu(I) is transferred from CCS1 to the entry site and then to the SOD1 active site by a thermodynamically driven affinity gradient. We also noted that efficient transfer from the entry site to active site is entirely dependent upon the oxidation of the conserved intra-subunit disulfide bond in SOD1. Our results herein provide a solid foundation for proposing a complete molecular mechanism for CCS1 activity and reclassification as a first-of-its- kind "dual chaperone.

Introduction

Cu is required for the activation of dioxygen, a function essential for the survival of aerobic organisms (1). Oddly enough, the electronic structure of Cu that permits its direct interaction with

oxygen also renders it toxic. Cells therefore possess systems to handle the uptake and distribution of Cu to prevent its toxic accumulation, while simultaneously ensuring adequate amounts are available in vivo (2). The discovery of trafficking proteins termed "metallo-chaperones" significantly expanded knowledge of these cellular control systems. Cu-chaperones acquire Cu from a membrane transporter, protect it from cytosolic scavenging molecules, and prevent deleterious redox reactions during delivery to various target proteins via specific protein-protein interactions [reviewed in (3-8)].

One prominent Cu-chaperone target protein is Cu-Zn superoxide dismutase (SOD1), an abundant homodimeric antioxidant enzyme that detoxifies superoxide anion through redox cycling of its catalytic Cu ion [$2O^- + 2H^+ \rightarrow H_2O_2 + O_2$] (9). Newly translated SOD1 is monomeric and inactive (10-12) and conversion to the active homodimer only occurs after several posttranslational modifications [reviewed in (13)]. The Cu chaperone for SOD1 (CCS1) mediates at least two of these modifications (14) by engaging nascent SOD1, inserting a Cu ion, and directing disulfide bond formation (15,16). However, increasing evidence supports additional roles for CCS1 during the SOD1 activation process (17-19). Metallo-chaperones are target specific as CCS1 does not recognize other metallo-proteins [reviewed in (6)] while, Cu-chaperones apart from CCS1 cannot activate SOD1 (14,20).

CCS1 proteins are comprised of three domains (D1, D2, and D3), each of which are key for SOD1 activation (20). The N-terminal domain (D1, residues 1-70 in yeast) is required for SOD1 activation under Cu-limiting growth conditions, suggesting its role may be to acquire Cu from the membrane transporter Ctr1 (2,20). D1 contains the metal-binding MxCxxC motif (where x is any amino acid) and a fold similar to the yeast Atx1 and human Atox1 Cu-chaperones that

escort Cu from the plasma membrane to the secretory pathway (21-23). The second domain (D2, residues 78-216) possesses sequence and structural homology with SOD1 (21) suggesting it recognizes SOD1 by mimicking SOD1•SOD1 homodimeric interactions. Supporting this notion, structures of yeast CCS1 alone (21) and in complex with yeast SOD1 (24,25) reveal D2- mediated interactions with SOD1. Mutations compromising the CCS1 D2 interface abrogate CCS1-mediated SOD1 activation (26). The C-terminal domain (D3, residues 217-249) contains an invariant CxC motif previously shown essential for complete SOD1 activation (14,20). Yeast CCS1 proteins completely lacking the D3 CxC motif fail to activate nascent SOD1 nor induce oxidation of the SOD1 disulfide bond (20,27).

Our recently published SOD1•CCS1 heterocomplex structure reveals a previously unobserved β-hairpin conformation of D3 that is stabilized by interactions with residues from SOD1, CCS1 D2, and the linker region between D1 and D2 (25). This novel conformer places the conserved CxC motif near the heterodimeric interface and creates an entry site for Cu delivery during SOD1 activation (25). Further analysis of the SOD1•CCS1 heterodimeric structure is suggestive of a possible 180° rotation of the D3 β- hairpin to transfer Cu(I) from the MxCxxC site in D1 to the SOD1•CCS1 "entry-site," as previously suggested (28). Our subsequent work showed that the D3 β-hairpin enhances the binding affinity to immature SOD1 and widens access for Cu delivery (29).

Contemporary reports from the laboratory of Lucia Banci utilize mass spectrometry and "in-cell" NMR to promote a mechanism for human CCS1, where D1 alone acquires Cu from the cell and actively delivers Cu to the SOD1 active site (30,31). Here, CCS1 D3 simply functions as a disulfide isomerase responsible for the oxidation of the SOD1 disulfide bond separately from Cu

delivery. Related work from this group points to molecular chaperone-like role(s) for CCS1 upon binding to variant forms of SOD1 (18). The mechanism of SOD1 maturation by CCS1 may not be universal as further evidenced by the conditional requirement for D1 in yeast (20), but not human (32), while other organisms have CCS1 molecules that lack the MxCxxC motif in D1 (33) or even CCS1 at all (34).

A comprehensive view of CCS1-mediated SOD1 activation is not only valuable for those investigating metallo-chaperones or Cu trafficking but is also potentially beneficial for the SOD1-linked amyotrophic lateral sclerosis (ALS) field. ALS is characterized as a protein aggregation-associated fatal neurogenerative disorder, where a fraction of cases are caused by dominant mutations in the gene expressing SOD1 (35,36). Laboratories characterizing inclusions taken from spinal cords of transgenic mice overexpressing pathogenic SOD1 mutants report the aggregates are enriched in pathogenic SOD1 proteins lacking Cu and disulfide bonds (37). The presence of immature SOD1 as the major component of these aggregates suggests that mutant forms of SOD1 may be unable to productively transact with CCS1, leaving them destabilized and aggregation prone (38). Work by our group and others supports a model where CCS1 possesses both Cu and molecular chaperoning roles that are impeded at specific points in the maturation process by pathogenic ALS mutants (17,19,25,39). However, related studies have purported that molecular chaperone-like functions of CCS1 actually work to target and stabilize disease-causing forms of SOD1 (18,40). Nevertheless, a detailed biochemical evaluation of these newly discovered molecular chaperoning functions of CCS1 is severely lacking.

Results

Conserved aromatic residues in CCS1 D3 promote binding and activation.

Our recent SOD1•CCS1 heterocomplex structure (25) reveals multiple interactions between CCS1 D3 and the disulfide loop of SOD1 (**SFig. 3.1 a,b**). The large indole side chain of W222 stacks with the side- chain of R105 from D2 and "anchors" the upstream region of the D3 β-hairpin in a groove between CCS1 D1 and SOD1. Another conserved tryptophan residue (W237) packs into a hydrophobic pocket on D2 and essentially works as a "latch" stabilizing the compact positioning of the D3 CxC motif near the SOD1•CCS1 interface. This significantly expands the SOD1•CCS1 interface beyond that of the SOD1 β-barrel and CCS1 D2 (**SFig. 3.1 c,d**). The binding affinities for CCS1 D3 variants W222A and W237A were tested and removal of either D3 tryptophan similarly hindered SOD1 (E,Zn-SOD1^{SH}) binding ~4-fold as compared to the wild-type (Wt) CCS1 protein measured previously by the same method (**Fig. 3.1a and Table 3.1**) (29). To test the ability of the same CCS1 variants to activate immature SOD1, a 5:1 ratio of Cu(I)-CCS1 to E,Zn-SOD1^{SH} was mixed at a minimum of 10-fold over the measured K_D in optimized reaction conditions (see Materials and Methods). SOD1 activated by Cu(I)-W222A CCS1 showed a decrease in activity to ~30% when compared to SOD1 with Wt Cu(I)- CCS1, while Cu(I)-W237A was completely unable to activate SOD1 (**Fig. 3.1b**). Cu occupancy of Wt and mutant forms of CCS1 were determined via Inductively coupled plasma-mass spectrometry (ICP-MS) and showed similar binding properties between Wt and the two Trp mutants (~1 Cu/monomer). Thus, the data suggests that the stability and correct positioning of the D3 β- hairpin critically effects SOD1 binding and activation by CCS1 with W237 playing a critical role.

Table 3.1. Affinity and activity of SOD1 with CCS1 variants

Construct	**K_D (nM)**	**SOD1 Activation**
Wt-yCCS1	114.0 ± 22.0	*****
yCCS1 W222A	452.7 ± 55.39	**
yCCS1 W237A	501.4 ± 104.2	No Activation
yCCS1 C16A/C20A	228.5 ± 27.74	*****
yCCS1 C229A/C231A	281.0 ± 28.95	No Activation
yCCS1 C16A/C20A/C229A/C231A	310.1 ± 19.48	No Activation
yCCS1 D3 truncation	552.0 ± 105.3	No Activation

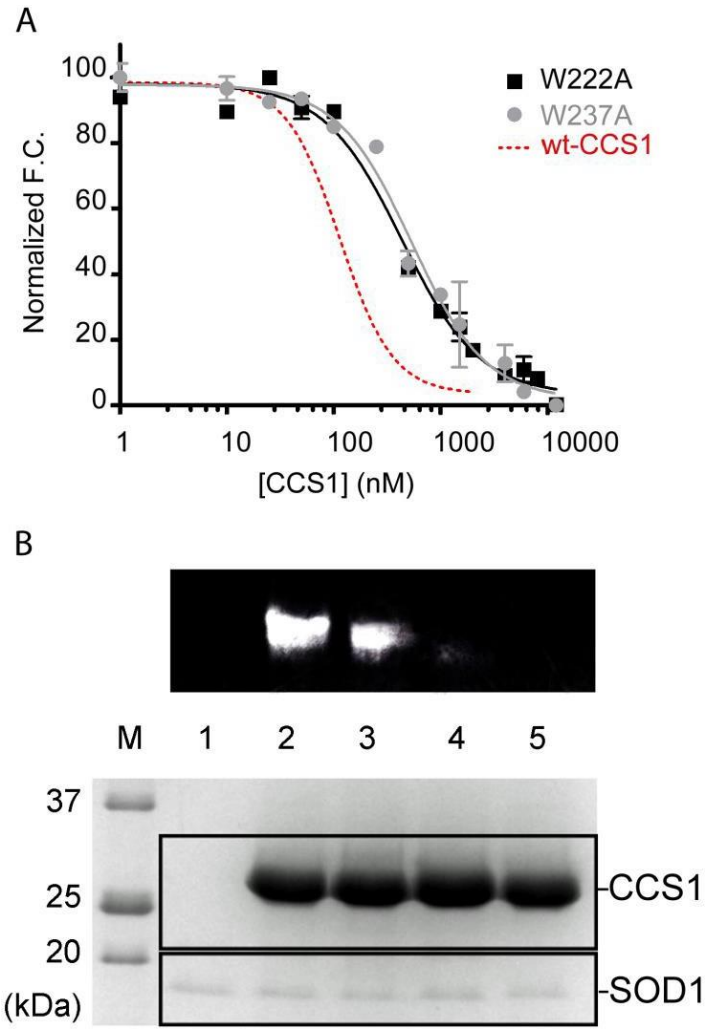

Figure 3.1. Immature SOD1 binding and activation by CCS1 D3 variants. (A) Fluorescent based binding studies for immature SOD1 (E,Zn-SOD1^{SH}) and D3 variant forms of CCS1. Both W222A and W237A mutations cause ~4-fold decrease in binding affinity compared to Wt-CCS1. Curves are normalized for comparison. (B) In vitro SOD1 activity assay. SOD1 activity is shown as white bands on the black background. Lane 1: E,Zn-SOD1^{SH}, Lane2: E,Zn-SOD1^{SH} with Cu(I)-Wt CCS1, Lane3: E,Zn- SOD1^{SH} with Cu(I)-W222A CCS1, Lane4: E,Zn-SOD1^{SH} with Cu(I)-W237A CCS1, Lane 5: H46R/H48Q/C146S SOD1 (X,Zn-SOD1X, cannot bind copper or form a disulfide bond) with Cu(I)-Wt CCS1. Below the activation gel are coomassie stained loading controls for the SOD1 and CCS1 proteins.

The CCS1 D3 CxC motif coordinates Cu(I) before delivery to SOD1.

Previous reports from numerous groups have provided conflicting results on the role of the D3 CxC motif in Cu ion coordination for delivery to SOD1 (20,28,30). Here, we take advantage of a form of CCS1 that has evolved to contain only the critically conserved D1 MxCxxC and D3 CxC cysteines (tomato CCS1) (41), as opposed to its functional homologues in yeast and human that have additional cysteines in D1 and D2 [reviewed in (4)]. Using the tCCS1 form allows for direct examination of the role for these two motifs in metal binding during SOD1 activation without further perturbation to the protein. Our motivation arises from observations that mutation of the additional cysteines (especially within the D2 β- barrel) of yCCS1 showed dramatic effects on protein folding and stability that would likely affect results in this assay. Here, we show that the wild type form of tCCS1 forms disulfide-linked homodimers under non-reducing conditions in vitro (**Fig. 3.2, top row of gels**). A D1 MxCxxC (C12A/C15A) mutant behaves similarly to the wild type. However, the D3 CxC (C204A/C206A) mutant and a mutant lacking all cysteines did not form dimers even in the presence of copper phenanthroline (CuP), which promotes disulfide bond formation. The data show that D3 CxC cysteines can form inter-subunit disulfide bonds, likely with the CxC cysteines covalently linking a pre-made D2-mediated tCCS1 homo-dimer. When tCCS1 is loaded with Cu(I), the same disulfide linkages do not form. These results strongly advocate that the D3 CxC cysteines participate in Cu(I) coordination and this form of tCCS1 can fully activate both immature tomato or yeast SOD1 (**Fig. 3.2, bottom right panel**).

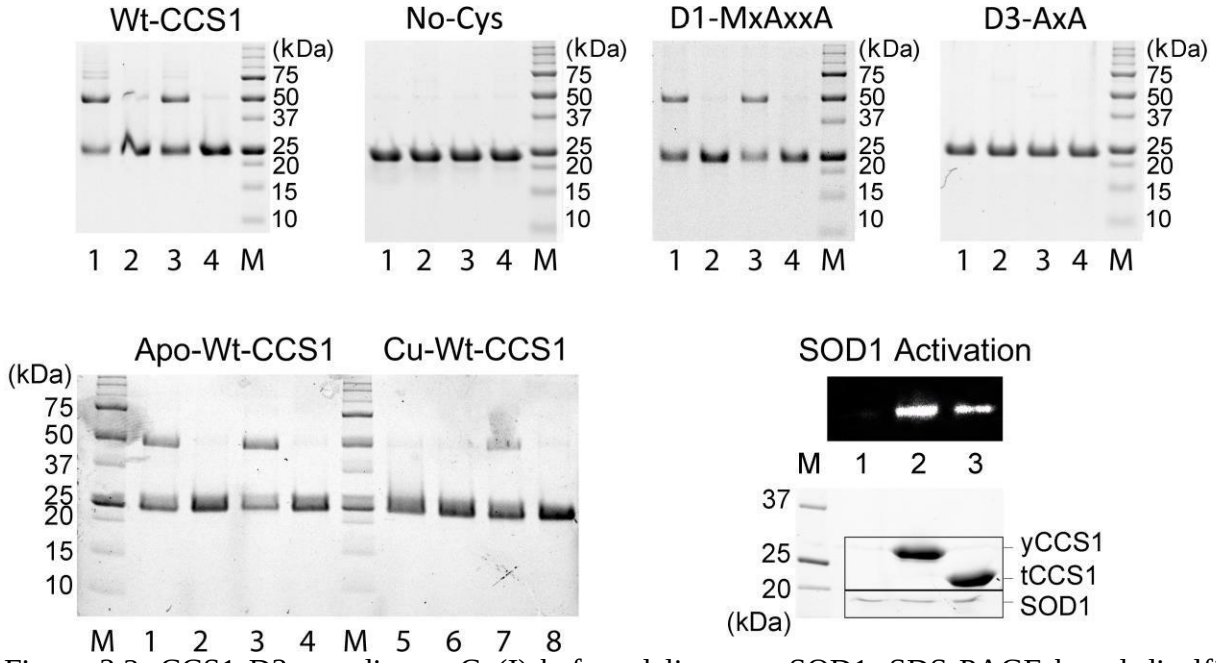

Figure 3.2. CCS1 D3 coordinates Cu(I) before delivery to SOD1. SDS-PAGE based disulfide crosslinking analysis of tCCS1. The top four gels are for the wild-type and cysteine variant forms of tCCS1 and are all setup in the same reaction order: Lane 1: Purified tCCS1 without βME, Lane 2: tCCS1 + 10 mM βME, Lane 3: tCCS1 + 25μM CuP/No βME, Lane 4: tCCS1 + 25μM CuP + 10 mM βME. tCCS1 monomer is the faster running (bottom band) and the disulfide crosslinked dimers are the top band. The bottom gel examines the consequence of Cu(I) addition to tCCS1. Lane 1: tCCS1 without βME, Lane 2: tCCS1 + 10 mM βME, Lane 3: tCCS1 + 25μM CuP/No βME, Lane 4: tCCS1 + 25μM CuP + 10 mM βME, Lane 5: Cu(I)-tCCS1 without βME, Lane 6: Cu(I)-tCCS1 + 10 mMβME, Lane 7: Cu(I)-CCS1 + 25μM CuP/No βME, Lane 8: Cu(I)-CCS1 + 25μM CuP + 10 mM βME. The SOD1 activation gel shows that Cu(I)-tCCS1 can activate the yeast SOD1 (Lane 3) to similar levels to that of yeast CCS1 (Lane 2). Lane 1 is immature yeast SOD1 alone. Below the activation gel are coomassie stained loading controls for the SOD1 and CCS1 proteins.

CCS1-mediated Cu(I)-delivery is a thermodynamically driven process.

We propose a model in which CCS1-mediated SOD1 activation involves Cu(I) transfer from CCS1 to SOD1 through a Cu ion entry site form where it is subsequently shuttled to the SOD1 active site. To verify whether this series of Cu(I) transfer events is thermodynamically driven, we determined the Cu(I)-binding affinity of Cu sites at progressive stages of Cu transfer from CCS1 to SOD1. We used a direct competition assay with two small molecule Cu(I) chelators

(L), BCA and BCS, that allow colorimetric quantification of their Cu-bound species (CuL2) upon competition with Cu(I)-bound CCS1 or SOD1 (**Table 3.2**). The known formation constants for BCA ($\beta2=1017.2M^{-2}$) and BCS ($\beta2=1019.8M^{-2}$) (42) allow for the determination of the Cu(I) dissociation constants for different binding sites on CCS1 and SOD1. To guarantee Cu(I) binding at specific sites in CCS1 and SOD1, site-specific mutants have been utilized. Previous studies, using indirect competition, reported that the Cu(I) affinity of D1 of CCS1 to be an order of magnitude greater than that of D3 (43).

Table 3.2. Cu(I) and Zn(II) dissociation constants for sites in CCS1 and SOD1

Cu(I) Sites	**K_D (M)**
CCS1-Domain 1	$3.61 \pm 1.00 \times 10^{-17}$
CCS1-Domain 3	$2.33 \pm 0.22 \times 10^{-17}$
Wt-SOD1 (Active Site)	$6.97 \pm 2.26 \times 10^{-21}$
H46R/H48Q-SOD1 + CCS1 (Entry Site)	$9.00 \pm 0.14 \times 10^{-19}$
H46R/H48Q/C57S-SOD1 + C231A CCS1	$1.29 \pm 0.05 \times 10^{-17}$
Zn(II) Constructs	**K_D (M)**
Cu,Zn-SOD1^{SS}	$8.46 \pm 2.83 \times 10^{-18}$
E,Zn-SOD1^{SH}	$1.60 \pm 0.24 \times 10^{-16}$
E,Zn-SOD1^{SH} + Wt-CCS1	$3.83 \pm 0.52 \times 10^{-17}$
E,Zn-SOD1^{SH} + W222A-CCS1	$1.62 \pm 0.21 \times 10^{-16}$
E,Zn-SOD1^{SH} + W237A-CCS1	$1.88 \pm 0.79 \times 10^{-16}$

However, using a standardized direct competition method in mutants where the Cu(I) binding residues have been mutated in each domain, we show that the CCS1 D1 and D3 domains possess nearly equal affinity for Cu(I), with D1 = $3.61 \pm 1.00 \times 10^{-17}$ M and D3 = $2.33 \pm 0.22 \times 10^{-17}$ M. On the other hand, the Cu(I) affinity in H46R/H48Q SOD1 (X,Zn-SOD1^{SH}, contains an ablated active site) , where Cu is bound at the entry site ($9.00 \pm 0.14 \times 10^{-19}$M), is nearly 2 orders of magnitude higher than the Cu(I) affinity for either CCS1 site, but significantly lower than the Cu(I) affinity at the active site of mature SOD1 (Cu,Zn-SOD1^{SS}), which we determine to be 6.97

± 2.26 x 10^{-21} M. Our results indicate that the transfer of Cu between D1 of CCS1 to D3 could involve dynamic Cu(I) equilibrium between their Cu(I) binding sites. Nevertheless, Cu(I) transfer from CCS1 to the entry site at the SOD1•CCS1 interface and then subsequently to the SOD1 active site is thermodynamically driven by a Cu(I) affinity gradient that allows a series of efficient Cu(I) transfer reactions.

Disulfide bond formation drives Cu(I)-delivery to the active-site. Based on the obtained Cu(I) binding affinities we propose a pathway of Cu delivery to SOD1 that involves the transfer from the 2S site in CCS1, to a Cu ion entry site with trigonal 2S and 1N/O coordination within SOD1•CCS1 (25), and subsequent transfer to the SOD1 active site, where Cu(I) is bound to 3 N/O ligands prior to oxidation to Cu(II) (25). We have performed detailed electronic absorption spectroscopic analysis to characterize differences in the Cu(I)-dependent electronic transitions arising from these sites, establish a platform to monitor Cu transfer from CCS1 to SOD1 and determine the rate at which it proceeds. The absorption spectrum of apo-CCS1, H46R/H48Q SOD1 (X,Zn-$SOD1^{SH}$) and Cu-free Wt-SOD1 (E,Zn-$SOD1^{SH}$) above 240nm are characterized by the presence of the electronic transitions originating from the aromatic residues (1Trp in SOD1, 4Trp and 6Tyr in CCS1) centered at ~280 nm. Binding of 1 Cu(I) equivalent to CCS1 give rise to a prominent metal-induced shoulder envelope at ~260 nm with tailing to 300 nm. These features are consistent with origin from the low energy CysS-Cu(I) LMCT transitions arising from the digonally thiolate-coordinated Cu(I) present at the CCS1 binding site. The metal-induced differential absorption (Cu(I)-CCS1/apo- CCS1) with a $\Delta\varepsilon = 5600\ M^{-1}\ cm^{-1}$ is consistent with the presence of 2 thiolate-Cu(I) bonds with an $\varepsilon \sim 2800\ M^{-1}\ cm^{-1}$ per bond (**Fig. 3.3**) (44). Similarly, reaction of Cu(I)-CCS1 with H46R/H48Q SOD1 resulting in the transfer of Cu to the SOD1 entry

site give rise to a prominent metal-induced shoulder at ~260 nm consistent with CysS-Cu(I) LMCT transitions origin. The metal induced differential absorption for Cu(I) binding to this 2S, 1N/O trigonal entry site shows a $\Delta\varepsilon = 6000\ M^{-1}\ cm^{-1}$ consistent with a minor $\Delta\varepsilon$ increase compared to Cu(I)-CCS1 likely arising from CysS-Cu(I) LMCT transitions in a changed coordination geometry environment. Removal of non-entry site coordinating cysteines in SOD1 (C146) and/or CCS1 D1 (C17/C20) does not hinder entry site Cu(I) binding while the mutation of the key entry site cysteines from SOD1 (C57) and CCS1 D3 (C231) eliminates all Cu binding away from CCS1 D1 and the SOD1 active site (**Table 3.2** and **Sfig. 3.2**).

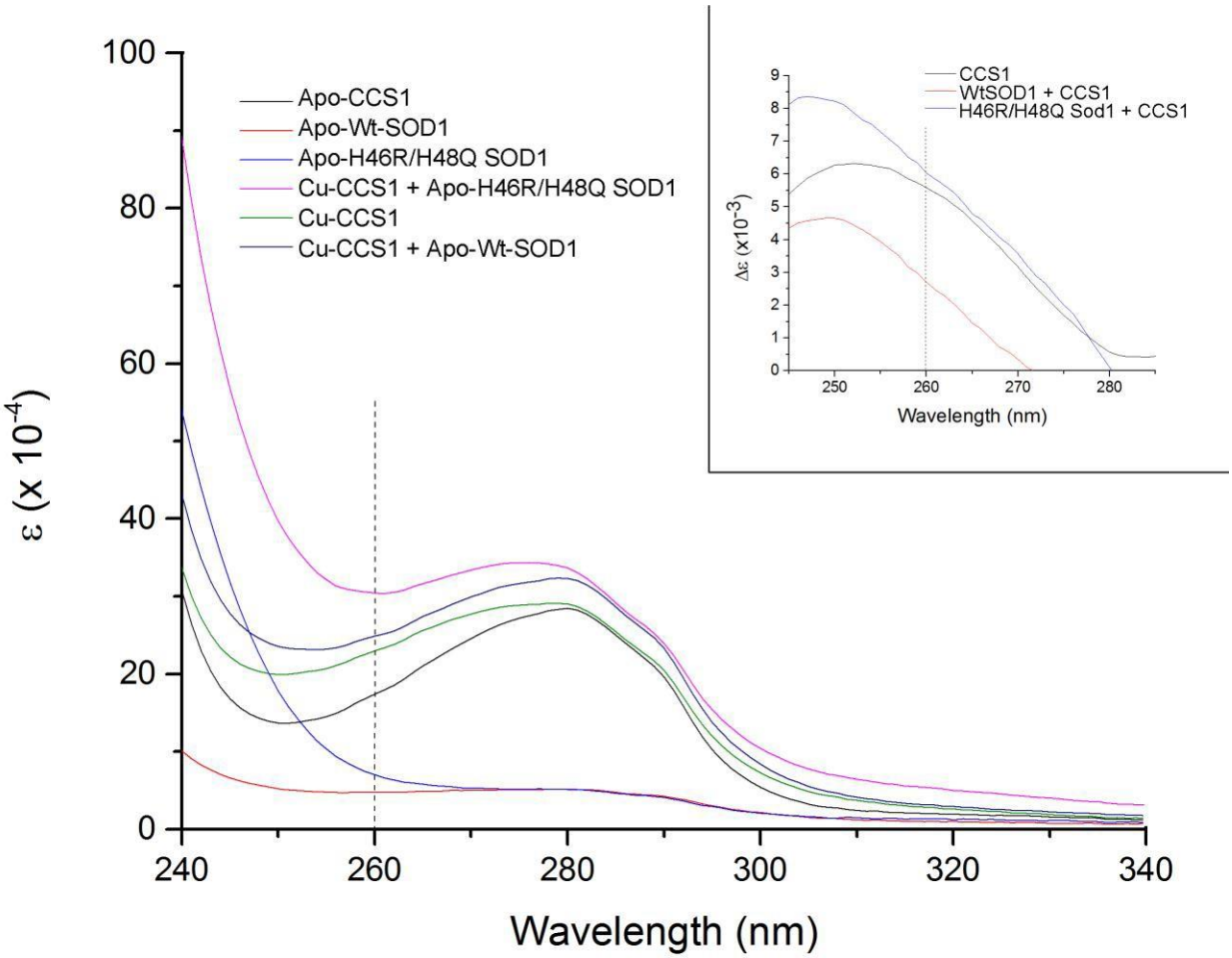

Figure 3.3. Electronic absorption analysis of Cu(I) transfer pathway between SOD1 and CCS1. UV-Vis absorption spectra of apo (metal-free) and Cu(I)-bound CCS1 and the absorbance shifts upon reaction with H46R/H48Q (X,Zn-SOD1^{SH}) and Wt E,Zn-SOD1^{SH}. In the insert, the differential absorption metal-induced contributions have been derived by subtracting the relevant apo-proteins spectra from the corresponding spectra recorded on the Cu(I)-bound transfer reaction products.

Relatedly, the reaction of Cu(I)-CCS1 with Wt E,Zn-SOD1^{SH} leads to significant shift of metal- induced features at 260 nm (with a marked Δε decrease) compared to Cu(I)-Ccs consistent with the expected shift to higher energy for N/O-Cu(I) LMCT (**Fig. 3.3**). This supports the transfer of Cu(I) to the SOD1 active site that is devoid of Cys ligands and for which a 3 N/O coordination has been determined by XAS (25) and numerous crystallographic analyses (45,46).

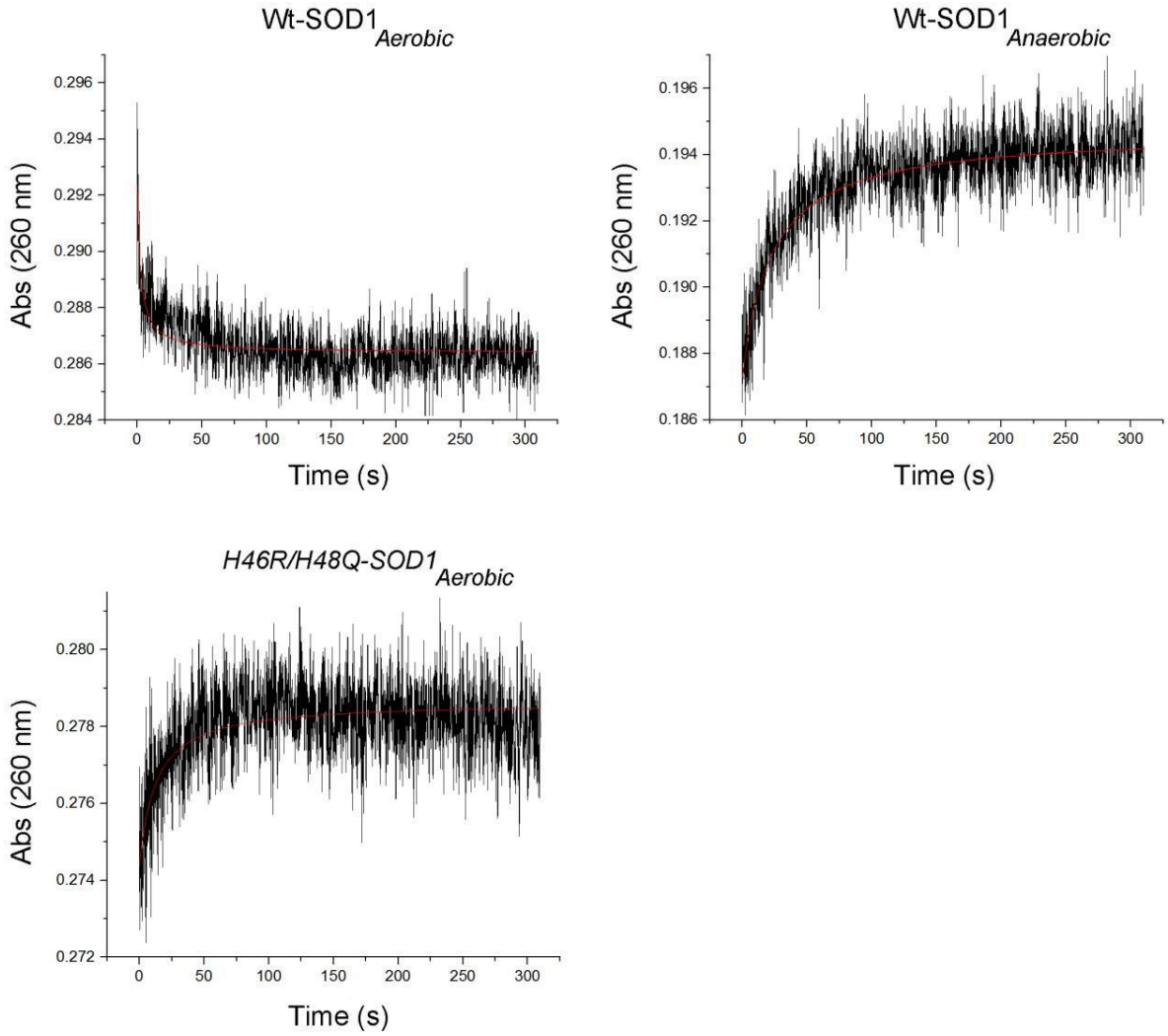

Figure 3.4. Kinetic analysis of CCS1 mediated copper delivery to sites on SOD1. Stopped-flow kinetic traces at 260 nm and corresponding curve fittings (red line) obtained upon rapid mixing of Cu(I)-Ccs (20μM) with equal volumes of apo H46R/H48Q (X,Zn-SOD1^{SH}) or Wt E,Zn-SOD1^{SH} (20μM) under aerobic or anaerobic conditions. The decreased absorbance at 260 nm (top left panel) corresponds to the copper ion moving from the cysteine coordination of CCS1 and/or SOD1 and entering the histidine coordination of the SOD1 active site. Increased absorbance at 260 nm shows the copper ion transfer from CCS1 cysteines to the SOD1•CCS1 2Cys/1His "entry-site."

Considering these differences, stopped-flow spectroscopic kinetic analysis at 260 nm following reactions between Cu(I)-CCS1 and SOD1, under anaerobic and aerobic conditions, monitor the kinetics of Cu transfer from CCS1 to the SOD1 entry site and then to the SOD1 active site. Reaction of Cu(I)-CCS1 with H46R/H48Q SOD1 (X,Zn-SOD1^{SH}) show increasing

absorbance traces at 260nm and are consistent with Cu(I) transfer to SOD1 stalled at the "entry-site." Results indicate a fast transfer reaction with an apparent second- order $k_{app} \sim 10^3\ M^{-1}s^{-1}$ (**Fig. 3.4, bottom panel**). Stopped-flow traces obtained upon mixing Cu(I)- CCS1 and Wt E,Zn-SOD1^{SH} in aerobic conditions yielded a fast 260nm absorbance decrease, suggesting very rapid Cu(I) transfer from CCS1 to the SOD1 active site where Cu(I) is coordinated by histidine residues, with second-order $k_{app} \sim 10^4\ M^{-1}s^{-1}$ (**Fig. 3.4, top left panel**). However, similar reactions between Cu(I)-CCS1 and Wt E,Zn- SOD1^{SH} in anaerobic conditions showed kinetic traces at 260nm consistent with the reaction using H46R/H48Q SOD1 (X,Zn-SOD1^{SH}). This is indicative of Cu(I) being stalled at the SOD1 entry site (**Fig. 3.4, top right panel**). CCS1-dependent SOD1 activation is known to require oxygen (15), as now explained by the oxygen-dependent transfer of Cu from the entry site to the SOD1 active site. Further spectroscopic studies performed by mixing Cu(I)-CCS1 and C146S SOD1 (E,Zn-SOD1X) mutant incapable of forming the disulfide bond showed a similar electronic absorption envelope as observed for H46R/H48Q SOD1 (X,Zn-SOD1^{SH}), corroborating the Cu stalling at the entry site when the disulfide bond cannot be formed.

CCS1 interaction stabilizes site-specific high- affinity Zn binding by SOD1. The acquisition of Zn by SOD1 is not well understood [reviewed in (4)] and has not been extensively studied (19). The yeast form of CCS1 does not bind Zn on its own (13) and immature SOD1 binds Zn with low affinity where the metal can leach from the protein in the presence of the weak Zn(II) chelator PAR (19,29). Here, we developed a competition method to monitor Zn binding in SOD1 using the high- affinity Zn chelator TPEN. After incubation and washing of Zn bound forms of SOD1 with competing concentrations of TPEN and subsequent removal of TPEN-Zn complex, we measured Zn loss in SOD1 by ICP-MS (**Fig. 3.5**). The Zn affinity of TPEN is 2.6×10^{-16}M (47).

The mature wild-type form of SOD1 (Cu,Zn-SOD1^{SS}) holds onto Zn the most stably (19.28 ± 0.24% Zn loss). The reduced form of the active site mutant H46R/H48Q SOD1 (X,Zn-SOD1^{SH}) showed a significantly reduced Zn(II) binding propensity (X,Zn-SOD1^{SH} = 86.47 ± 1.32% Zn loss)). However, complex formation between the X,Zn- SOD1^{SH} and CCS1 significantly increased the SOD1 affinity for Zn (resulting in 51.94 ± 0.56% Zn loss). Interestingly, X,Zn-SOD1^{SH} binding by the CCS1 D3 mutants W222A and W237A, which destabilize the D3 β-hairpin, do not provide the same level of Zn protection as Wt-CCS1. In fact, the levels of Zn loss mimic X,Zn-SOD1^{SH} alone (86.03 ± 3.27% for W222A and 88.33 ± 2.52% for W237A) CCS1 D3 CxC mutants did not have the same effect and behave more similar to the levels of Wt-CCS1 protection.

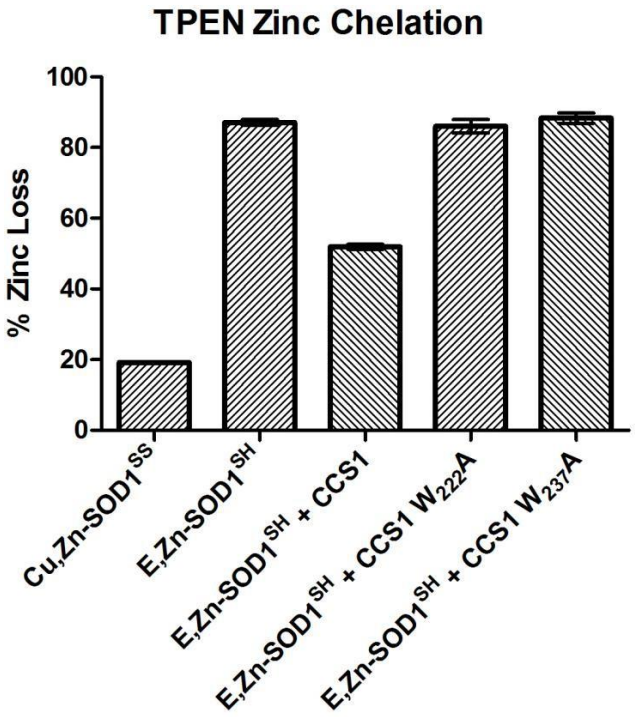

Figure 3.5. Zinc competition between SOD1 and the Zn(II)-chelator TPEN. Immature forms of SOD1 (E,Zn-SOD1^{SH}) can be readily outcompeted for zinc by the Zn(II) chelator TPEN. SOD1 maturation events (i.e. copper binding and disulfide formation) increase SOD1 affinity for zinc as seen by the decrease in Zn(II) loss for Cu,Zn-SOD1^{SS}. CCS1 binding alone (i.e. apo-CCS1 with no copper delivery) promotes zinc binding by immature SOD1 (reduces Zn(II) loss). The removal

of key tryptophan residues within CCS1 D3 (W222 and W237) eliminates this zinc protection ability of CCS1.

Next, using an in-line equilibrium cell and the known Zn affinity of TPEN, we developed a competition method with stringent volume control to, for the first time, determine the Zn affinity of SOD1 at various stages in maturation (**Table 3.2**). Fully mature wild-type SOD1 (Cu,Zn-$SOD1^{SS}$) binds Zn with the highest affinity ($8.46 \pm 2.83 \times 10^{-18}$ M). The active site mutant H46R/H48Q SOD1 (X,Zn-$SOD1^{SH}$) has a significantly weaker affinity for Zn ($1.60 \pm 0.24 \times 10^{-16}$ M), but upon complex formation with CCS1, the affinity of X,Zn-$SOD1^{SH}$ (mimicking immature SOD1) for Zn increases by nearly an order of magnitude ($3.83 \pm 0.52 \times 10^{-17}$ M). Once again, the Zn affinity values for X,Zn-$SOD1^{SH}$ bound by the CCS1 D3 mutants W222A ($1.62 \pm 0.21 \times 10^{-16}$) and W237A ($1.88 \pm 0.79 \times 10^{-16}$) mimic that of X,Zn-$SOD1^{SH}$ without Wt-CCS1 binding. These K_D values substantiate our Zn loss assay results (above) and promote a mechanism where CCS1 binding to immature SOD1 induces/stabilizes a conformation suitable for stable Zn binding, thereby accelerating subsequent Cu delivery and disulfide formation.

Discussion

Our data predicts that yeast CCS1 functions beyond a standard metallo-chaperone and promotes all levels of SOD1 post translation modification. We have shown that CCS1 preferentially binds a completely immature SOD1 molecule (E,E-$SOD1^{SH}$) and this interaction promotes high-affinity Zn binding by SOD1 (29), **Fig. 3.5,** and **Table 3.2**. An expanded SOD1•CCS1 interface involving the disulfide loop of SOD1 and the CCS1 D3 β-hairpin likely stabilizes Zn ligand residues in this region (e.g. H63, H71, and H80). Intercalation of the SOD1 disulfide loop by CCS1 D3 concomitantly forms a Cu ion drop-off point or entry site (25). Cu transfer follows a favorable thermodynamic affinity gradient from CCS1 to the entry site and

eventually the SOD1 active site. In conjunction, kinetics show that the transfer process is fast and delivery to the active site is directed by SOD1 disulfide formation. In all, this supports and greatly advances our understanding of the order, rates and forces guiding the multiple SOD1 maturation events coordinated by CCS1 (25).

It has been generally assumed that SOD1 diffusively acquires Zn from the available pool within the cell as the first step in its maturation process [reviewed in (13)]. This is supported by the lack of Zn specific metallo-chaperones that have been discovered, to date, and that wild-type SOD1 purified from yeast lacking CCS1 are devoid of Cu, yet enriched with Zn (>1 Zn/monomer) (25). However, this can be misleading as those SOD1 molecules examined after purification are improperly metallated (i.e. Zn bound in both the Cu and Zn sites) and represent only a portion of the whole SOD1 population, much of which fell within the insoluble fraction as metal deplete and disulfide reduced (14,25). It has also been shown that pathogenic SOD1 variants that cannot productively interact with CCS1, including D124V and C57S, show improper metallation (i.e. Cu free and Zn bound at the Cu site) and are disulfide reduced (39). Even more recent studies have shown that the major form of SOD1 found within cultured HEK293 cells lacking CCS1 are completely metal free and disulfide reduced (30). Taken together, these data argue that CCS1 facilitates proper Zn metallation, though the mechanism of action remains unclear. In support of this model, we have very recently shown that CCS1 recognizes a completely immature form of SOD1 (E,E-SOD1^{SH}) and binding then promotes stable Zn uptake by CCS1-bound SOD1 (29). Our present results provide a molecular basis for proper high-affinity Zn binding by SOD1 that is induced by interaction with CCS1 (**Table 3.2**). We find that conserved aromatic residues (W222 and W237) that stabilize the β-hairpin conformation of CCS1 D3 and are critical for overall SOD1

activation are also critical for this function. We have previously asserted (29), and our current data reinforces the notion that CCS1 D3 stabilizes a loop region of SOD1 containing multiple Zn-liganding residues and generates a complete Zn binding site in SOD1. It is important to realize that stable Zn binding by SOD1 must occur before Cu insertion and disulfide oxidation can ensue (30,48). Without CCS1 present, the population of SOD1 disintegrates into an assorted collection of improperly metallated molecules ranging from completely Zn-free to conformers with 2 Zn ions per monomer [reviewed in (13)]. CCS1 likely plays an all-encompassing faciliatory role during SOD1 activation that starts with guaranteeing "correct" Zn status of the SOD1 molecule.

The compact β-hairpin conformation of CCS1 D3 expands the SOD1•CCS1 dimeric interface outside that of the SOD1 β-barrel and CCS1 D2 (**SFig. 3.1**). Two highly conserved tryptophan residues secure the β-hairpin against CCS1 D2 and place the CxC cysteines near dimeric interface and disulfide cysteines of SOD1 forming what we have termed the Cu ion "entry-site." W222 anchors the first six amino acids of D3 within a narrow groove between SOD1 and CCS1 D1. Within the D3 β-hairpin, W237 interacts with a hydrophobic patch on D2 stabilizing this section of D3 downstream of W222 that is commonly unstructured in the absence of Cu coordination or SOD1 binding (21,28). Substitution of either residue resulted in a similar ~4-fold loss in binding affinity compared to Wt CCS1 (**Fig. 3.1a**) and (49). These values also compare quite well with a CCS1 truncation that lacks D3 (**Table 3.1**) and (29), suggesting that without W222 or W237, CCS1 D3 does not complete the observed notch-into-groove interactions guided by the D3 β-hairpin and unfurled SOD1 disulfide loop as pictured in **SFig. 3.1** and (25).

Removal of these key tryptophan residues in CCS1 D3 significantly hindered SOD1 activation. Both mutants can be loaded in vitro to normal (e.g. similar to wild type) levels of Cu

binding. The W222A mutant retains some capacity to activate SOD1, but only ~1/3 of wild type CCS1. The W237A mutant abolishes any SOD1 activation. The lack of cohesion between the W222 and W237 variants where both deter binding ~4-fold, yet their SOD1 activation propensities show some disparity could be explained kinetically. While both tryptophan residues likely stabilize the positioning of the D3 β-hairpin, without W222 the W237 could likely still find its spot for a subset of CCS1 molecules making the CxC motif available for Cu ion entry site formation. However, without W237, this localization may take much longer or exist less stably. Other related CCS1 variants were tested and are shown in **Table 3.1**.

The structural and biochemical framework first generated around our SOD1•CCS1 complex demonstrates a tuned mechanism for the transfer of Cu from CCS1 to the SOD1•CCS1 entry site and subsequent release to the nearby active site. The transient Cu(I) coordination at the entry site is prompted by a ligand exchange reaction where the introduction of an additional coordinating ligand switches from a 2S digonal Cu(I) site (in CCS1) to a 2S1N/O trigonal environment (in SOD1•CCS1) that results in a nearly two orders magnitude increase in Cu(I) affinity (**Table 3.2**). This resembles processes observed in other Cu- trafficking proteins, where sulfur-coordinated Cu(I) sites with low coordination numbers (2–3) by 'soft' ligands such as Cys (or Met) side chains are selected to guarantee fast ligand exchange between residues of donor and acceptor sites (50).

From the entry site in SOD1•CCS1, Cu(I) is then delivered to the SOD1 active site where a 3N coordination occurs (25,30). Based on Pearson HSAB theory (hard and soft, acid and bases) which predicts the "soft" nature of both Cu(I) and thiolate ligands, it is surprising that the SOD1 active site shows an 80-fold increase in Cu(I) binding affinity compared to the entry site (with histidine

being in nature “harder” than thiolates) (51,52) . However, despite the known identity of the Cu(I) coordinating active site histidines (H46, H48, H6 and H120), the exact role of these residues in Cu translocation to the active site remain ambiguous [reviewed in (13)]. H63 also coordinates Zn(II) and can act as bridging ligand, its “non-standard” side chain acidity and altered “hardness” could facilitate Cu(I) transfer. H120 is both an active site and entry site Cu ligand and this may diminish the affinity of the competing “incomplete” active site (e.g. only 3 free histidines) when liganding Cu(I) as a part of the “entry-site.” Delivery is achieved exclusively when disulfide formation occurs, thus, it appears that stability of Cu(I) bound at the active site in mature SOD1 is modulated by both oxidation of the coordinating thiolate ligand in the entry site (C57) (preventing Cu(I) coordination) as well as possible structural constrains imposed to the active site by the disulfide bridge formation. This fits well with previous work showing that C57S and C146S SOD1 variants isolated from yeast show negligible active site Cu and an overabundance of Zn (~ 2 Zn ions/SOD1 monomer) (53).

It appears that yeast CCS1 is a multipurpose “helper” protein with conditionally/temporally dependent chaperoning roles during SOD1 activation (**Fig. 3.6**). The overall functionality of CCS1 is significantly more complex than a standard metallo-chaperone. Related work on the human form of CCS1 has shown an ability to stabilize select disease-causing SOD1 mutants, though any role in SOD1-dependent ALS is unclear (18). Our results support a model where initial binding of immature SOD1 by CCS1 facilitates site-appropriate Zn binding by stabilizing liganding residues present in the disulfide loop of SOD1 (**Fig. 3.6b,c and d,e**). The second step in the SOD1 maturation process will be dependent on the level of available Cu. During limiting Cu conditions, CCS1 D1 will have likely acquired the necessary Cu(I) from the Cu transporter Ctr1 (54) for

delivery to the SOD1 "entry site" (25) (**Fig. 3.6a**). Our previous work has established that at this point, the entry site bound Cu ion will react with a superoxide/peroxide attracted to a nearby electropositive hole and promote sulfenylation at C146 on SOD1 (**Fig. 3.6c**) and (25). Sulfenylation of C146 prompts disulfide exchange reactions between nearby cysteines, concluding in formation of the SOD1 intra-subunit disulfide, Cu release into the SOD1 active site (**Fig. 3.6g**). (25). Disulfide bond formation also terminates interaction with CCS1 and the mature SOD1 molecule (Cu,Zn-SOD1^{SS}) can find another Cu,Zn-SOD1SS molecule to form the complete homodimeric enzyme (**Fig. 3.6g**). When Cu levels are higher, Cu(I)-GSH will likely provide the Cu to CCS1 and/or directly to the SOD1•CCS1 entry site (**Fig. 3.6e**). In this instance CCS1 may serve to stabilize a conformation of SOD1 that displays an available entry site and then that of a disulfide oxidase after Cu drop-off by Cu(I)-GSH (**Fig. 3.6e,f,g**) (25). In all, CCS1 has a complex mode of action that is honed to specifically activate immature SOD1 during differing cellular conditions in an extremely efficient manner.

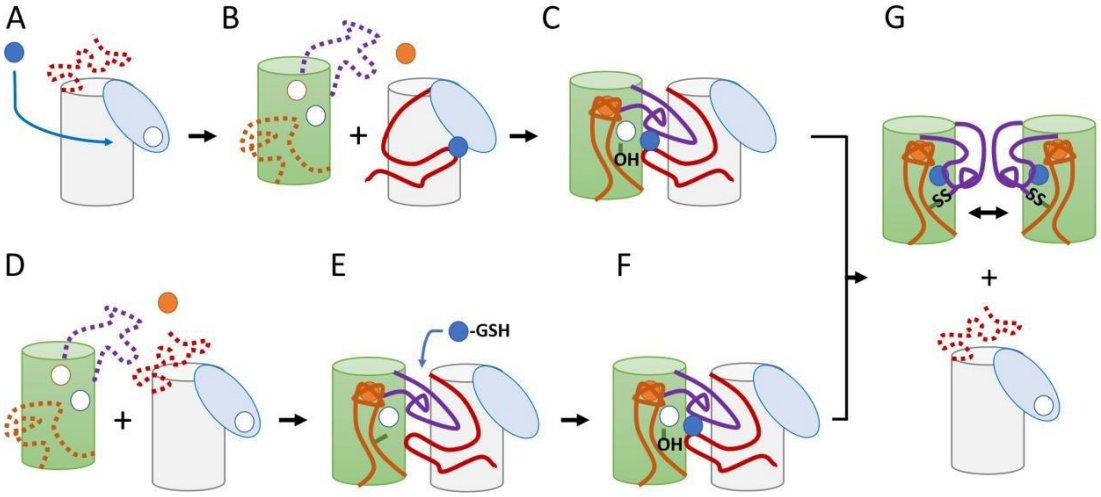

Figure 3.6. Copper dependent models for SOD1 activation by yeast CCS1. (A) CCS1 domains are shown as a blue oval (D1), grey cylinder(D2) and red strand (D3); Under copper limiting conditions Cu(I) (blue circle) is first acquired by D1 and binding stabilizes an unfolded D3. (B) CCS1 binding to immature SOD1 (green β-barrel, purple "disulfide loop" and orange electrostatic loop) orders the conserved loop elements of SOD1 and promotes proper Zn(II) (orange circle)

binding. (C) Cu(I) is bound at the entry site promoting sulfenylation at a nearby cysteine in SOD1. (G) Disulfide bond formation in SOD1 keys Cu(I) release to the active site, terminates interaction with CCS1 and promotes homodimerization with another mature SOD1 molecule. (D-E) When labile copper is abundant, Cu(I) may be provided to the entry site by reduced glutathione (GSH) after SOD1•apo-CCS1 complex formation. (F) Cu(I) is bound at the entry site promoting sulfenylation at a nearby cysteine in SOD1. (G) Mature Sod1 homodimerizes and CCS is free to proceed the same as before.

Experimental Procedures

Materials.

DTT (dithiotreitol) and IPTG (isopropyl1-thio-beta-D-galactopyranoside), and tris(2-carboxyethyl)phosphine (TCEP) were purchased from GoldBio. Yeast extract, tryptone, NaCl, Bis-Tris, Tris-Base, glycine, beta- mercaptoethanol (βME), agar, ammonium persulfate (APS), sodium acetate, acetic acid, EDTA, and TEMED were purchased from Thermo Fisher Scientific. Nitro Blue Tetrozolium salt (NBT) and bathocuproine sulfonate (BCS) were obtained from Alfa Aesar. Imidazole, Zn2SO4, and Cu(II)2SO4, Imidazole, monobasic and dibasic sodium phosphate and acetonitrile were purchased from Sigma-Aldrich. MES, glutathione, and trichloroethanol (TCE) were purchased from Acros Organics. Cu1-(CH3CN4)PF6 was obtained from Strem Chemicals and 1,10 phenanthroline from Toronto Research Chemicals. Primers for mutagenesis were purchased from Sigma-Aldrich and the Phusion Site-Directed Mutagenesis Kit from Thermo Fisher Scientific. TPEN (N,N,N′,N′-tetrakis(2-pyridinylmethyl)-1,2- ethanediamine) was purchased from Tocris Bioscience. Alexa-546 fluorescent dye for labeling was purchased from Life Technologies. Bacterial strains used were DH5α (Invitrogen), BL21 pLysS (DE3) E.coli (Promega), and XL1-Blue (Stratagene). Chromatography columns were purchased from GE. Antibodies used in this study were mouse monoclonal 6x-His epitope tag antibody (MA1-21315, Invitrogen) and rabbit polyclonal SOD1 antibody (PA1-30195, Thermo Fisher Scientific).

hSOD1 Cloning, Expression and Purification.

DNA fragments encoding wild-type and mutants forms of SOD1 were amplified by PCR and ligated into the YEP351-hSOD plasmid, where expression of the SOD1 protein is directed under the control of its own promoter. The protein was expressed, purified, and characterized as previously described (19) with the addition of a DEAE-Sephadex chromatography step between the hydrophobic interaction chromatography and gel filtration column steps. Metal content of purified SOD1 proteins was determined using inductively-coupled plasma mass spectrometry (ICP-MS).

CCS1 Cloning, Expression and Purification.

DNA fragments encoding yCCS1 were generated by polymerase chain reaction (PCR) from plasmids originally supplied by J.S. Valentine (UCLA). CCS1 constructs were cloned into a pkA6H vector, which contains an inducible LacZ promoter, a 6x-N-terminal His-tag, and a tobacco etch virus (TEV) cleavage site. Residues 238-240 of CCS1 D3 were changed to alanine via quick-change mutagenesis. These substitutions convert the highly conserved 237WEER240 motif found in CCS1 DIII to WAAA. Alanine at these sites enhanced the yield of CCS1 approximately 5-fold and also appeared to inhibit the C-terminal proteolysis observed in identically prepared, unsubstituted CCS1 during storage 4oC. yCCS1 proteins were expressed in Escherichia coli BL21 (DE3). Cells containing these expression plasmids were grown in LB media at 37oC to an OD600 of 0.6 to 0.8. After induction with IPTG (1mM), the cells were transferred to 30oC for an additional 4 hours before being harvested. yCCS1 proteins were purified using a HisTrap HP Ni^{2+} affinity column purchased from Amersham using buffer A (20mM Tris pH8, 300mM NaCl, and 2mM DTT) and buffer B (20mM Tris pH8, 300mM NaCl, 2mM TCEP, and 1M imidazole). The column

was washed with 2% of buffer B for 10 bed volumes. yCCS1 was eluted with a gradient from 2% to 100% in 80ml. After purification, the hexa-His-tag was removed from the CCS1 proteins using TEV protease (A280=1 OD) produced in-house and engineered to contain its own non-cleavable hexa- His tag. After digestion overnight at room temperature, the cleaved His tag and TEV protease was removed from the CCS1 sample by a final pass through the nickel column. This procedure leaves a two residue (Gly-His) extension on the CCS1 N-terminus. The metal content of purified CCS1 proteins was determined using inductively- coupled plasma mass spectrometry (ICP-MS, Agilent 7900) facility here at UTD. Samples for ICP-MS were digested with 1% HNO3 for analysis.

Microplate-based binding assays. The preparation and completion of the binding assays were done in following the details of past work (55). Here, binding experiments were done with a reaction buffer containing 20 mM Tris pH 7.5, 150 mM NaCl, 1 mM TCEP and 0.01% of both octyl glucoside and CHAPS. The plates (or gels) were imaged using a GE Typhoon FLA 9500 using filters specific for the fluorophore's excitation. The binding experiments are completed in replicative quadruplicate on the same plate for comparative and statistical analysis. The fluorescence change was then quantified using Image-Quant TL and then analyzed and figures constructed using GraphPad Prism.

SOD1 activity assays. Metals were removed from SOD1 by dialysis in 10mM EDTA pH 3.8 followed by 1mM EDTA pH 5.5. Dialysis in 10mM EDTA buffer was done for 8 hours followed by dialysis in the 1mM EDTA buffer overnight (all at 4°C). 0.5 mM EDTA was used to remove trace metals from tubes, tips, and glassware for activation experiments. Cu loading was always performed under anaerobic conditions using a glove box. CCS1 protein was mixed in 1:1

stoichiometric ratio with Cu1-(CH3CN4)PF6 (Strem Chemicals) for 2-3 hours in a buffer containing 50mM Tris, pH 8, 10mM TCEP, and 150mM NaCl. Unbound Cu was removed by washing the protein with degassed buffer using a spin-filter (EMD Millipore). Activity assays were set up in an aerobic environment with a 5:1 molar ratio of CCS1 to SOD1. The reaction buffer contains 50mM Tris pH 8, 100mM NaCl, 0.5mM TCEP, 20μM Zn2SO4, and 200μM BCS. Samples were incubated for 20 minutes prior to running the reactions out on a 8% Native-PAGE and followed by visualization using the Nitro Blue Tetrazolium (NBT) gel method. All experiments were completed in at least 3 separate gels for comparative analysis.

Disulfide crosslinking assays. Tomato Ccs (10μm) was incubated for 15 minutes with Cu 1,10 phenanthroline (CuP) (25μm) in reaction buffer (20mM Tris pH 7.5 and 300mM NaCl). Samples were prepared with and without the addition of BME and boiled 10 min prior to visualization on 14% BIS-TRIS gels made with trichloroethanol (TCE). BIS-TRIS gels were run in MES running buffer for 25 min at 200V. All experiments were completed in at least 3 separate gels for comparative analysis.

Determination of Cu binding affinity to Ccs and SOD1 using BCA and BCS. Cu binding affinity experiments were performed in a nitrogen- purged anaerobic glovebox. Samples were made oxygen-free with at least three vacuum/nitrogen cycles on a Schlenk-line. Cu(I)-CCS samples (20 μM, pH 7.4) were reacted with 1mM BCA and incubated for 15 h. For Cu(I)-SOD samples, 40 μM samples were reacted with 1mM BCS for H46R/H48Q SOD1 and 5mM BCS for Wt SOD1 and incubated for 15 h. The absorbance of the [Cu(I)L2]3- complex formed was then measured using Cary 300 UV-Vis Spectrophotometer (Agilent) at 562 nm for L = BCA (ε=7,900 M^{-1} cm^{-1}) and at 483 nm for L = BCS (ε= 13,000 M^{-1} cm^{-1}). All samples were run in triplicate to

ensure proper statistical analysis. The dissociation constants were calculated according to the following equations, using the formation constants β2 = 1017.2 M^{-2} for BCA and β2=1019.8 M^{-2} for BCA (42).

Detection of Cu Transfer from Cu1-CCS1 to SOD1.

Samples of SOD1 (20μM in 20mM Na2PO4, pH 7.6, 50mM NaCl, 0.5mM TCEP) were incubated with Cu(I)-CCS1 (20μM in 20mM Na2PO4, pH 7.6, 50mM NaCl, 0.5mM TCEP) for 20 minutes. UV-Vis absorption spectra were recorded before and after the Cu transfer reactions using a Cary 300 UV-Vis Spectrophotometer (Agilent) in 1-cm Quartz cuvettes. Kinetics of Cu

$$P - Cu + 2L \rightleftharpoons P + CuL_2$$

$$K_D\beta_2 = \frac{\frac{[P]_{total}}{[P-Cu]} - 1}{\left(\frac{[L_{total}]}{[CuL_2]} - 2\right)^2 [CuL_2]}$$

transfer was measured using a stopped-flow SX-20 spectrometer (Applied Photophysics) with a temperature-controlled sample cell. Equal volumes of the Wt or mutant SOD1 samples and Cu(I)-CCS1 samples (both 20μM) were injected and mixed and the absorbance monitored at 260 nm for 300s at 25°C. All buffers for this experiment were rendered metal-free by treatment with Chelex resin (Bio-Rad).

Zn loss assays of SOD1 using TPEN. SOD1 samples (10μM in 50mM Tris, 150mM NaCl) were incubated with 100μM TPEN (N,N,N′,N′- tetrakis(2-pyridinylmethyl)-1,2-ethanediamine, Tocris Bioscience) for 20 minutes at 25°C. 3K ultrafiltration spin columns (Sartorius) were used to separate Zn-TPEN complex from SOD1. The SOD1 samples were washed with 12.5X the reaction volume. Zn-TPEN and Zn bound to SOD1 were determined by measuring Zn concentrations via ICP-MS (Agilent 7900) in the flow through and supernatant respectively.

Samples for ICP-MS were digested with 1% HNO3 prior to analysis. All buffers for the experimental setup were made metal-free by treatment with Chelex resin. Each sample was analyzed in triplicate for statistical analysis.

Determination of Zn affinity of SOD1, apo- SOD1, and apo-SOD1 in complex with CCS1 by equilibrium dialysis. Zn binding affinity experiments were performed at pH 7.4 using a - Bel-Art In-line Equilibrium Cell (1ml). The dialysis membrane was treated with EDTA and boiled to remove any metal and sulfide contaminants. One side of the chamber for each reaction was filled with a solution of TPEN at 100µM. The other side contained 10µM protein- Zn complex and 100µM TPEN. The Zn exchange reaction was allowed to proceed at room temperature overnight under agitation. ICP-MS was used to analyze the Zn concentrations on both sides. The KD has previously been determined for TPEN at pH 7.4 to be 2.6×10^{-16} (41). We used this value to determine Zn affinity values. All samples were analyzed in triplicate and from multiple preps in order to provide meaningful statistical analysis.

Acknowledgments

We thank Dr. P. John Hart for generously providing numerous reagents. This research was supported in part by R01 GM120252 from the National Institutes of Health awarded to D.D.W. The work was also supported by the Robert A. Welch Foundation (Grant: AT-1935-20170325) and by the National Institute of General Medical Sciences of the National Institutes of Health under Award Number R35GM128704 awarded to G.M., and by funds from the University of Texas at Dallas. The content is solely the responsibility of the authors and does not necessarily represent the official views of the National Institutes of Health.

Conflicts of Interest

The authors declare that they have no conflicts of interest with the contents of this article.

References

1. Solomon, E. I., and Lowery, M. D. (1993) Electronic structure contribu- tions to function in bioinorganic chemistry. Science 259, 1575–1581 CrossRef Medline

2. Dancis, A., Haile, D., Yuan, D. S., and Klausner, R. D. (1994) The Saccha- romyces cerevisiae copper transport protein (Ctr1p): biochemical charac- terization, regulation by copper, and physiologic role in copper uptake. J. Biol. Chem. 269, 25660 –25667 Medline

tion between SOD1 and hCCS in neurodegenerative disease. Sci. Rep. 6, 27691 CrossRef Medline

18. Luchinat, E., Barbieri, L., and Banci, L. (2017) A molecular chaperone activity of CCS restores the maturation of SOD1 fALS mutants. Sci. Rep. 7, 17433 CrossRef Medline

19. Winkler, D. D., Schuermann, J. P., Cao, X., Holloway, S. P., Borchelt, D. R., Carroll, M. C., Proescher, J. B., Culotta, V. C., and Hart, P. J. (2009) Struc- tural and biophysical properties of the pathogenic SOD1 variant H46R/ H48Q. Biochemistry 48, 3436 –3447 CrossRef Medline

20. Schmidt, P. J., Rae, T. D., Pufahl, R. A., Hamma, T., Strain, J., O'Halloran,

T. V., and Culotta, V. C. (1999) Multiple protein domains contribute to the action of the copper chaperone for superoxide dismutase. J. Biol. Chem. 274, 23719 –23725 CrossRef Medline

21. Lamb, A. L., Wernimont, A. K., Pufahl, R. A., Culotta, V. C., O'Halloran,

T. V., and Rosenzweig, A. C. (1999) Crystal structure of the copper chap- erone for superoxide dismutase. Nat. Struct. Biol. 6, 724 –729 CrossRef Medline

22. Rosenzweig, A. C., Huffman, D. L., Hou, M. Y., Wernimont, A. K., Pufahl,

R. A., and O'Halloran, T. V. (1999) Crystal structure of the Atx1 metal- lochaperone protein at 1.02 Å resolution. Structure 7, 605– 617 CrossRef Medline

23. Wernimont, A. K., Huffman, D. L., Lamb, A. L., O'Halloran, T. V., and Rosenzweig, A. C. (2000) Structural basis for copper transfer by the met- allochaperone for the Menkes/Wilson disease proteins. Nat. Struct. Biol. 7, 766 –771 CrossRef Medline

24. Lamb, A. L., Torres, A. S., O'Halloran, T. V., and Rosenzweig, A. C. (2001) Heterodimeric structure of superoxide dismutase in complex with its metallochaperone. Nat. Struct. Biol. 8, 751–755 CrossRef Medline

25. Fetherolf, M. M., Boyd, S. D., Taylor, A. B., Kim, H. J., Wohlschlegel, J. A., Blackburn, N. J., Hart, P. J., Winge, D. R., and Winkler, D. D. (2017) Cop- per-zinc superoxide dismutase is activated through a sulfenic acid inter- mediate at a copper ion entry site. J. Biol. Chem. 292, 12025–12040 CrossRef Medline

26. Schmidt, P. J., Kunst, C., and Culotta, V. C. (2000) Copper activation of superoxide dismutase 1 (SOD1) in vivo: role for protein-protein inter- actions with the copper chaperone for SOD1. J. Biol. Chem. 275, 33771–33776 CrossRef Medline

27. Proescher, J. B., Son, M., Elliott, J. L., and Culotta, V. C. (2008) Biological effects of CCS in the absence of SOD1 enzyme activation: implications for disease in a mouse model for ALS. Hum. Mol. Genet. 17, 1728 –1737 CrossRef Medline

28. Rae, T. D., Torres, A. S., Pufahl, R. A., and O'Halloran, T. V. (2001) Mech- anism of Cu,Zn-superoxide dismutase activation by the human metal- lochaperone hCCS. J. Biol. Chem. 276, 5166 –5176 CrossRef Medline

29. Boyd, S. D., Liu, L., Bulla, L., and Winkler, D. D. (2018) Quantifying the interaction between copper-zinc superoxide dismutase (Sod1) and its copper chaperone (Ccs1). J. Proteomics Bioinform. 11, 473 Medline

30. Banci, L., Bertini, I., Cantini, F., Kozyreva, T., Massagni, C., Palumaa, P., Rubino, J. T., and Zovo, K. (2012) Human superoxide dismutase 1 (hSOD1) maturation through interaction with human copper chaperone for SOD1 (hCCS). Proc. Natl. Acad. Sci. U.S.A. 109, 13555–13560 CrossRef Medline

31. Banci, L., Cantini, F., Kozyreva, T., and Rubino, J. T. (2013) Mechanistic aspects of hSOD1 maturation from the solution structure of Cu(I)-loaded hCCS domain 1 and analysis of disulfide-free hSOD1 mutants. Chembi- ochem 14, 1839 –1844 CrossRef Medline

32. Caruano-Yzermans, A. L., Bartnikas, T. B., and Gitlin, J. D. (2006) Mech- anisms of the copper-dependent turnover of the copper chaperone for superoxide dismutase. J. Biol. Chem. 281, 13581–13587 CrossRef Medline

33. Kirby, K., Jensen, L. T., Binnington, J., Hilliker, A. J., Ulloa, J., Culotta, V. C., and Phillips, J. P. (2008) Instability of superoxide dismutase 1 of Drosoph- ila in mutants deficient for its cognate copper chaperone. J. Biol. Chem. 283, 35393–35401 CrossRef Medline

34. Jensen, L. T., and Culotta, V. C. (2005) Activation of CuZn superoxide dismutases from Caenorhabditis elegans does not require the copper chaperone CCS. J. Biol. Chem. 280, 41373–41379 CrossRef Medline

35. Deng, H. X., Hentati, A., Tainer, J. A., Iqbal, Z., Cayabyab, A., Hung, W. Y., Getzoff, E. D., Hu, P., Herzfeldt, B., and Roos, R. P. (1993) Amyotrophic lateral sclerosis and structural defects in Cu,Zn superoxide dismutase. Science 261, 1047–1051 CrossRef Medline

36. Rosen, D. R., Siddique, T., Patterson, D., Figlewicz, D. A., Sapp, P., Hentati, A., Donaldson, D., Goto, J., O'Regan, J. P., and Deng, H. X. (1993) Muta- tions in Cu/Zn superoxide dismutase gene are associated with familial amyotrophic lateral sclerosis. Nature 362, 59–62 CrossRef Medline

37. Jonsson, P. A., Graffmo, K. S., Andersen, P. M., Bra¨nnstro¨m, T., Lindberg, M., Oliveberg, M., and Marklund, S. L. (2006) Disulphide-reduced super- oxide dismutase-1 in CNS of transgenic amyotrophic lateral sclerosis models. Brain 129, 451– 464 CrossRef Medline

38. Karch, C. M., Prudencio, M., Winkler, D. D., Hart, P. J., and Borchelt, D. R. (2009) Role of mutant SOD1 disulfide oxidation and aggregation in the

pathogenesis of familial ALS. Proc. Natl. Acad. Sci. U.S.A. 106, 7774 –7779 CrossRef Medline

39. Seetharaman, S. V., Winkler, D. D., Taylor, A. B., Cao, X., Whitson, L. J., Doucette, P. A., Valentine, J. S., Schirf, V., Demeler, B., Carroll, M. C., Culotta, V. C., and Hart, P. J. (2010) Disrupted zinc-binding sites in struc- tures of pathogenic SOD1 variants D124V and H80R. Biochemistry 49, 5714 –5725 CrossRef Medline

40. Luchinat, E., Barbieri, L., Rubino, J. T., Kozyreva, T., Cantini, F., and Banci,

L. (2014) In-cell NMR reveals potential precursor of toxic species from SOD1 fALS mutants. Nat. Commun. 5, 5502 CrossRef Medline

41. Zhu, H., Shipp, E., Sanchez, R. J., Liba, A., Stine, J. E., Hart, P. J., Gralla, E. B., Nersissian, A. M., and Valentine, J. S. (2000) Cobalt(2+) binding to human and tomato copper chaperone for superoxide dismutase: implications for the metal ion transfer mechanism. Biochemistry 39, 5413–5421 CrossRef Medline

42. Xiao, Z., Brose, J., Schimo, S., Ackland, S. M., La Fontaine, S., and Wedd,

A. G. (2011) Unification of the copper(I) binding affinities of the metallo- chaperones Atx1, Atox1, and related proteins: detection probes and affin- ity standards. J. Biol. Chem. 286, 11047–11055 CrossRef Medline

43. Allen, S., Badarau, A., and Dennison, C. (2012) Cu(I) affinities of the do- main 1 and 3 sites in the human metallochaperone for Cu,Zn-superoxide dismutase. Biochemistry 51, 1439 –1448 CrossRef Medline

44. Pountney, D. L., Schauwecker, I., Zarn, J., and Vasa´k, M. (1994) Formation of mammalian Cu8-metallothionein in vitro: evidence for the existence of two Cu(I)4-thiolate clusters. Biochemistry 33, 9699 –9705 CrossRef Medline

45. Tainer, J. A., Getzoff, E. D., Richardson, J. S., and Richardson, D. C. (1983) Structure and mechanism of copper, zinc superoxide dismutase. Nature 306, 284 –287 CrossRef Medline

46. Hart, P. J., Balbirnie, M. M., Ogihara, N. L., Nersissian, A. M., Weiss, M. S., Valentine, J. S., and Eisenberg, D. (1999) A structure-based mechanism for copper-zinc superoxide dismutase. Biochemistry 38, 2167–2178 CrossRef Medline

47. Jakob, U., Eser, M., and Bardwell, J. C. (2000) Redox switch of hsp33 has a novel zinc-binding motif. J. Biol. Chem. 275, 38302–38310 CrossRef Medline

48. Lamb, A. L., Torres, A. S., O'Halloran, T. V., and Rosenzweig, A. C. (2000) Heterodimer formation between superoxide dismutase and its copper chaperone. Biochemistry 39, 14720 – 14727 CrossRef Medline

49. Winkler, D. D., Luger, K., and Hieb, A. R. (2012) Quantifying chromatin- associated interactions: the HI-FI system. Methods Enzymol. 512, 243–274 CrossRef Medline

50. Boal, A. K., and Rosenzweig, A. C. (2009) Structural biology of copper trafficking. Chem. Rev. 109, 4760 – 4779 CrossRef Medline

51. Pearson, R. G. (1990) Hard and soft acids and bases: the evolution of a chemical concept. Coordin. Chem. Rev. 100, 403– 425 CrossRef

52. Lopachin, R. M., Gavin, T., Decaprio, A., and Barber, D. S. (2012) Appli- cation of the hard and soft, acids and bases (HSAB) theory to toxicant–target interactions. Chem. Res. Toxicol. 25, 239 –251 CrossRef Medline

53. Sea, K., Sohn, S. H., Durazo, A., Sheng, Y., Shaw, B. F., Cao, X., Taylor,

A. B., Whitson, L. J., Holloway, S. P., Hart, P. J., Cabelli, D. E., Gralla, E. B., and Valentine, J. S. (2015) Insights into the role of the unusual disulfide bond in copper-zinc superoxide dismutase. J. Biol. Chem. 290, 2405–2418 CrossRef Medline

54. Aller, S. G., and Unger, V. M. (2006) Projection structure of the human copper transporter CTR1 at 6-Å resolution reveals a compact trimer with a novel channel-like architecture. Proc. Natl. Acad. Sci. U.S.A. 103, 3627–3632 CrossRef Medline

CHAPTER 4

ACTIVATION OF SUPEROXIDE DISMUTASE 1 BY THE HUMAN COPPER CHAPERONE

Abstract

Superoxide dismutase 1 (Sod1) is an antioxidant enzyme with high levels of activity and dozens of critical functions within the cell. The copper chaperone for Sod1 (Ccs) activates Sod1, which is necessary for these functions to proceed normally. Because of their importance to cell function, both Sod1 and Ccs have been thoroughly studied for decades and many models of Sod1 activation by Ccs have been proposed. We have previously shown a mechanism of Sod1 activation by Ccs in the model organism S. cerevisiae, which has Sod1 and Ccs that are structurally and functionally homologous to human. Despite this, there are still many questions on how applicable this model is for the activation mechanism in human cells, with some data in seeming conflict with the proposed mechanism. The data presented here helps to disambiguate these conflicts. We will show that the activation of Sod1 by Ccs in humans is broadly the same as in S. cerevisiae, but there are some important differences.

Introduction

Superoxide dismutase 1 (Sod1) is a Cu, Zn antioxidant critical to the healthy function of cells (1, 2). It is thought to be the first antioxidant in our evolutionary history, with a functional homologue present in every aerobic organism (3). It is a perfect enzyme that catalyzes the dismutation of reactive oxygen species (ROS) to water and hydrogen peroxide (4). In humans, it

is present in all tissues and almost every intracellular compartment but is mainly found in the cytosol (5). In addition to its antioxidant function, it also acts as a signal either by binding to DNA as a transcription factor or by directing the action of other enzymes by changing local hydrogen peroxide concentrations (6, 7).

Considering the robust activity and prevalence of Sod1, it is no surprise that it plays a role in many cell functions, from apoptosis to cell division (8, 9). It is also no surprise that abnormal Sod1 activity corresponds to many different disease states, including neurodegenerative diseases like amyotrophic lateral sclerosis (ALS) or Parkinson's disease and many types of cancer (10-12). For all of these reasons, Sod1 has been a popular topic of research for decades and may be one of the most studied enzymes.

Sod1 does not begin existence with all these amazing abilities, however. It is translated in an immature state that lacks activity and must be matured to gain its full function (13). The maturation process requires three post-translational modifications (PTMs) to be complete: addition of zinc, addition of copper, and formation of a disulfide bond (14). The copper chaperone of Sod1 (Ccs) assists Sod1 in all three modifications by stabilizing zinc binding, delivering copper, and catalyzing the formation of the disulfide bond (15).

Ccs is one of several copper chaperones that deliver copper to target enzymes within cells (16). Copper is a reactive metal and must be prevented from engaging in damaging interactions with carbon-based molecules (17). Ccs has three domains that each contribute to its function (18). Domain 1 has a conserved copper-binding motif, MxCxxC, and is similar in structure to another copper chaperone, Atox1 (19). Domain 2 is structurally homologous to Sod1 and contains the binding site for immature Sod1 (20). In human Ccs (hCcs), the zinc-binding loop of Sod1 is also

conserved in this region and binds zinc (21). Domain 3 contains another copper-binding motif, CxC, and is known to form the disulfide bond on Sod1 (22). This domain is the smallest of the three and is unstructured in most crystal images (13). Ccs picks up a copper from one of the sources in the cell, such as Ctr1, and binds the copper until it is delivered to Sod1, thus fulfilling its copper chaperone role (16).

In addition to the standard copper chaperone function, we have recently reported a molecular chaperone function for Ccs (15). Binding of Ccs to Sod1 helps to stabilize the zinc affinity of Sod1. This is likely due to a Ccs-driven change in the conformation of the zinc-binding loop of Sod1 which stabilizes it in a favorable conformation for zinc to bind.

We have previously published a mechanism for the activation of Sod1 by Ccs in S. cerevisiae, which we are referring to as "yeast" in this manuscript (14). Yeast Ccs (yCcs) and yeast Sod1 (ySod1) are structural and functional homologues for human Ccs (hCcs) and Sod1 (hSod1) and can rescue each other's function within cells. Ccs was first discovered in yeast, and yeast Ccs has been an important point of study in understanding the activation of Sod1 (18). In our mechanism, domain 3 forms a β-hairpin structure upon binding copper and pivots from interacting with yCcs domain 1 to interacting with Sod1 at an "entry site" at the residues where the disulfide bond will form. This pivot mechanism involves a "hinge" residue, W222, that must allow the motion, and a "latch" residue, W237, that stabilizes the position of domain 3. The copper is drawn toward the high-affinity active site of Sod1 and formation of the disulfide bond locks it in place. The formation of the disulfide bond is initiated by the addition of a transient sulfenic acid group on Sod1 by Ccs domain 3 (13, 14).

Despite this clear mechanism in yeast, there still exists some contention on how the hCcs mechanism proceeds. Some data suggests that hCcs domain 1 is responsible for the transfer of copper to Sod1, rather than domain 3 as shown in yeast (23). This would mean that hCcs domain 3 is solely responsible for the formation of the disulfide bond on Sod1 and has been proposed to not occur through formation of sulfenic acid intermediates, but through a disulfide shuffle mechanism where a pre-formed disulfide bond on domain 3 is transferred to Sod1. Here, we will show results that clarify these questions about the hCcs activation of Sod1 mechanism and discuss the similarities and differences found in the two mechanisms.

Materials and Methods

Construct generation

Constructs of hSod1 and hCcs were originally gifted by Dr. John Hart in pAG8H vectors for bacterial expression with an N-terminal His8 tag and tobacco etch virus (TEV) site. Mutations were made using a Site-Directed Mutagenesis Kit by Promega. Mutations were confirmed by Sanger sequencing through Macrogen, now Psomagen.

Constructs of hSod1 and hCcs for expression in S. cerevisiae were ordered from Vector Builder. The cDNA for the hSod1 gene was inserted with a C-terminal Strep tag into a pYAC vector containing leu2. This was placed under the control of the yeast endogenous promoter for Sod1, which was the same genetic region previously described.(22) The cDNA for the hCcs gene was similarly placed under the control of the yeast endogenous promoter for yCcs on a pYAC vector containing his3. Mutations to these constructs were made also using a Site-Directed Mutagenesis Kit by Promega and confirmed by Sanger sequencing through Macrogen, now Psomagen.

Bacterial expression

Constructs were transformed into competent E. coli BL21 DE3 pLysS and grown at 37°C to an OD600 between 0.6-0.8. These were induced with isopropyl 1-thio-β-D-galactopyranoside (1 mM) and grown for 4 hours at 37°C 250 rpm. Each protein was purified with a HisTrap 5 mL Ni column using a 20 mM Tris, pH 8.0, 300 mM NaCl, 2 mM dithiothreitol (DTT).

Yeast expression

Saccharomyces cerevisiae strains were grown in SC-glucose (dextrose) (SCD) medium at 30 °C unless otherwise noted. BY4741 strain containing a double deletion (ΔySod1/ΔyCcs) was generously gifted by Dr. Val Culotta. Yeast were chemically transformed using the protocol described by Dr. Gietz.(24) Strains were grown to an OD600 of 1.0 before harvesting.

Copper affinity

Cu-binding affinity experiments were performed in a nitrogen-purged anaerobic glovebox. Samples were made oxygen-free with at least three vacuum/nitrogen cycles on a Schlenk line. Cu(I)-CCS samples (20 μM, pH 7.4) were reacted with 1 mM Bathocuproinedisulfonic acid (BCS) and incubated for 15 h. The absorbance of the (Cu(I)L2)3- complex formed was then measured using Cary 300 UV-visible spectrophotometer (Agilent) at 483 nm for L = BCS (ε = 13,000 M-1 cm-1). Calculations were done as previously described. (15) Affinity assays were performed in a 50 mM Tris, pH 7.4, 150 mM NaCl, 0.5 mM Tris(2-carboxyethyl)phosphine (TCEP) buffer.

Activation of Sod1

Bacterially expressed Ccs mutants were anaerobically loaded with Cu(I) at a 1:1 protein:copper ratio and excess copper was removed by buffer exchange with a degassed buffer. Bacterially expressed Sod1 was stripped of metals and disulfide reduced by incubation overnight

at 4°C in a 100 mM acetic acid, pH 3.8, 10 mM Ethylenediaminetetraacetic acid (EDTA), 10 mM TCEP buffer, followed by incubation overnight at 4°C in a 100 mM sodium acetate, pH 5.5, 150 mM NaCl buffer that was treated to remove free metals. The metal-free Sod1 (apo-Sod1) was then buffer exchanged to a 50 mM Tris, pH 7.6, 150 mM NaCl, 0.5 mM TCEP, 200 μM BCS buffer for experiments. During activation assays, Ccs was incubated with Sod1 in a 5:1 ratio to ensure maximum activation was achieved. Reactions were incubated at room temperature in atmospheric oxygen for 20 minutes. After this, 5% glycerol was added and an equal amount of each reaction was loaded onto a metal-free non-reducing PAGE gel and run in a metal-free buffer. The gel was then incubated in a mixture of riboflavin and nitro blue tetrazolium in the dark for 15 minutes, then transferred to a 0.01% Tetramethylethylenediamine (TEMED) solution and incubated for another 15 minutes in the dark. Finally, the gel was exposed to light and developed and images were taken on a ChemiDoc. Band intensities were compared to determine qualitative activation strength.

Pulldown assay of yeast lysate

Yeast expressing hSod1 and hCcs were lysed by sonication in a 50 mM Tris, pH 7.6, 150 mM NaCl, 2 mM TCEP buffer and centrifuged to remove the pellet. Lysate supernatant was incubated with Strep-tactin beads for 1 hour at room temperature. Beads were washed 3 times with buffer, then boiled in 100 μL 2x Laemmli dye with β-mercaptoethanol (BME) to elute protein. Equal amounts of supernatant were loaded on a 14% SDS-PAGE gel and transferred to nitrocellulose membrane for western blotting. Rabbit-α-Sod1 and rabbit-α-Ccs primary antibodies were incubated on the membrane in a 1:10,000 TBS-T solution. Goat-α-rabbit-HRP secondary was used to image blot. Images were taken with a ChemiDoc.

Sulfenic acid identification

Yeast cells were lysed in a 50 mM Tris, pH 7.6, 150 mM NaCl, 2 mM TCEP, 2.5 mM dimedone buffer. Dimedone binds specifically to sulfenic acid and can be detected by and antibody as described previously. (22) Lysate supernatant was incubated on Strep-tactin beads for 1 hour at room temperature. Beads were washed 3 times and eluted by boiling in 100 μM 2x Laemmli dye with BME. Equal amounts of elutions were run on a 14% SDS-PAGE gel and transferred to a nitrocellulose membrane. A 1:10,000 rabbit-α-dimedone/sulfenic acid primary antibody and a 1:10,000 goat-α-rabbit-HRP secondary antibody were used to detect the presence of the sulfenic acid on Sod1.

Results

Domains 1 and 3 work together to bind copper.

Table 4.1. Copper affinities of hCcs.

Ccs mutants	**Cu(I) affinity (M)**
hCcs	$3.40 \pm 0.23\ E^{-19}$
MxAxxA	$4.29 \pm 1.09\ E^{-18}$
AxA	$1.59 \pm 1.42\ E^{-18}$

hCcs has two copper binding motifs, an MxCxxC motif in domain 1 and a CxC motif in domain 3. Alanine substitutions made in the cysteine residues of one motif allow us to measure the Cu(I) affinity only at the other motif. The affinity for each motif to bind one Cu(I) ion or for the wild-type Ccs to bind one Cu(I) ion is shown above (**Table 4.1**). The affinity of either copper motif alone is approximately 10-fold less than when both are present. This increase in affinity shows that both domain 1 and domain 3 are participating in binding one Cu(I) ion.

While domain 1 is necessary for function, domain 3 delivers copper.

Ccs function was measured by assaying Sod1 activity (**Fig. 4.1**). Mutations made to the MxCxxC motif (MxAxxA) showed little effect on Sod1 activation, while mutations to the CxC motif (AxA) showed a pronounced lack of Sod1 activity (**Table 4.2**). This indicates that the CxC motif in domain 3 is necessary and sufficient for activation of Sod1, able to both deliver Cu(I) and form the disulfide bond by itself. However, if domain 1 is completely removed from Ccs (D1D), then Ccs loses the ability to activate Sod1 almost completely (**Table 4.2**). This shows that domain 1 is playing some role other than copper binding or delivery that is necessary for Sod1 activation. As expected, domain 3 deletion (D3D) behaves similarly to AxA, and mutating both copper motifs severely reduces Sod1 activation as there is very little chance that Sod1 can pick up a copper and activate (**Table 4.2**). Since AxA has a pronounced effect on Sod1 activation, mutations were made in each of the cysteine residues (C244A and C246A) to determine if one has a more pronounced role than the other. Mutations to either of the CxC cysteines only slightly decreased Sod1 activation (**Table 4.2**). This shows that one cysteine in domain 3 is enough to successfully activate, and that it does not matter which residue is present.

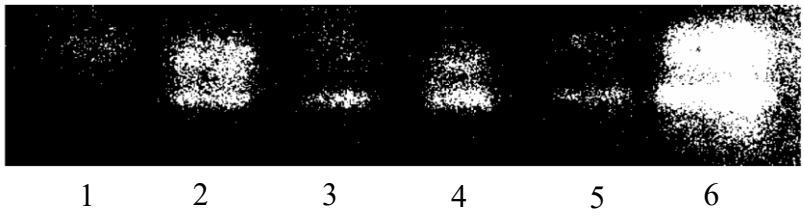

Fig. 4.1. Activation assays measure Ccs function. This is a sample Sod1 activation assay showing that the level of Sod1 activity changes when mutations are made to Ccs. Lane 1: apo-Sod1, Lane 2: apo-Sod1 + Cu(I) MxAxxA Ccs, Lane 3: apo-Sod1 + Cu(I) AxA Ccs, Lane 4: apo-Sod1 + Cu(I) D3D Ccs, Lane 5: apo-Sod1 + Cu(I) MxAxxA/AxA Ccs, Lane 6: apo-Sod1 + Cu(I) Ccs. Similar assays were performed for each mutant, contributing to the table below.

Table 4.2. Ability of hCcs mutants to activate Sod1. One * is little/no activity.

Ccs mutant	**Sod1 activation**
Ccs	*****
MxAxxA	****
AxA	*
MxAxxA/AxA	*
D1D	*
D3D	*
C244A	****
C246A	****
F237A	*
W252A	**

The two residues homologous to the yCcs “hinge” and “latch” were mutated to see if the same physical motion could explain both mechanisms (**Table 4.2**). The homologous “hinge” mutant (F237A) showed almost no activity, while the homologous “latch” mutant (W252A) showed some activity. This is opposite what was observed in yeast and does not support the hypothesis that the same motion is present in hCcs.

Disulfide formation is not the result of disulfide shuffling.

Aside from delivery of Cu(I), the other major task of Ccs in Sod1 activation is the formation of the disulfide bond. It has been suggested that Sod1 may form the disulfide bond through a disulfide shuffling event where a pre-formed disulfide bond on Ccs domain 3 is transferred to Sod1.(23) This is already made very unlikely by the fact that either cysteine in domain 3 is able to activate Sod1 alone (**Table 4.2**) as it is not possible to have a pre-formed disulfide bond on one cysteine. To see if it was possible to form the sulfenic acid intermediate on Sod1 without the presence of a pre-formed disulfide bond, we moved the CxC motif cysteines into adjacent positions (C245/C246). With the two residues immediately adjacent to each other it is impossible to form a disulfide bond between them. A pulldown was performed on yeast lysate expressing hSod1 and a mutant of hCcs (**Fig. 4.2**). When hCcs is unable to activate hSod1, it forms a stable complex with the immature Sod1 and will be pulled down with it. From the assay, we see that C244A and C246A are both able to activate Sod1, as confirmed by the in vitro assays above (**Fig. 4.1**). AxA hCcs is unable to activate Sod1 and forms a stable complex, appearing in the western. C245/C246 hCcs activates Sod1 and so does not remain bound to it. We therefore see that hCcs is able to form the disulfide bond on Sod1 when it cannot have a pre-formed disulfide bond on domain 3.

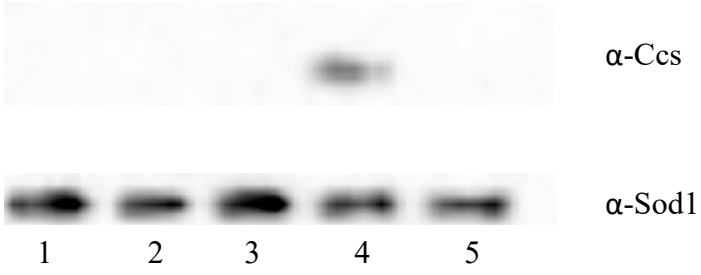

Figure 4.2. The disulfide bond is not pre-formed. Western blot showing the elutions of a pulldown of yeast lysate expressing hSod1 and a variant of hCcs. hSod1 was pulled down using Strep-tactin

beads. Lane 1: hSod1 + hCcs, Lane 2: hSod1 + C244A Ccs, Lane 3: hSod1 + C246A hCcs, Lane 4: hSod1 + AxA hCcs, Lane 5: hSod1 + C245/C246 hCcs.

Previously, we reported that the disulfide bond was formed through addition of a sulfenic acid intermediate to Sod1 by Ccs. In vitro, we found that either C57 or C146 of hSod1 could accept the sulfenic acid, however it was unclear if this was an artifact of performing the experiment in atmospheric levels of oxygen. To confirm this result, C57S hSod1 and C146S hSod1 were expressed in yeast cells with hCcs at endogenous levels. The yeast provided a reducing cellular environment that could be compared to previous results. It was found that both C57 and C146 of hSod1 could accept the sulfenic acid intermediate in the cellular environment, confirming the accuracy of our in vitro assay (**Figure 4.3**).

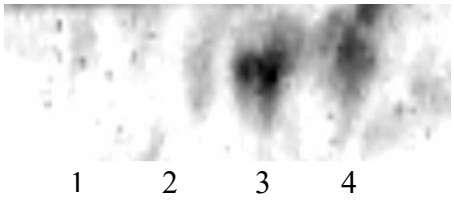

Figure 4.3. Sulfenic acid forms on either C57 or C146 of hSod1. Yeast expressing hCcs and a variant of hSod1 were lysed and incubated with 2.5 mM dimedone. The hSod1 was then pulled down using Strep-tactin beads. Lane 1: beads alone, Lane 2: hSod1 + hCcs, Lane 3: C57S hSod1 + hCcs, Lane 4: C146S hSod1 + hCcs. Sulfenic acid was detected strongly on both mutants.

All three Ccs domains work synergistically

Domain 2 of hCcs is structurally similar to Sod1 and retains the zinc loop and zinc binding ability. While this zinc site has been known for decades, it was previously impossible to measure the affinity as there were no zinc chelators with competitive affinities available. Using a new chelator, TPEN, with a technique we previously established by measuring Sod1 zinc affinity, we were able to measure the zinc affinity of Ccs. Surprisingly, we found the zinc affinity to be very high, at $2.01 \pm 0.34\ E^{-19}$ M, which has been published prior to this (15). We then examined if

mutations to domain 1 or 3 might affect zinc affinity. When domain 1 or 3 were deleted, there was a significant decrease in affinity corresponding to almost a 10-fold drop (**Table 4.3**). To further examine this, the copper binding mutants were tested to see if the reactive cysteines in these motifs might be contributing. We found that the AxA mutant had a slight decrease in zinc affinity, but the MxAxxA mutant had a very dramatic decrease of almost 100-fold (**Table 4.3**). Mutations made to either of the cysteines in the MxCxxC motif of domain 1 (C22A and C25A) decreased the zinc affinity by approximately half of what was seen when both are mutated (**Table 4.3**), suggesting that each contributes approximately equally to the overall weakening of affinity. This highlights the inter-connected nature of hCcs, where all three domains are synergistically working together, and failure of any part affects the whole.

Table 4.3**.** Zinc affinity of hCcs mutants.

Ccs mutant	**Zinc affinity (M)**
hCcs	**$2.01 \pm 0.34\ E^{-19}$**
D1D	**$6.54 \pm 0.06\ E^{-18}$**
D3D	**$3.74 \pm 0.05\ E^{-18}$**
MxAxxA/AxA	**$2.24 \pm 0.04\ E^{-18}$**
MxAxxA	**$2.95 \pm 0.10\ E^{-17}$**
AxA	**$8.45 \pm 0.01\ E^{-19}$**
C22A	**$1.81 \pm 0.42\ E^{-18}$**
C25A	**$1.91 \pm 0.50\ E^{-18}$**

Discussion

The first point of comparison between human and yeast Ccs is their ability to bind copper. We had previously reported that domain 1 of yCcs binds copper at $3.61 \pm 1.00 \times 10^{-17}$ M and domain 3 can bind copper at $2.33 \pm 0.22 \times 10^{-17}$ M (14). We have also seen that wild-type yCcs binds one copper ion more tightly than either domain can alone, at $1.15 \pm 0.52 \times 10^{-19}$ M (unpublished data). We show that hCcs has a similar trend, with domain 1 and 3 binding at similar affinities, $4.29 \pm 1.09\ E^{-18}$ M and $1.59 \pm 1.42\ E^{-18}$ M and the wild-type binding at $3.40 \pm 0.23\ E^{-19}$ M (**Table 4.1**). Human Ccs has an overall higher affinity for copper than yCcs, but the wild-type affinity is about 10-fold higher in both proteins. The increase in affinity when both domains are able to bind shows that the copper sites of domain 1 and 3 are cooperatively binding the ion, which supports other group's results that Cu(I) was bound between cysteines on domain 1 and 3 on Ccs (25).

The activation of Sod1 by Ccs is an important measure of Ccs functionality. Previously, domain 1 was shown to be highly important as the deletion of this domain abolished copper delivery to Sod1. Similarly, we show that deletion of domain 1 also halts Sod1 activation, however the mutation of only the copper binding residues in domain 1 had little effect on Sod1 activation. This indicates that domain 1 has a critical function not involving copper binding necessary for Sod1 activation, possibly some kind of necessary conformational change or stabilizing effect. However, this disagrees with a model in which domain 1 delivers copper to Sod1. When domain 3 is deleted or the copper binding motif is mutated, there is a significant decrease in Sod1 activation. This supports a model where domain 3 is primarily responsible for copper delivery. If we consider that domain 1 and 3 are cooperatively binding the copper before Sod1 binding to Ccs

initiates delivery of that copper by domain 3, this indicates a model where Ccs domain 3 pivots between interaction with domain 1 via Cu(I) and Sod1, exactly what was seen in the yeast model.

The cysteines in domain 3 of yCcs are not equally important to Sod1 activation. C231, which is positioned closer to Sod1 during interaction, is much more important to Sod1 activation. Mutation of this residue results in an almost complete inability to activate Sod1, accounting for almost all functionality of yCcs domain 3. A mutation made to the homologous residue of hCcs, C246A, showed almost no decrease in activation of Sod1. A mutation made to the other domain 3 cysteine, C244A, had similarly little effect. In contrast to yCcs, hCcs does not seem to have the same rigid importance of position, with either cysteine residue in domain 3 able to complete the activation of Sod1.

Previously, activation assays were performed on yCcs to a “hinge” amino acid (F237A) and a “latch” amino acid (W252A) showing that the hinge was less restrictive than the latch (15). Homologous residues in hCcs were similarly mutated, however the results were the opposite of those seen in yeast. The hypothesized “latch” was less restrictive than the “hinge” in Sod1 activation. This indicates that the movement of domain 3 in hCcs is different to that in yCcs in an unknown way, even though the function of the movement is the same.

In our yCcs model for Sod1 activation, we showed that yCcs domain 3 forms the disulfide bond on Sod1 via a sulfenic acid intermediate (22). We demonstrated that this occurs in vitro on both hSod1 and ySod1, however ySod1 is more restricted in which cysteine can accept the sulfenic acid. Only C57 in ySod1 contained the intermediate, but both C57 and C146 of hSod1 had been modified in approximately equal numbers. It was suggested that this may be due to the greater propensity of hSod1 to become oxidized than ySod1, so these tests were repeated with hSod1 and

hCcs expressed in yeast cells at endogenous yeast levels. A large portion of the wild-type Sod1 is activated, so few intermediates were detected. When C57 or C146 are mutated to serine, it becomes impossible for the disulfide bond to form and sulfenic acid intermediates can be "trapped" and measured via addition of dimedone. Both C57S Sod1 and C146S Sod1 showed sulfenic acid additions, indicating that the difference between ySod1 and hSod1 is not due to different sensitivities to environmental oxidation.

Finally, the main difference between yCcs and hCcs was examined: the ability to bind zinc. This is specific to hCcs domain 2, which more closely resembles Sod1 than yCcs (13, 26). We find that hCcs has a much stronger affinity for zinc than Sod1, which was unexpected as the zinc site is structurally homologous to the Sod1 site. One possible reason for the strengthened affinity is that domain 1 and/or 3 are contributing to the zinc affinity of domain 2, so each domain was deleted and the zinc affinity tested. We found that deletion of either domain weakened the zinc affinity significantly, with a slightly higher effect from domain 1. This supports the theory that domain 1 plays a structural role in hCcs.

Overall, we find that the mechanism of Sod1 activation by hCcs is highly similar to yCcs. Each of the domains performs a similar role, with domain 1 helping to bind copper, domain 2 binding Sod1, and domain 3 delivering copper and catalyzing the formation of the disulfide bond. At the same time, there are clear differences. Domain 1 of hCcs has greater importance to its function, likely by helping the structure stabilize in a favorable conformation for Sod1 activation. Domain 2 has an additional zinc binding function. Domain 3 does not seem to "pivot" in the same way as domain 3 of yCcs, and the function of each cysteine residue is more flexible in the human protein. In yCcs, each function is assigned to a specific domain, or even a specific residue, and

these are carried out independently of what other parts are doing. In contrast, hCcs spreads out it roles across multiple parts that work synergistically. In some cases, this adds resilience where a mutation in one residue or domain does not eliminate the function as is the case in domain 3 where the mutation of either cysteine does not abort function. In other cases, it seems to create fragility, where problems in one area weaken the whole, which is seen in the zinc affinity where mutations made in domain 1 or 3 have a strong impact on domain 2. The reason for this may be the greater regulation necessary in multicellular organisms, as compared to single-celled organisms. Human Ccs must activate Sod1 in a variety of tissues for a variety of reasons; a simple mechanism where one structural component has one function may not be the most efficient way to address this variety of roles.

References

1. J. M. McCord, I. Fridovich, Superoxide dismutase. An enzymic function for erythrocuprein (hemocuprein). J Biol Chem 244, 6049-6055 (1969).

2. A. G. Reaume et al., Motor neurons in Cu/Zn superoxide dismutase-deficient mice develop normally but exhibit enhanced cell death after axonal injury. Nat Genet 13, 43-47 (1996).

3. G. N. Landis, J. Tower, Superoxide dismutase evolution and life span regulation. Mech Ageing Dev 126, 365-379 (2005).

4. J. M. McCord, I. Fridovich, Superoxide Dismutase: An Enzymic Function for Erythrocuprein (Hemocuprein). J. Biol. Chem. 244, 6049-6055 (1969).

5. C. JD, O. T, R. C, Slot JW, C. LY. (Proc Natl
Acad Sci U S A, 1992 Nov 1), vol. 89, pp. 10405-10409.

6. C. K. Tsang, Y. Liu, J. Thomas, Y. Zhang, X. F. Zheng, Superoxide dismutase 1 acts as a nuclear transcription factor to regulate oxidative stress resistance. Nat Commun 5, 3446 (2014).

7. J. C. Juarez et al., Superoxide dismutase 1 (SOD1) is essential for H2O2-mediated oxidation and inactivation of phosphatases in growth factor signaling. Proc Natl Acad Sci U S A 105, 7147-7152 (2008).

8. H. L. Liang et al., Partial attenuation of cytotoxicity and apoptosis by SOD1 in ischemic renal epithelial cells. Apoptosis 14, 1176-1189 (2009).

9. E. Cova et al., G93A SOD1 alters cell cycle in a cellular model of Amyotrophic Lateral Sclerosis. Cell Signal 22, 1477-1484 (2010).

10. M. E. Gurney et al., Motor neuron degeneration in mice that express a human Cu,Zn superoxide dismutase mutation. Science 264, 1772-1775 (1994).

11. B. G. Trist et al., Accumulation of dysfunctional SOD1 protein in Parkinson's disease is not associated with mutations in the SOD1 gene. Acta Neuropathol 135, 155-156 (2018).

12. L. Papa, G. Manfredi, D. Germain, SOD1, an unexpected novel target for cancer therapy. Genes Cancer 5, 15-21 (2014).

13. M. M. Fetherolf, S. D. Boyd, D. D. Winkler, D. R. Winge, Oxygen-dependent activation of Cu,Zn-superoxide dismutase-1. Metallomics 9, 1047-1059 (2017).

14. S. D. Boyd, L. Liu, L. Bulla, D. D. Winkler, Quantifying the Interaction between Copper-Zinc Superoxide Dismutase (Sod1) and its Copper Chaperone (Ccs1). J Proteomics Bioinform 11, (2018).

15. S. D. Boyd et al., The yeast copper chaperone for copper-zinc superoxide dismutase (CCS1) is a multifunctional chaperone promoting all levels of SOD1 maturation. J Biol Chem 294, 1956-1966 (2019).

16. S. D. Boyd, M. S. Ullrich, A. Skopp, D. D. Winkler, Copper Sources for Sod1 Activation. Antioxidants (Basel) 9, (2020).

17. E. R. Stadtman, Berlett, B. S., Fenton Chemistry: Amino Acid Oxidation. JBC 266, 17201-17211 (1991).

18. V. C. Culotta et al., The copper chaperone for superoxide dismutase. J Biol Chem 272, 23469-23472 (1997).

19. T. D. Rae, Torres, A. S., Pufahl , R. A., and O'Halloran, T. V., Mechanism of Cu,Zn-superoxide dismutase activation by the human metallochaperone hCCS. Journal of Biological Chemistry 276, (2001).

20. P. J. Schmidt et al., Multiple Protein Domains Contribute to the Action of the Copper Chaperone for Superoxide Dismutase. J. Biol. Chem. 274, 23719-23725 (1999).

21. P. J. Schmidt, M. Ramos-Gomez, V. C. Culotta, A Gain of Superoxide Dismutase (SOD) Activity Obtained with CCS, the Copper Metallochaperone for SOD1. J. Biol. Chem 274, 36952-36956 (1999).

22. M. M. Fetherolf et al., Copper-zinc superoxide dismutase is activated through a sulfenic acid intermediate at a copper ion entry site. J Biol Chem 292, 12025-12040 (2017).

23. L. Banci, Bertini, I., Cantini, F., Kozyreva, T., Massagni, C., Palumaa, P., Rubino, J. T. and Zovo, K., Human superoxide dismutase 1 (hSOD1) maturation through interaction with human copper chaperone for SOD1 (hCCS). Proc Natl Acad Sci U S A 109, 13555-13560 (2012).

24. R. D. Gietz, Yeast transformation by the LiAc/SS carrier DNA/PEG method. Methods Mol Biol 1205, 1-12 (2014).

25. J. F. Eisses, J. P. Stasser, M. Ralle, J. H. Kaplan, N. J. Blackburn, Domains I and III of the Human Copper Chaperone for Superoxide Dismutase Interact via a Cysteine-Bridged Dicopper(I) Cluster. Biochemistry 39, 7337-7342 (2000).

26. T. D. Rae, A. S. Torres, R. A. Pufahl, T. V. O'Halloran, Mechanism of Cu,Zn-Superoxide Dismutase Activation by the Human Metallochaperone hCCS. J. Biol. Chem. 276, 5166-5176 (2001).

CHAPTER 5

MUTATIONS IN SUPEROXIDE DISMUTASE 1 (SOD1) LINKED TO FAMILIAL AMYOTROPHIC LATERAL SCLEROSIS CAN DISRUPT HIGH-AFFINITY ZINC-BINDING PROMOTED BY THE COPPER CHAPERONE FOR SOD1 (CCS)

Stefanie D. Boyd, Morgan S. Ullrich, Jenifer S. Calvo, Fatemeh Behnia, Gabriele Meloni, and Duane D. Winkler

The Department of Biological Sciences, BSB12
The Department of Chemistry and Biochemistry, BSB13

The University of Texas at Dallas

800 West Campbell Road

Richardson, Texas 75080-3021

Abstract

Zinc (II) ions (hereafter simplified as zinc) are important for the structural and functional activity of many proteins. For Cu, Zn superoxide dismutase (Sod1), zinc stabilizes the native structure of each Sod1 monomer, promotes homo-dimerization and plays an important role in activity by "softening" the active site so that copper cycling between Cu(I) and Cu(II) can rapidly occur. Previously, we have reported that binding of Sod1 by its copper chaperone (Ccs) stabilizes a conformation of Sod1 that promotes site-specific high-affinity zinc binding. While there are a multitude of Sod1 mutations linked to the familial form of amyotrophic lateral sclerosis (fALS), characterizations by multiple research groups have been unable to realize strong commonalities among mutants. Here, we examine a set of fALS-linked Sod1 mutations that have been well-characterized and are known to possess variation in their biophysical characteristics. The zinc affinities of these mutants are evaluated here for the first time and then compared with the previously established value for wild-type Sod1 zinc affinity. Ccs does not have the same ability to promote zinc binding to these mutants as it does for the wild-type version of Sod1. Our data provides a deeper look into how (non)productive Sod1 maturation by Ccs may link a diverse set of fALS-Sod1 mutations.

Introduction

Zinc ions are essential trace metals necessary for life. Zinc plays an important structural role in many proteins needed for cell function [1] and there are families of enzymes that use zinc as a catalytic cofactor [2,3]. However, it is not well understood how proteins acquire zinc. Zinc transporters are responsible for importing the ion into the cell and moving it to intracellular compartments such as the endoplasmic reticulum, golgi or nucleus where many proteins requiring

zinc are metallated [4]. It has been hypothesized that zinc ions are acquired from a labile pool that exists within the cell, but no conclusive evidence exists related to an exact mechanism [5,6].

One of the proteins that requires zinc is Cu, Zn superoxide dismutase (Sod1), an antioxidant enzyme constitutively expressed in humans and other aerobic organisms [7]. Sod1 catalyzes the dismutation of superoxide; turning superoxide radical into water and hydrogen peroxide in a two-step "ping-pong" reaction [8]. It is present throughout the cell, but is most abundant in the cytosol [9]. Sod1 must be "activated", which requires three post-translational modifications: zinc binding, copper insertion and formation of an intramolecular disulfide bond [8,10,11]. We and others have shown strong evidence that the copper chaperone for Sod1 (Ccs) assists Sod1 in obtaining each of these modifications [10,12,13].

Zinc plays a dual role in Sod1, as it supports both structural stability and enzyme function [13,14]. The binding of zinc by Sod1 stabilizes a region of the enzyme called the "zinc loop", which significantly decreases Sod1 misfolding and degradation [15]. Zinc binding also assists the enzymatic proficiency of Sod1. Sod1 binds a copper ion in its active site that cycles between Cu(I) and Cu(II) redox states as Sod1 rids the cell of superoxide anions. When the copper is in a reduced form, it binds three histidine residues (H46, H48, H120), and when it is oxidized it binds four histidines (H46, H48, H120, and H63). Zinc is bound in a nearby site by three histidine residues (H63, H71, H80) and a single aspartate (D83). H63 "bridges" the copper and zinc ions, easing the transition between Cu(I) and Cu(II),thereby increasing enzymatic activity 10-fold [6,16].

Mutations to the gene coding for Sod1 are linked to an inherited form of amyotrophic lateral sclerosis (fALS), a neurodegenerative disease resulting in paralysis and eventual death [17,18]. Mutations in Sod1 are the cause of 20% of fALS cases, where a point mutation in a single

copy of the sod1 gene leads to fALS through a toxic "gain-of-function" [19]. There are a multitude of Sod1 mutations that are known to cause fALS, and upwards of 130 sites in Sod1 are disease related. Aggregates containing Sod1 and Ccs can be found in neural tissue expressing fALS-Sod1 mutants, which often lack correct binding of one or both metals and the disulfide bond [20–23].

While all of the fALS-Sod1 mutations lead to the same disease and outcome, the rates of disease progression vary widely between mutations [24,25]. A4V is the most common mutation in North America, accounting for 50% of Sod1-linked fALS cases [26]. It is also one of the most aggressive forms of ALS, with average survival persisting less than 2 years after diagnosis [27,28]. A4V Sod1 can reach full maturity (copper and zinc bound with an oxidized disulfide bond (i.e., Cu,Zn-Sod1^{SS})) in the cell [29] and has even been shown to have a stronger affinity for copper than wild-type Sod1 [30]. Interestingly, unlike many other fALS-Sod1 mutations, there is no mouse model for A4V, as transgenic mice do not exhibit any symptoms [31].

G93A is another frequently studied mutation. It was one of the earliest established mouse models for the disease and is well-characterized [32]. In this model, metal-free (apo) disulfide reduced G93A (E,E-G93A^{SH}) is the primary component of intracellular aggregates, yet a significant amount of fully metallated G93A is present in the soluble fraction [33]. The G85R Sod1 mutation is a commonly used model as the onset of paralytic symptoms corresponds well with the appearance of Sod1 aggregation bundles in neural cells [34]. This form of Sod1 is consistently disulfide reduced, under metallated and/or mis-metallated inside cells [33,35]. The crystal structure shows a novel zinc-coordinating water molecule present in the zinc loop that is speculated to affect zinc affinity [28,36].

Unlike the previous mutations discussed, H80R Sod1 is a metal-binding mutant. H80 is one of the 4 residues responsible for binding zinc, and its mutation to arginine completely abolishes zinc binding at the zinc loop. However, the crystal structure shows that a zinc ion is coordinated at the adjacent active site in place of copper (Zn,E-H80R^{SH}) [37]. This type of mis-metallation is often observed in fALS-Sod1 mutants, even when an intact zinc site is present [38].

Each of these well-studied mutants has different inherent characteristics and locations within the Sod1 structure (**Figure 5.1**); however, all of them lead to the same disease. It is currently unknown what mutual characteristic links these proteins to acquiring fALS symptoms. Additionally, there has lacked clear data showing the effect these mutations have on zinc affinity and the chaperoning actions of Ccs. In this work, we aim to analyze this effect by examining the zinc affinity of these mutations in various stages of maturation. The role of Ccs in facilitating zinc acquisition by Sod1 has been recently published [16]. Here, we further elucidate the changes caused in this interaction by fALS mutations. By providing this missing characteristic, we draw closer to understanding the behavior of Sod1 and any potential role(s) for Ccs in fALS.

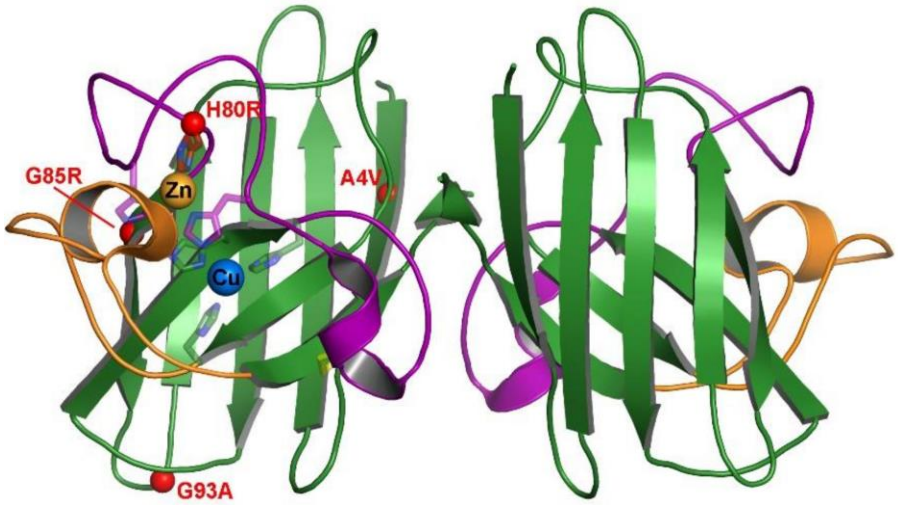

Fig 5.1. Position of select fALS mutations on mature hSod1. The crystal structure is of wild-type Sod1 (1PU0) with the β-barrel colored green, the electrostatic loop colored orange and the connecting zinc and disulfide loops colored purple. The metal binding residue sidechains are

shown as sticks and the metals are shown in their binding sites as labeled spheres. Each of the 4 fALS mutations are shown as small red spheres at their position within the protein structure for visual comparison.

Results

Fluorescent-Labeling of Immature Sod1 Mutants

Sod1 contains two native cysteine residues involved in the essential intra-subunit disulfide bond (C57-C146). Each fALS-Sod1 variant studied here has an additional C146S background mutation, used to enable specific labeling of Sod1 at position C57 with an Alexa-488 fluorescent dye, which also maintains Sod1 immaturity (i.e., disulfide reduced). Ccs will only bind the reduced form of Sod1 [13]. The labeled proteins were individually purified by size exclusion chromatography in order to separate the $Sod1_{488}$ from unbound label (**Figure 5.2**). The fluorescent label is necessary for measuring fine differences in the Sod1•Ccs apparent dissociation constants (K_Ds) as it allows the use of an extremely sensitive detection method (HI-FI) [13,39,40].

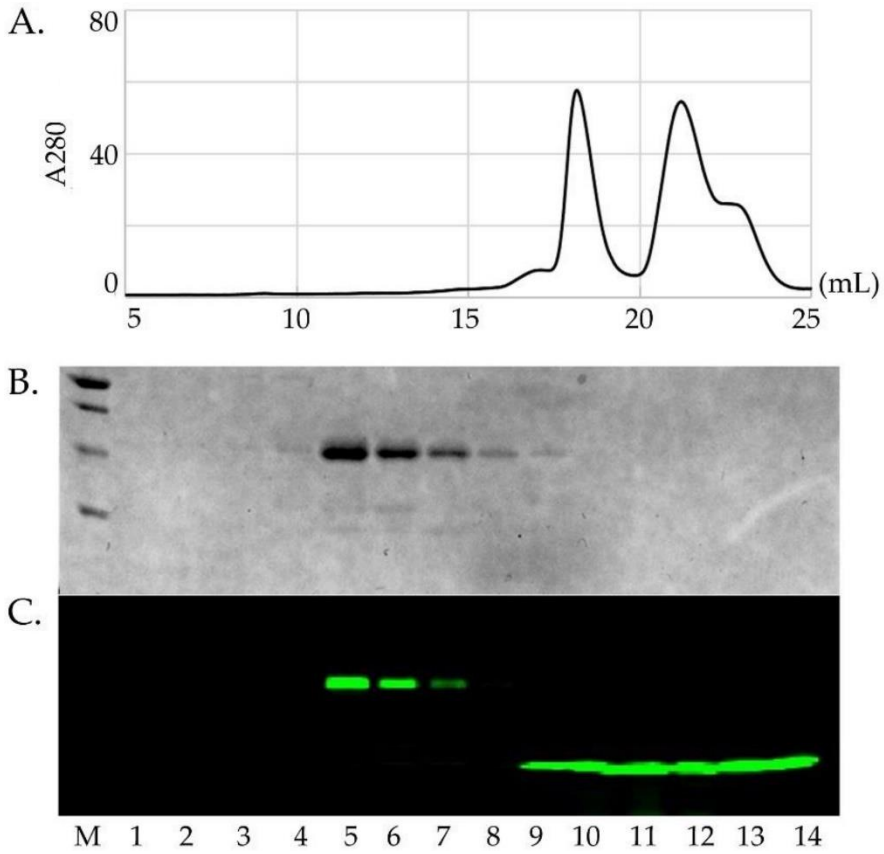

Fig 5.2. Fluorescent labeling and purification of Sod1. Panel (A) shows the purification of an Sod1 protein (left peak, 17–20 mL) after labeling with Alexa488 from the remaining free dye (right peak, 20–24 mL). Panel (B) shows the SDS-PAGE gel of the peak samples imaged by Coomassie staining. Although the free Alexa488 dye shows up in the SEC chromatogram, it does not show up in the Coomassie stained gel. Panel (C) shows the same gel that has been imaged using a fluoro-imager set for the emission wavelength for Alexa488. This shows that the Sod1 protein (lanes 4–8) has been stably conjugated with the dye and separated from the remaining free dye (lanes 9–14).

Ccs Is Not Prevented from Binding Select fALS-Sod1 Mutants

Quantitative binding assays were performed to evaluate differences between fALS-Sod1 interactions with Ccs. The fALS mutants were chosen in an attempt to span the wide variety of metal binding properties (e.g., complete metal binding, mis-metallation, and direct zinc-site disruption) that are seen across the family of pathogenic mutants. Each fALS-Sod1 mutant was kept metal-free (confirmed via ICP-MS) and disulfide reduced (E,E-Sod1^{SH}) using the C146S

mutation. This results in monomeric Sod1 proteins whose dissociation constants can be compared to previously reported data. The binding affinity between Ccs and fALS E,E-Sod1^{SH} are all extremely tight and within the low nano-molar range, showing that these fALS mutations do not inhibit Ccs binding (**Figure 5.3**). The fALS-Sod1•Ccs binding affinities measured: A4V (K_D = 42.06 ± 8.2 nM), H80R (K_D = 67.60 ± 9.4 nM), G85R (K_D = 35.50 ±3.0 nM), and G93A (K_D = 33.42 ± 4.7 nM). Previously, we established the affinity of Ccs for wild-type E,E-Sod1^{SH} as K_D = 22 ± 6.0 nM [13]. This is the first time that the interaction between Ccs and these fALS-Sod1 mutants have been quantified and shows that their aberrant behavior is not due to a lack of Ccs binding by the immature forms of the proteins.

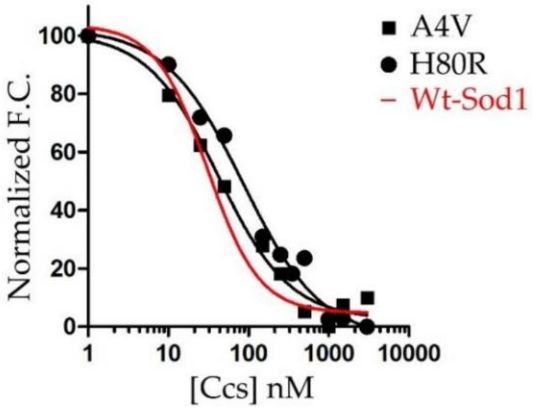

Ccs Interaction with fALS-Sod1	
	KD (nM)
A4V	42.06 +/- 8.2
H80R	67.60 +/- 9.4
G85R	35.50 +/- 3.0
G93A	33.42 +/- 4.7

Fig 5.3. fALS-Sod1 mutants binding with Ccs. The left panel is a combined plot of binding curves for select fALS-Sod1 mutants and Ccs. As shown, the binding curves are comparable to the wT-Sod1 binding curve that we determined previously (red). The right panel shows a list of the fALS-Sod1 mutants that were of focus, here. The KDs are all very similar to that of wild-type Sod1 and show that these particular mutations do not hinder Ccs interaction. All binding assays were performed with the human forms of Sod1 and Ccs.

Ccs Binds Zinc with a High-Affinity

The human form of Ccs binds zinc in its Sod1-like domain 2 (D2) coordinated by residues homologous to those found in the Sod1 β-barrel [8]. We have previously shown that Ccs preferentially binds to a completely immature form of Sod1 (E,E-Sod1^{SH}) [13] and others have

suggested that Ccs may act directly or indirectly to deliver zinc to immature Sod1 [16,41]. Therefore, we wanted to measure the affinity of the Ccs D2 binding site for zinc and expected that the similar nature of Ccs and Sod1 zinc-binding sites would result in similar affinities. Here, using a TPEN-based zinc-chelation assay, we show that the wild-type Ccs zinc dissociation constant is $2.01 \pm 0.34 \times 10^{-19}$ M. This was somewhat surprising as it is ~40-fold tighter than the zinc site in fully mature wild-type Sod1, which was previously measured to be $8.46 \pm 2.83 \times 10^{-18}$ M [16].

Ccs Promotes Site-Specific Metalation of H80R Sod1

Arginine substitution of the zinc-liganding residue H80 prevents zinc binding at the "zinc-site". A previously determined crystal structure of H80R (PDB: 3QQD) shows zinc aberrantly bound at the copper/active site and a reduced disulfide bond (Zn,E-H80R^{SH}) [37]. Since many ALS-Sod1 patient samples have been reported with this kind of mis-metallation [27,42], we used this mutant to measure the affinity of zinc in the copper site. The immature H80R protein bound zinc with an affinity of $2.78 \pm 1.30 \times 10^{-16}$ M (**Table 5.1**). This value is ~32-fold weaker than the zinc binding affinity for the "zinc-site" in wild-type Sod1 and over four orders of magnitude less than the affinity for Cu(I) at this site [16]. Notably, zinc loading into the active site was nearly saturated in the samples, with ~94% of the copper/active sites occupied with zinc (measured by ICP-MS after metal reconstitution and exhaustive washing and listed in **Table 5.1**).

Table 5.1. Zn(II) dissociation constants and occupancies for fALS-Sod1 mutants.

Immature hSod1	**K_D (M)**	**Zn(II) Occupancy**
A4V	$1.91 \pm 0.56 \times 10^{-16}$	49%
H80R		94%
G85R	$1.11 \pm 0.53 \times 10^{-16}$	36%
G93A		20%
hSod1 in complex with yCcs	Fold-Change to measured K_D	
A4V	~2-fold weaker	78%
H80R	2-3-fold weaker	37%
G85R	No Significant change	84%
G93A	No Significant change	73%
Mature hSod1	Fold-Change to measured K_D	
A4V	~9-fold weaker	~100%
G85R	No Significant change	~100%
G93A	~3-fold stronger	~100%

We then formed a complex between H80R Sod1 (hSod1) and yeast Ccs (yCcs). If human Ccs was used here, the result would be an average of the Sod1 zinc affinity and the Ccs zinc affinity. Therefore, we utilized the yeast form of Ccs, which does not bind zinc, but is a structural and functional homologue of human Ccs that binds and promotes Sod1 maturation in a nearly indistinguishable manner [10]. The H80R•yCcs complex was purified and then loaded with zinc under the same conditions as the noncomplexed sample described above. The zinc occupancy was a mere 37% and the K_D for zinc was measured to be $7.72 \pm 1.90 \times 10^{-16}$ M (**Table 5.1**). Ccs binding weakens the affinity of the copper/active site held zinc by nearly 3-fold, while dramatically decreasing the total amount of zinc loading into the copper/active site by ~60%. These results suggest that Ccs interaction promotes "site-specific" zinc binding in Sod1 by discouraging mis-metallated zinc binding in the copper/active site [16].

Ccs Has Little to No Effect on Zinc Affinity in G93A and G85R Mutations of Sod1

The G93A and G85R mutations are both located on β-strands, but at very different locations within the Sod1 β-barrel. G93 is located at a seemingly innocuous position near a loop between strands 5 and 6 and is commonly termed a "wild-type-like mutant" (WTL). G85, on the other hand, is located near the "zinc-loop" that contains all of the zinc-coordinating residues and is grouped as a "metal-binding region mutant" (MBR) [36]. The zinc affinity of immature G93A was determined to be $2.01 \pm 0.19 \times 10^{-16}$ M. The G93A hSod1•yCcs complex zinc affinity was measured $1.36 \pm 0.579 \times 10^{-16}$ M. Unlike the H80R mutation, G93A Sod1 can accept copper at the copper site and become fully mature. Therefore, its zinc affinity when fully mature (Cu,Zn-G93ASS) was determined to be $6.09 \pm 0.01 \times 10^{-17}$ M (**Table 5.1**).

The zinc affinity of immature G85R was $1.11 \pm 0.53 \times 10^{-16}$ M. The G85R hSod1•yCcs complex was measured as $3.47 \pm 4.10 \times 10^{-16}$ M. Finally, the mature G85R (Cu,Zn-G85ASS) zinc affinity was determined to be $3.24 \pm 1.18 \times 10^{-16}$ M (**Table 5.1**). Ccs binding to G93A and G85R could not promote zinc affinity to the levels of wt-Sod1. However, the zinc occupancy of both Sod1 mutants increased upon Ccs binding (**Table 5.1**). All proteins were loaded and extensively washed under the same conditions, then checked for the percentage of zinc bound by ICP-MS. G93A was found to be ~20% loaded, but when bound to Ccs this increased to 73%. Similarly, G85R was 36% loaded when alone and 84% loaded when complexed with Ccs. Zinc binding never exceeded a 1:1 ratio for these mutants, ensuring that extraneous zinc-binding in the copper site is not occurring. Zinc binding will always preferentially bind to an accessible zinc-site due to the several orders of magnitude difference in affinity over the copper site (demonstrated here) and shown in previous structural and biochemical analysis of these mutants, along with A4V, isolated

from yeast and reconstituted with metals [28,36]. This suggests that Ccs is providing a beneficial effect on the kinetics of zinc binding by these mutants, although it cannot strengthen their decreased affinities.

A4V Shows Decreased Zinc Affinity with Each Step of Maturation

Similar to G93A and G85R described above, the A4V mutation affects the stability of the β-barrel in Sod1. In a correlated manner, A4V Sod1 also behaves similarly to G93A Sod1 and G85R Sod1 when acquiring zinc. Alone, A4V Sod1 bound zinc at 49% when immature; this increased to 78% when bound by Ccs (both measurements taken after reconstitution and washing). However, when looking at zinc affinity, the A4V mutation sharply contrasts what has been observed for other mutants. The dissociation constant of immature A4V was determined to be 1.91 ± 0.56 × 10^{-16} M for zinc, A4V hSod1•yCcs had an affinity of 3.39 ± 1.04 × 10^{-16} M, and fully mature A4V (Cu,Zn-A4V^{SS}) was 1.68 ± 0.10 × 10^{-15} M (**Table 5.1**). This shows a decrease in zinc affinity with each incremental step toward maturation. This pattern suggests that the A4V mutation has an inhibitory effect on Sod1 maturation.

Ccs Binding Prevents "wild-Type-Like" Sod1 mutant Oligomerization and Insoluble Aggregation in Vitro

It has previously been reported that A4V and G93A mutations in Sod1 are significantly less stable than wild-type in their immature forms [43]. This same trend does not carry over to many members of the metal-binding region mutants like H80R and G85R. We confirmed early on that, particularly in their disulfide-reduced forms, these two mutations were prone to oligomerization and aggregation within a week after purification, whereas H80R and G85R (and wild-type) Sod1 can remain stable for weeks (Figure 4, panel A, top gel and panel B). Conversely,

the A4V and G93A mutations became much less prone to these oligomerization events while in stable complex with an apo (e.g., copper-free) form of Ccs when held under the same conditions and over the same time period (**Figure 5.4, panel A, bottom gel**). The use of apo-Ccs is essential to ensure that Ccs cannot perform its activating functions on Sod1 and the interaction is stalled. Ccs confers stability to fALS-Sod1 mutants simply through stable interaction.

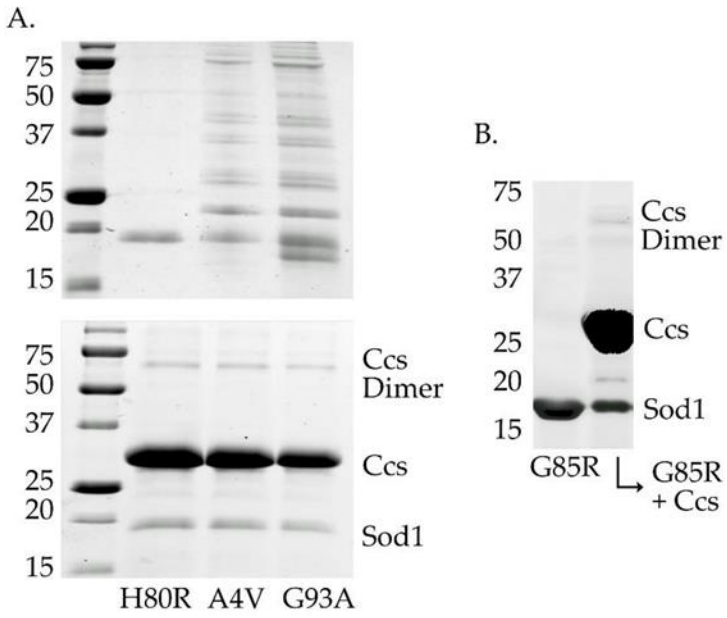

Fig 5.4. Stabilization of fALS-Sod1 mutants by Ccs. The top gel in panel A (the left two gels) compares the stability of two WTL mutants with the metal-binding-region mutant H80R (and G85R in panel B (right gel), lane 1), after 4 days at 4 ◦C. The WTL mutants are highly oligomerized (A4V and G93A lanes) as compared to the two MBR mutants. The bottom gel in panel A shows that the same WTL proteins are protected from severe oligomerization if incubated as a complex with an apo (metal-free) form of Ccs. The complexes shown here are between human Sod1 and human Ccs.

Discussion

Aberrant zinc binding of fALS-Sod1 mutants has been a topic of much speculation, but little direct evidence for this notion has been provided by the field. In previous work, we showed that wt-Sod1 binds zinc with a very tight affinity compared to other known zinc binding proteins

and that interaction Ccs stabilizes site-specific zinc binding by immature Sod1 [16]. To further this work, we have examined how a set of pathogenic fALS mutations directly affect zinc binding by Sod1 and whether or not Ccs interaction can promote high-affinity site-specific zinc binding as observed for the wild-type form of Sod1.

We first wanted to ensure that the cross section of fALS-Sod1 mutants examined could bind Ccs with a similar affinity to the wild-type version of Sod1. All of the fALS mutants tested showed very comparable Ccs binding affinities to what we have previously reported for wild-type Sod1 (KDs in the low nano-molar range) [13,16]. However, it would be expected that fALS mutations that occur at the Sod1•Ccs dimeric interface would likely hinder or even eliminate binding, thus preventing any and all Ccs action.

The human form of Ccs is known to bind zinc at its "Sod1-like" domain 2 and contains matching residues at the same sites as the zinc-binding residues in Sod1 [44]. Yeast and other lower eukaryotic forms of Ccs do not contain a complete zinc binding site [12]. Interestingly, Ccs binds zinc with a 100-fold stronger affinity than fully mature wild-type Sod1. It is possible that the adjacent copper-binding domains (D1 and D3) of Ccs, which are not present in Sod1, may play an indirect role in stabilizing zinc-binding in D2. This also argues against Ccs directly supplying zinc to immature Sod1 as metallo-chaperones have been shown to function by simply following an affinity gradient of binding sites between chaperone and target protein binding sites [45].

The fALS-Sod1 mutant H80R does not bind zinc in the canonical zinc site. It does, however, bind zinc in the copper/active site as observed in the crystal structure (PDB: 3QQD) [38]. We use this mutant to examine the zinc affinity in the copper/active site as this and other forms of zinc mis-metallation have been noted in fALS samples [33]. Zinc binding at this site is

considerably weaker than the canonical zinc-binding site on Sod1 and Ccs binding further decreased the affinity and occupancy of zinc at this site. This strongly suggests a role for Ccs in guiding proper zinc coordination by Sod1 during the maturation process.

G93A and G85R Sod1 are both β-barrel mutations that are relatively close in sequence, but locations with regard to the zinc-binding site are quite different [28,36]. The G93A mutant structure (PDB: 3GZO) is nearly identical to that of wild-type Sod1 (PDB: 1PU0), from β-barrel conformation, loop placement and metal occupancies. The protein in this crystal structure comes from a small fraction of the total protein has undergone Ccs-mediated maturation and likely misrepresents the majority of the G93A protein expressed in the yeast cells. For instance, it is known that immature G93A (E,E-G93A^{SH}) is severely destabilized as compared to wt-Sod1 (common for most WTL fALS mutants) and it is very likely that a large portion of this protein does not reach maturity [20]. The G85R mutant, on the other hand, is proximal to the zinc coordinating residues and zinc loop on Sod1. The crystal structures of G85R (PDBs: 3CQP, 3CQQ, 2VR6-8) display decreased metal occupancy, mis-metallation (zinc in copper site) and disordered loop elements. G85R and many other MBR mutants are quite stable in their immature forms, unlike that of the WTL β-barrel mutants, yet cannot bind metals effectively [36]. Though biophysically very different, both mutants showed a decreased zinc affinity at all stages of maturation when compared to wild-type Sod1 and direct interaction with Ccs was unable to significantly rescue their zinc affinity. However, stable interaction with Ccs did dramatically improve the overall stability and resistance to oligomerization/aggregation for G93A (**Figure 5.4**).

A4V is another a β-barrel mutation (located near the Sod1 homodimeric interface) that causes one of the most severe and rapidly progressing forms of fALS [31]. The A4V mutation is

not located near the "zinc loop" and does not directly affect its orientation. In fact, the crystal structure of A4V is almost identical to wt-Sod1, with only minor changes throughout the structure (PDB: 1UXM). However, this mutation showed a decreased affinity for zinc that actually worsens with each step of maturation, in direct contradiction to that of wt-Sod1 (Table 1). It has been previously speculated that the conformation of the A4V zinc loop when copper is bound might lower its affinity for zinc, and this data provides further evidence for this idea [46]. Stable interaction with Ccs further weakened the zinc affinity of A4V, but as with G93A, Ccs binding repressed oligomerization events (**Figure 5.4**). This mutation seems to actively impede each maturation step, which may serve to increase the time needed to reach full maturity. It is interesting to consider if these unique characteristics of the A4V mutant contribute to how such a seemingly innocuous mutation leads to the rapid disease progression suffered by patients. fALS-Sod1 mutants have been closely examined and compared by researchers for decades [20,28,37,46–49]. The mutants examined here were chosen because they are all commonly studied, well-characterized and represent a broad cross-section within the large pool of pathogenic mutants [28,36,37]. We show that the zinc-binding affinities for each mutant are consistently worse than what is observed in wt-Sod1, but the magnitude and pattern of these differences vary by mutation (**Table 5.1**). We also show that the zinc occupancy levels are decreased, likely due to varying fractions of these proteins existing as misfolded/off-pathway states commonly observed for these fALS mutants (reviewed in [27,49]). For each fALS-Sod1 mutant possessing a complete zinc-binding site, Ccs binding increased overall zinc occupancy. However, unlike wt-Sod1, zinc binding affinity actually decreased. Ccs binding to immature wt-Sod1 induces a conformation of the disulfide/zinc loop region that promotes high-affinity site-specific zinc binding [10]. Subsequent copper delivery and

disulfide bond formation complete Sod1 maturation and secures zinc coordination in a nearly irreversible manner. Mature wt-Sod1 (Cu,Zn-Sod1^{SS}) is stable and active under very harsh conditions (e.g., incubation with high concentrations of denaturant and the strong metal ion chelator EDTA) [50–52]. This supports the idea, recently described by us and others, that Ccs functions in a molecular-chaperone-like manner where binding alone induces a more stable conformation of Sod1 [10,16,48,53]. This simply may not be true for fALS-Sod1 mutants. The inability of Ccs to improve zinc binding status of examined fALS mutants to the levels of the wild-type form provides another point of evidence that the link between the diverse pool of fALS-Sod1 mutants may be an inability to fully complete transaction with Ccs (**Figure 5.5**) and [8,27,53]. The argument against this idea has been that Ccs KO mice do not show ALS-like symptoms [54] and Ccs overexpression in mice expressing pathogenic forms of Sod1 actually have earlier symptomatic onset [34]. These data seem to contradict a role for Ccs in fALS pathology. For the former, it is important to note that only a small fraction of Sod1 activity is needed for normal cellular function and the Ccs-independent pathway for Sod1 maturation (found in mammals) can take care of this need. Additionally, the wild-type form of Sod1 is not prone to aggregation in any form [15]. Furthermore, an overabundance of Ccs (overexpression) in the presence of fALS-Sod1 likely exacerbates the problem by forming nonproductive complexes with Sod1 mutants, as previously described [8,10]. The Ccs protein is then likely pulled into the Sod1 laden toxic oligomers. A role for Ccs in Sod1 zinc acquisition is gaining momentum and the concept that

fALS-Sod1 mutations deter this function serves to highlight the multifaceted nature of Ccs function and a potential role in fALS-Sod1 pathology.

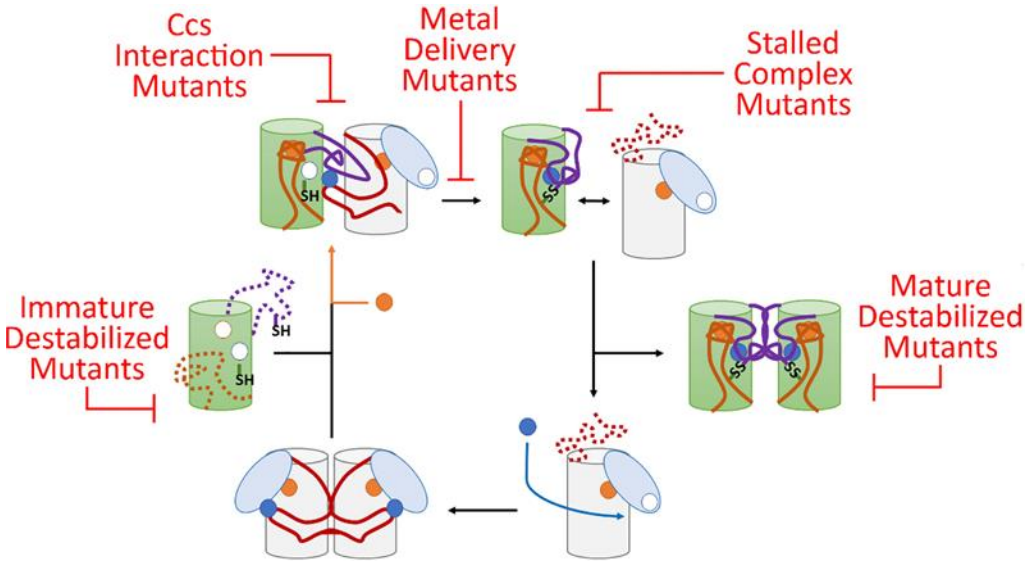

Fig 5.5. A model for fALS-Sod1 mutations blocking Ccs-mediated Sod1 maturation. In this maturation cycle Sod1 is colored green with the conserved loops colored orange and purple (same as Figure 1). The Ccs molecule is colored by its three domains (D1—light blue, D2—white and D3—red). The copper ions are shown as blue circles and zinc are orange circles. The cycle normally begins as Ccs acquires copper from the cell which stabilizes D3 and homo-dimerization. Recognition and binding to a completely immature (E,E-Sod1^{SH}) Sod1 molecule induces site-specific zinc binding in Sod1 followed by Ccs-directed copper delivery and disulfide bond formation. This latter event keys separation of the Sod1•Ccs heterodimer. The mature Sod1 monomer is now free to find another mature Sod1 monomer to form a highly stable Sod1 homodimer that is now a fully active enzyme. The apo-Ccs molecule can now bind another copper ion and enter the maturation cycle again. There are at least five sites within this Ccs-mediated maturation cycle that can be disrupted by fALS mutations and these sites can be populated by a nearly comprehensive list of potential fALS mutant proteins. For example, immature destabilized mutants include L126Z, interaction mutants include I113T, delivery mutants include H80R, stalled complex mutants include C146S, and mature destabilized mutants include A4V, G85R, and G93A.

Lastly, a large percentage of known fALS-Sod1 mutants can be easily divided into groups that would hinder specific points in the Ccs-mediated Sod1 maturation cycle (**Figure 5.5**) and [27]. First, mutants destabilized in their immature state include A4V, G37R, G93A, I113T, L126Z and numerous other WTL mutants. Many of these proteins can reach a full maturity when bound and activated by Ccs, but since Ccs is highly outnumbered by Sod1 in vivo, it is likely that many of

these proteins begin the oligomerization/aggregation process before Ccs can do its job. Mutations that preclude direct interaction with Ccs (ex., T54R, I113T, G114A, T116R to name a select few) may be stable in their immature state, but the majority will not ever reach full maturity, since stable Ccs interaction is required for Ccs-mediated maturation, leading to the buildup of immature conformers. Many mutations that directly affect copper binding or delivery have been shown to have stability similar to that of wild-type Sod1 in their immature states [55]. However, these MBR mutants cannot reach maturity due to direct alteration of the metal binding sites in Sod1 (ex., H46R, H48Q, D124V, H80R and many others). Over time this population of immature Sod1 molecules will likely induce pathological effects in the cell. fALS-Sod1 mutations that prevent complete Sod1 maturation produce "stalled complexes" with Ccs where dissociation of the heterodimer does not readily occur. This will include a wide swath of mutants including additional mutants not mentioned in previous groups (ex., C57R, C146R, G85R, and many others in the conserved disulfide loop region). Lastly, there are a group of mutants that can reach maturity, but are severely destabilized in this conformation (ex., A4V, L38V, L84V, G93R and many others) [55]. There is a small fraction of mutants that have characteristics at each step of maturity and activity levels almost identical to wild-type Sod1. Interestingly, some of these mutants happen to fall in established aggregation-forming segments on the Sod1 surface [56].

In conclusion, this work provides new insight into zinc binding by fALS-Sod1 mutants and the role of Ccs in Sod1 zinc acquisition. Each of the examined fALS mutants possess a decreased zinc affinity (as compared with wt-Sod1) that could not be rescued by Ccs binding. These novel properties have been acquired via pathogenic fALS mutation and suggest that a role for zinc acquisition in the fALS phenotype deserves closer examination.

Materials and Methods

Yeast extract, tryptone, NaCl, BisTris, Tris-base, glycine, β-mercaptoethanol (BME), agar, ammonium persulfate, sodium acetate, acetic acid, EDTA, and TEMED were purchased from Thermo Fisher Scientific (Hampton, NH, USA). DTT, isopropyl 1-thio–d-galactopyranoside, and tris(2-carboxyethyl)phosphine (TCEP) were purchased from GoldBio (St. Louis, MO, USA). Imidazole, Zn2SO4, and Cu(II)2SO4, imidazole, monobasic and dibasic sodium phosphate, and acetonitrile were purchased from Sigma-Aldrich (St. Louis, MO, USA). Trichloroethanol was purchased from Acros Organics. Primers for mutagenesis were purchased from Sigma-Aldrich, and the Phusion site-directed mutagenesis kit was from Thermo Fisher Scientific. TPEN was purchased from Tocris Bioscience (Bristol, United Kingdom). Alexa-488 fluorescent dye for labeling was purchased from Life Technologies (Carlsbad, CA, USA). Bacterial strains used were DH5alpha (Invitrogen, St. Louis, MO, USA), BL21 pLysS (DE3) E. coli (Promega, Madison, WI, USA), and XL1-Blue (Stratagene, St. Louis, MO, USA). Chromatography columns were purchased from GE Healthcare (Marlborough, MA, USA).

Sod1 and Ccs Cloning, Expression and Purification

DNA fragments encoding yCcs1 were generated by PCR from plasmids originally supplied by J. S. Valentine (UCLA). Both yeast Ccs and human Ccs constructs were cloned into a pkA8H vector that contains both contain an inducible LacZ promoter, an 8x-Nterminal His-tag, and a tobacco etch virus (TEV) protease cleavage site and gifted from the Hart lab (UTHSCSA, San Antonio, TX, USA). The A4V and G93A human Sod1 clones were also gifted from the Hart lab. Site specific amino acid changes in Sod1 were done via quick-change mutagenesis to generate G85R and H80R mutants. Sod1 and Ccs1 proteins were expressed in Escherichia coli BL21 (DE3)

pLysS. Cells containing these expression plasmids were grown in LB media at 37 °C to an OD_{600} of 0.6 to 0.8. After induction with IPTG, the cells were transferred to 37 °C for an additional 4 hours before being harvested. Overexpressed proteins were purified using a HisTrap HP Ni2+ affinity column purchased from GE. After purification, the 8x-His-tag was removed from the proteins using TEV protease produced in-house and engineered to contain its own non-cleavable 8X-His-tag. After digestion, the cleaved His-tag and TEV protease are removed from the sample by a final pass through the nickel column. This procedure leaves a two residue (Gly-His) extension on the N-terminus of the purified protein. Sod1•Ccs complexes were purified by size exclusion chromatography. The metal content of purified proteins and protein complexes was determined using inductively-coupled plasma mass spectrometry (ICP-MS), here at UTD (Richardson, TX, USA). Samples for ICP-MS were digested with 1% HNO_3 for analysis.

Labeling of Sod1 with Fluorescent Labels

The Alexa-488 C5-maleimide dyes (Invitrogen) was mixed at a 1:1 ration with purified apo-C146S Sod1 mutants in a buffer containing 20 mM Tris pH 7.4, 300 mM NaCl and 1 mM TCEP. The mixture incubated in the dark at 4 ◦C overnight. The micromolar concentration of the protein is kept low to avoid aggregation events. The following morning, the protein was concentrated in spin concentrators to lower the total volume and remove some of the excess dye. The sample was loaded onto a Superdex 200 SEC column from GE. The column was wrapped in foil to keep the sample in the dark during the separation. The sample was fractionated and then run on SDS-PAGE. The excess dye elutes near the bed volume of the column.

Microplate-Based Binding Assays

The preparation and completion of the binding assays were performed as detailed in previous work (13). Binding experiments were done with a reaction buffer containing 20 mM Tris, pH 7.5, 150 mM NaCl, and 1 mM TCEP. The plates were imaged using a GE Typhoon FLA 9500 (UTD, Richardson, TX, USA) scanner using filters specific for the fluorophore's 488 nm excitation. The binding experiments were completed in replicative quadruplicate on the same plate for comparative and statistical analysis. The fluorescence change was then quantified using Image-Quant TL (UTD, Richardson, TX, USA) and then analyzed, and figures were constructed using GraphPad Prism.

Measuring Zn Affinity of Sod1 Mutants, Sod1 Mutants in Complex with Ccs, and Mature Sod1 Mutants by Equilibrium Dialysis

Proteins and protein complexes were loaded with zinc and washed repeatedly with metal-free buffer to remove any unbound zinc. Complexes were formed using human Sod1 mutants and yeast Ccs, as it does not bind zinc and will not affect affinity calculations. ICP-MS was performed on samples to determine the protein-Zn concentration. Zn-binding affinity experiments were performed at pH 7.4 using a Bel-Art in-line equilibrium cell (1 mL). The dialysis membrane was treated with EDTA and boiled to remove any metal and sulfide contaminants. One side of the chamber for each reaction was filled with a solution of TPEN at 100 µM. The other side contained 10 µM protein–Zn complex and 100 µM TPEN. Excess Sod1 protein that was unbound is considered unable to bind zinc. The zinc-exchange reaction proceeded at room temperature overnight under agitation. ICP-MS was used to analyze the Zn concentrations on both sides. The KD for TPEN at pH 7.4 has previously been determined to be 2.6×10^{-16} M [16]. We used this

value to determine Zn affinity values. All samples were analyzed in triplicate and from multiple preparations to provide meaningful statistical analysis. Experiments were performed under aerobic conditions and the disulfide bond status was not directly examined in all cases.

Protein Degradation Assay

Purified ALS-Sod1 protein samples were kept at 4 °C for 4 days, then run on a 14% SDS-PAGE gel and visualized with Coomassie stain. ALS-Sod1•Ccs complex samples were kept at 4 °C for 4 days then run on a 14% SDS-PAGE gel and visualized with Coomassie stain.

Author Contributions: D.D.W. devised the research plan. S.D.B., M.S.U. and F.B. performed the research and wrote the initial manuscript. D.D.W and G.M. edited the manuscript and made the final figures. J.S.C. and G.M. provided technical help over the course of the research. All authors have read and agreed to the published version of the manuscript.

Funding: This research was supported in part by R01 GM120252 from the National Institutes of Health awarded to D.D.W. The work was also supported by the Robert A. Welch Foundation (Grant: AT-1935-20170325) and bythe National Institute of General Medical Sciences of the National Institutes of Health under Award Number R35GM128704 awarded to G.M., and by funds from the University of Texas at Dallas. The content is solely the responsibility of the authors and does not necessarily represent the official views of the National Institutes of Health.

Conflicts of Interest: The authors declare that they have no conflicts of interest with the contents of this article.

References

1. Hambidge, M. Human zinc deficiency. J. Nutr. 2000, 130, 1344S–1349S. [CrossRef]

2. Kochan´czyk, T.; Drozd, A.; Kre¸z˙el, A. Relationship between the architecture of zinc coordination and zinc binding affinity in proteins–insights into zinc regulation. Metallomics 2015, 7, 244–257. [CrossRef]

3. Cousins, R.J.; Liuzzi, J.P.; Lichten, L.A. Mammalian zinc transport, trafficking, and signals. J. Biol. Chem.
2006, 281, 24085–24089. [CrossRef]

4. Eide, D.J. Zinc transporters and the cellular trafficking of zinc. Biochim. Biophys. Acta 2006, 1763, 711–722. [CrossRef]

5. Sekler, I.; Sensi, S.L.; Hershfinkel, M.; Silverman, W.F. Mechanism and regulation of cellular zinc transport. Mol. Med. 2007, 13, 337–343. [CrossRef]

6. Pelmenschikov, V.; Siegbahn, P.E. Copper-zinc superoxide dismutase: Theoretical insights into the catalytic mechanism. Inorg. Chem. 2005, 44, 3311–3320. [CrossRef] [PubMed]

7. Lyons, T.J.; Gralla, E.B.; Valentine, J.S. Biological chemistry of copper-zinc superoxide dismutase and its link to amyotrophic lateral sclerosis. Met. Ions Biol. Syst. 1999, 36, 125–177. [PubMed]

8. Fetherolf, M.M.; Boyd, S.D.; Winkler, D.D.; Winge, D.R. Oxygen-dependent activation of Cu,Zn-superoxide dismutase-1. Metallomics 2017, 9, 1047–1059. [CrossRef] [PubMed]

9. Sturtz, L.A.; Diekert, K.; Jensen, L.T.; Lill, R.; Culotta, V.C. A fraction of yeast Cu,Zn-superoxide dismutase and its metallochaperone, CCS, localize to the intermembrane space of mitochondria. A physiological role for SOD1 in guarding against mitochondrial oxidative damage. J. Biol. Chem. 2001, 276, 38084–38089. [PubMed]

10. Fetherolf, M.M.; Boyd, S.D.; Taylor, A.B.; Kim, H.J.; Wohlschlegel, J.A.; Blackburn, N.J.; Hart, P.J.; Winkler, D.D. Copper-zinc superoxide dismutase is activated through a sulfenic acid intermediate at a copper ion entry site. J. Biol. Chem. 2017, 292, 12025–12040. [CrossRef] [PubMed]

11. Banci, L.; Bertini, I.; Cantini, F.; Kozyreva, T.; Massagni, C.; Palumaa, P.; Rubino, J.T.; Zovo, K. Human superoxide dismutase 1 (hSOD1) maturation through interaction with human copper chaperone for SOD1 (hCCS). Proc. Natl. Acad. Sci. USA 2012, 109, 13555–13560. [CrossRef] [PubMed]

12. Culotta, V.C.; Klomp, L.W.J.; Strain, J.; Casareno, R.L.B.; Krems, B.; Gitlin, J.D. The Copper Chaperone for Superoxide Dismutase. J. Biol. Chem. 1997, 272, 23469–23472. [CrossRef]

13. Boyd, S.D.; Liu, L.; Bulla, L.; Winkler, D.D. Quantifying the Interaction between Copper-Zinc Superoxide Dismutase (Sod1) and its Copper Chaperone (Ccs1). J. Proteom. Bioinform. 2018, 11, 473. [CrossRef] [PubMed]

14. Arnesano, F.; Banci, L.; Bertini, I.; Martinelli, M.; Furukawa, Y.; O'Halloran, T.V. The Unusually Stable Quaternary Structure of Human Cu,Zn-Superoxide Dismutase 1 Is Controlled by Both Metal Occupancy and Disulfide Status. J. Biol. Chem. 2004, 279, 47998–48003. [CrossRef] [PubMed]

15. Furukawa, Y.; O'Halloran, T.V. Amyotrophic lateral sclerosis mutations have the greatest destabilizing effect on the apo- and reduced form of SOD1, leading to unfolding and oxidative aggregation. J. Biol. Chem. 2005, 280, 17266–17274. [CrossRef] [PubMed]

16. Boyd, S.D.; Calvo, J.S.; Liu, L.; Ullrich, M.S.; Skopp, A.; Meloni, G.; Winkler, D.D. The yeast copper chaperone for copper-zinc superoxide dismutase (CCS1) is a multifunctional chaperone promoting all levels of SOD1 maturation. J. Biol. Chem. 2019, 294, 1956–1966. [CrossRef]

17. Rosen, D.R. Mutations in Cu/Zn superoxide dismutase gene are associated with familial amyotrophic lateral sclerosis. Nature 1993, 364, 362. [CrossRef]

18. Bowling, A.C.; Schulz, J.B.; Brown, R.H., Jr.; Beal, M.F. Superoxide Dismutase Activity, Oxidative Damage, and Mitochondrial Energy Metabolism in Familial and Sporadic Amyotrophic Lateral Sclerosis. J. Neurochem. 1993, 61, 2322–2325. [CrossRef]

19. Reaume, A.G.; Elliott, J.L.; Hoffman, E.K.; Kowall, N.W.; Ferrante, R.J.; Siwek, D.F.; Wilcox, H.M.; Flood, D.G.; Beal, M.F.; Brown, R.H.; et al. Motor neurons in Cu/Zn superoxide dismutase-deficient mice develop normally but exhibit enhanced cell death after axonal injury. Nat. Genet. 1996, 13, 43–47. [CrossRef]

20. Watanabe, M.; Dykes-Hoberg, M.; Culotta, V.C.; Price, D.L.; Wong, P.C.; Rothstein, J.D. Histological evidence of protein aggregation in mutant SOD1 transgenic mice and in amyotrophic lateral sclerosis neural tissues. Neurobiol. Dis. 2001, 8, 933–941. [CrossRef]

21. Bourassa, M.W.; Brown, H.H.; Borchelt, D.R.; Vogt, S.; Miller, L.M. Metal-deficient aggregates and diminished copper found in cells expressing SOD1 mutations that cause ALS. Front. Aging Neurosci. 2014, 6, 1–6.

22. Shaw, B.F.; Valentine, J.S. How do ALS-associated mutations in superoxide dismutase 1 promote aggregation of the protein? Trends Biochem. Sci. 2007, 32, 78–85. [CrossRef] [PubMed]

23. Fukuoka, M.; Tokuda, E.; Nakagome, K.; Wu, Z.; Nagano, I.; Furukawa, Y. An essential role of N-terminal domain of copper chaperone in the enzymatic activation of Cu/Zn-superoxide dismutase. J. Inorg. Biochem. 2017, 175, 208–216. [CrossRef] [PubMed]

24. Sugaya, K.; Nakano, I. Prognostic role of "prion-like propagation" in SOD1-linked familial ALS: An alternative view. Front. Cell. Neurosci. 2014, 8, 359. [CrossRef] [PubMed]

25. Valentine, J.S.; Doucette, P.A.; Zittin Potter, S. Copper-zinc superoxide dismutase and amyotrophic lateral sclerosis. Annu. Rev. Biochem. 2005, 74, 563–593. [CrossRef]

26. Saeed, M.; Yang, Y.; Deng, H.X.; Hung, W.Y.; Siddique, N.; Dellefave, L.; Gellera, C.; Andersen, P.M.; Siddique, T. Age and founder effect of SOD1 A4V mutation causing ALS. Neurology 2009, 72, 1634–1639. [CrossRef]

27. Seetharaman, S.V.; Prudencio, M.; Karch, C.; Holloway, S.P.; Borchelt, D.R.; Hart, P.J. Immature copper-zinc superoxide dismutase and familial amyotrophic lateral sclerosis. Exp. Biol. Med. 2009, 234, 1140–1154. [CrossRef]

28. Galaleldeen, A.; Strange, R.W.; Whitson, L.J.; Antonyuk, S.V.; Narayana, N.; Taylor, A.B.; Schuermann, J.P.; Holloway, S.P.; Hasnain, S.S.; Hart, P.J. Structural and biophysical properties of metal-free pathogenic SOD1 mutants A4V and G93A. Arch. Biochem. Biophys. 2009, 492, 40–47. [CrossRef]

29. Cudkowicz, M.E.; McKenna-Yasek, D.; Chen, C.; Hedley-Whyte, E.T.; Brown, R.H. Limited Corticospinal Tract Involvement in Amyotrophic Lateral Sclerosis Subjects with the A4V Mutation in the Copper/Zinc Superoxide Dismutase Gene. Ann. Neurol. 1998, 43, 703–710. [CrossRef]

30. Watanabe, S.; Nagano, S.; Duce, J.; Kiaei, M.; Li, Q.-X.; Tucker, S.; Tiwari, A.; Brown, R., Jr.; Beal, M.H.; Hayward, L.J.; et al. Increased affinity for copper mediated by cysteine 111 in forms of mutant superoxide dismutase 1 linked to amyotrophic lateral sclerosis. Free Radic. Biol. Med. 2007, 42, 1534–1542. [CrossRef]

31. Cardoso, R.M.; Thayer, M.M.; DiDonato, M.; Lo, T.P.; Bruns, C.K.; Getzoff, E.D.; Tainer, J.A. Insights into Lou Gehrig's disease from the structure and instability of the A4V mutant of human Cu,Zn superoxide dismutase. J. Mol. Biol. 2002, 324, 247–256. [CrossRef]

32. Gurney, M.E. Transgenic-mouse model of amyotrophic lateral sclerosis. N. Engl. J. Med. 1994, 331, 1721–1722. [CrossRef] [PubMed]

33. Lelie, H.L.; Liba, A.; Bourassa, M.W.; Chattopadhyay, M.; Chan, P.K.; Gralla, E.B.; Miller, L.M.; Borchelt, D.R.; Valentine, J.S.; Whitelegge, J.P. Copper and zinc metallation status of copper-zinc superoxide dismutase from amyotrophic lateral sclerosis transgenic mice. J. Biol. Chem. 2011, 286, 2795–2806. [CrossRef] [PubMed]

34. Son, M.; Puttaparthi, K.; Kawamata, H.; Rajendran, B.; Boyer, P.J.; Manfredi, G.; Elliott, J.L. Overexpression of CCS in G93A-SOD1 mice leads to accelerated neurological deficits with severe mitochondrial pathology. Proc. Natl. Acad. Sci. USA 2007, 104, 6072–6077. [CrossRef] [PubMed]

35. Haidet-Phillips, A.M.; Hester, M.E.; Miranda, C.J.; Meyer, K.; Braun, L.; Frakes, A.; Song, S.; Likhite, S.; Murtha, M.J.; Foust, K.D.; et al. Astrocytes from familial and sporadic ALS patients are toxic to motor neurons. Nat. Biotechnol. 2001, 29, 824–828. [CrossRef] [PubMed]

36. Cao, X.; Antonyuk, S.; Seetharaman, S.V.; Whitson, L.J.; Taylor, A.B.; Holloway, S.P.; Strange, R.W.; Doucette, P.A.; Valentine, J.S.; Tiwari, A.; et al. Structures of the G85R variant of SOD1 in Familial Amyotrophic Lateral Sclerosis. JBC 2008, 283, 16169–16177. [CrossRef]

37. Seetharaman, S.V.; Winkler, D.D.; Taylor, A.B.; Cao, X.; Whitson, L.J.; Doucette, P.A.; Valentine, J.S.; Schirf, V.; Demeler, B.; Carroll, M.C.; et al. Disrupted zinc-binding sites in structures of pathogenic SOD1 variants D124V and H80R. Biochemistry 2010, 49, 5714–5725. [CrossRef]

38. Strange, R.W.; Antonyuk, S.V.; Hough, M.A.; Doucette, P.A.; Valentine, J.S.; Hasnain, S.S. Variable metallation of human superoxide dismutase: Atomic resolution crystal structures of Cu-Zn, Zn-Zn and as-isolated wild-type enzymes. J. Mol. Biol. 2006, 356, 1152–1162. [CrossRef]

39. Skopp, A.; Boyd, S.D.; Ullrich, M.S.; Liu, L.; Winkler, D.D. Copper-zinc superoxide dismutase (Sod1) activation terminates interaction between its copper chaperone (Ccs) and the cytosolic metal-binding domain of the copper importer Ctr1. Biometals 2019, 32, 695–705. [CrossRef]

40. Winkler, D.D.; Luger, K.; Hieb, A.R. Quantifying chromatin-associated interactions: The HI-FI system. Methods Enzym. 2012, 512, 243–274.

41. Furukawa, Y.; Torres, A.S.; O'Halloran, T.V. Oxygen-induced maturation of SOD1: A key role for disulfide formation by the copper chaperone CCS. EMBO J. 2004, 23, 2872–2881. [CrossRef]

42. Hwang, Y.M.; Stathopulos, P.B.; Dimmick, K.; Yang, H.; Badiei, H.R.; Tong, M.S.; Rumfeldt, J.A.; Chen, P.; Karanassios, V.; Meiering, E.M. Nonamyloid aggregates arising from mature copper/zinc superoxide dismutases resemble those observed in amyotrophic lateral sclerosis. J. Biol. Chem. 2010, 285, 41701–41711. [CrossRef]

43. Sheng, Y.; Chattopadhyay, M.; Whitelegge, J.; Valentine, J.S. SOD1 Aggregation and ALS: Role of Metallation States and Disulfide Status. Curr. Top. Med. Chem. 2012, 12, 2560–2572. [CrossRef]

44. Lamb, A.L.; Wernimont, A.K.; Pufahl, R.A.; O'Halloran, T.V.; Rosenzweig, A.C. Crystal structure of the second domain of the human copper chaperone for superoxide dismutase. Biochemistry 2000, 39, 1589–1595. [CrossRef]

45. Banci, L.; Cantini, F.; Kozyreva, T.; Rubino, J.T. Mechanistic aspects of hSOD1 maturation from the solution structure of Cu(I) -loaded hCCS domain 1 and analysis of disulfide-free hSOD1 mutants. Chembiochem 2013, 14, 1839–1844. [CrossRef]

46. Schmidlin, T.; Kennedy, B.K.; Daggett, V. Structural changes to monomeric CuZn superoxide dismutase caused by the familial amyotrophic lateral sclerosis-associated mutation A4V. Biophys. J. 2009, 97, 1709–1718. [CrossRef]

47. Banci, L.; Bertini, I.; Boca, M.; Girotto, S.; Martinelli, M.; Valentine, J.S.; Vieru, M. SOD1 and Amyotrophic Lateral Sclerosis: Mutations and Oligomerization. PLoS ONE 2008, 3. [CrossRef]

48. Luchinat, E.; Barbieri, L.; Banci, L. A molecular chaperone activity of CCS restores the maturation of SOD1 fALS mutants. Sci. Rep. 2017, 7, 17433. [CrossRef]

49. Furukawa, Y.; O'Halloran, T.V. Posttranslational modifications in Cu,Zn-superoxide dismutase and mutations associated with amyotrophic lateral sclerosis. Antioxid. Redox Signal. 2006, 8, 847–867. [CrossRef]

50. Forman, H.J.; Fridovich, I. On the stability of bovine superoxide dismutase. The effects of metals. J. Biol. Chem. 1973, 248, 2645–2649.

51. Forman, H.J.; Evans, H.J.; Hill, R.L.; Fridovich, I. Histidine at the active site of superoxide dismutase. Biochemistry 1973, 12, 823–827. [CrossRef]

52. Hartz, J.W.; Deutsch, H.F. Preparation and physicochemical properties of human erythrocuprein. J. Biol. Chem. 1969, 244, 4565–4572.

53. Winkler, D.D.; Schuermann, J.P.; Cao, X.; Holloway, S.P.; Borchelt, D.R.; Carroll, M.C.; Proescher, J.B.; Culotta, V.C.; Hart, P.J. Structural and biophysical properties of the pathogenic SOD1 variant H46R/H48Q. Biochemistry 2009, 48, 3436–3447. [CrossRef]

54. Wong, P.C.; Waggoner, D.; Subramaniam, J.R.; Tessarollo, L.; Bartnikas, T.B.; Culotta, V.C.; Price, D.L.; Rothstein, J.; Gitlin, J.D. Copper chaperone for superoxide dismutase is essential to activate mammalian Cu/Zn superoxide dismutase. Proc. Natl. Acad. Sci. USA 2000, 97, 2886–2891. [CrossRef]

55. Rodriguez, J.A.; Shaw, B.F.; Durazo, A.; Sohn, S.H.; Doucette, P.A.; Nersissian, A.M.; Faull, K.F.; Eggers, D.K.; Tiwari, A.; Hayward, L.J.; et al. Destabilization of apoprotein is insufficient to explain Cu,Zn-superoxide dismutase-linked ALS pathogenesis. Proc. Natl. Acad. Sci. USA 2005, 102, 10516–10521. [CrossRef]

56. Ivanova, M.I.; Sievers, S.A.; Guenther, E.L.; Johnson, L.M.; Winkler, D.D.; Galaleldeen, A.; Sawaya, M.R.; Hart, P.J.; Eisenberg, D.S. Aggregation-triggering segments of SOD1 fibril formation support a common pathway for familial and sporadic ALS. Proc. Natl. Acad. Sci. USA 2014, 111, 197–201. [CrossRef]

CHAPTER 6

CHARACTERIZATION OF THE ONLY KNOWN DISEASE-ASSOCIATED CCS MUTATION

Abstract

Superoxide dismutase 1 (Sod1) is an antioxidant enzyme that requires a specific copper chaperone (Ccs) to become active. Sod1 is associated with many neurological diseases, most notably amyotrophic lateral sclerosis (ALS), but Ccs is not understood to directly cause disease. One mutation in Ccs, R163W, has been identified to potentially cause disease, which warrants further investigation. This study biochemically characterizes R163W Ccs metal affinities, determining the Sod1 affinity, and revealing the presence of a novel copper-binding site in domain 2. Previous efforts to characterize this mutant observed that it has an increased propensity for degradation, which we show can be rescued by the deletion of R163W Ccs domain 3. Finally, we examine the functionality of R163W Ccs and some explanations for why its aberrant and disease-associated behavior may be occurring.

Introduction

The antioxidant Sod1 is a perfect enzyme catalyzing the dismutation of reactive oxygen species (ROS) to water and hydrogen peroxide (1). It is highly expressed and shows strong activity, and so was one of the first enzymes identified and characterized (2). It is known that a wide variety of mutations in Sod1 lead to ALS, a neurodegenerative disease affecting motor neurons which results in paralysis and death (3). Sod1 is created in an immature state, where it lacks metal cofactors (apo-Sod1), and must be activated by its copper chaperone, Ccs, which delivers copper

and forms a disulfide bond (4). Maturation also requires Sod1 to bind a zinc ion, which Ccs assists with by stabilizing Sod1 in a conformation that encourages zinc binding (5).

Ccs has 3 domains, each of which contain a metal binding site (6). Domain 1 and 3 each have a copper-binding motif and provide the copper chaperone function that Ccs is named for (7). These domains bind a single copper ion tightly between their two copper motifs to prevent unwanted and damaging copper reactions from occurring within the cell (8). Domain 2 is similar in structure to Sod1 and has a homologous zinc binding site (9). Ccs binds zinc more tightly than Sod1 due to all 3 domains interacting to help strengthen the zinc affinity in domain 2 (Chapter 4). Domain 2 is also the location of the binding interface where Sod1 docks with Ccs during the maturation process (10).

Because of the strong association between Ccs and Sod1, Ccs has previously been examined as a possible cause for some forms of ALS where a mutation in Sod1 is not found (11). Removal of Ccs from human cell lines has little effect, as the cells are able to maintain viable levels of Sod1 activity (20-25%) even without Ccs (12). Deletion of Ccs from mouse models has a more severe effect, causing neurological development and muscular problems thought to be caused by high levels of ROS within those cell types. However, this does not result in motor neuron degeneration or other ALS symptoms in these animals (13). The prevailing theory has been that ALS is caused by some function inherent to Sod1 and Ccs is simply a bystander to the toxic effect of Sod1 (14).

A mutation in Ccs was discovered that somewhat questions this view (15). A single patient from a consanguineous relationship was being studied for several neurological problems. The patient had several known rare mutations that caused multiple neurological diseases to manifest

symptoms in the central nervous system, but also experienced symptoms associated with ALS. As a genetic sequence was available, it was checked for any mutations known to cause ALS and the patient was found to have none. However, both Ccs genes had the same point mutation, R163W, making the patient homozygous for this Ccs mutant. This mutation was thought to be a possible source for the ALS-like symptoms for the same reasons that Ccs had previously been considered a possible source for ALS.

Two groups have now done biochemical assays of R163W Ccs (15, 16). The mutant Ccs has been found to be less stable overall, showing a propensity for aggregation that is not seen in wild-type Ccs. This caused it to form aggregated protein bundles in cells, which mimics the aggregation function of ALS-mutants of Sod1. One proposed explanation for this loss of stability was the loss of a zinc binding function in domain 2, despite the fact that the R163W mutation does not occur within the putative zinc binding site. Here, we will continue the biochemical analysis of R163W Ccs and test some of the proposed reasons for its disfunction.

Materials and Methods

Expression of mutant Ccs

Original constructs of Ccs for bacterial expression were gifts from the lab of Dr. John Hart. Mutations were generated using a Site-directed mutagenesis kit from Promega. Constructs were transformed into competent E. coli and grown at 37°C to an OD600 of 0.6-0.8. Expression was induced with isopropyl 1-thio-β-D-galactopyranoside (1 mM). Cells were harvested, lysed, and purified on an AKTA Pure with a HisTrap Ni column. Buffer A contained 20 mM Tris, pH 8.0, 300 mM NaCl, 2 mM dithiothreitol. The N-terminal His tag was removed by cleavage with tobacco etch virus protease.

Zinc affinity

Zinc affinity was assayed with 4-(2-pyridylazo)resorcinol (PAR), which removed all zinc added to the protein. Zinc was then incubated with R163W Ccs for 20 minutes at room temperature and the protein was buffer exchanged to a metal-free buffer. Induced coupled plasma mass spectroscopy (ICP-MS) showed that no zinc remained in the protein sample and all zinc was accounted for in the buffer. Based on this, we concluded that zinc did not even weakly bind to exposed residues. All affinity assays were conducted in 50 mM Tris, pH 7.4, 150 mM NaCl, 0.5 mM Tris(2-carboxyethyl)phosphine (TCEP).

Copper affinity

Cu(I) was incubated in a 1:1, 1:2, and 1:3 protein:copper ratio anaerobically. Unbound copper was removed by buffer exchange to a metal-free buffer and bound copper was measured by ICP-MS. Affinity assays were conducted in 50 mM Tris, pH 7.4, 150 mM NaCl, 0.5 mM TCEP. Samples were made oxygen-free with at least three vacuum/nitrogen cycles on a Schlenk line. Cu(I)-CCS samples (20 μM, pH 7.4) were reacted with 1 mM Bathocuproinedisulfonic acid (BCS) and incubated for 15 h. The absorbance of the (Cu(I)L2)3- complex formed was then measured using Cary 300 UV-visible spectrophotometer (Agilent) at 483 nm for L = BCS (ε = 13,000 M-1 cm-1). Calculations were done as previously described. (17)

Activation assays

Bacterially expressed Sod1 was stripped of metals and disulfide reduced by incubation overnight at 4°C in a 100 mM acetic acid, pH 3.8, 10 mM Ethylenediaminetetraacetic acid (EDTA), 10 mM TCEP buffer, followed by incubation overnight at 4°C in a 100 mM sodium acetate, pH 5.5, 150 mM NaCl buffer that was treated to remove free metals. The metal-free Sod1

(apo-Sod1) was then buffer exchanged to a 50 mM Tris, pH 7.6, 150 mM NaCl, 0.5 mM TCEP, 200 μM BCS buffer for experiments. During activation assays, Ccs was incubated with Sod1 in a 5:1 ratio to ensure maximum activation was achieved. Reactions were incubated at room temperature in atmospheric oxygen for 20 minutes. After this, 5% glycerol was added and an equal amount of each reaction was loaded onto a metal-free non-reducing PAGE gel and run in a metal-free buffer. The gel was then incubated in a mixture of riboflavin and nitro blue tetrazolium in the dark for 15 minutes, then transferred to a 0.01% Tetramethylethylenediamine (TEMED) solution and incubated for another 15 minutes in the dark. Finally, the gel was exposed to light and developed and images were taken on a ChemiDoc. Band intensities were compared to determine qualitative activation strength. For assays requiring Zn-free Ccs, bacterially expressed and purified Ccs was incubated overnight at 4°C in a 50 mM Tris, pH 7.5, 10 mM EDTA, 150 mM NaCl, 10 mM TCEP buffer. Amount of zinc bound was confirmed by ICP-MS.

Results

Zinc binding is lost, but Sod1 binding is not

The R163W mutation affects domain 2 of Ccs, which contains both the zinc binding region and the Sod1 binding interface. It was previously reported that R163W has lost all affinity for zinc, despite the mutation not affecting any of the zinc binding residues. We therefore checked to confirm that the zinc binding ability has been lost and to see if this interfered with Sod1 binding.

R163W Ccs was completely unable to bind zinc. Any zinc chelator tried was able to completely remove zinc from the sample. Even buffer exchange to a zinc-free buffer was sufficient to remove all zinc. To all appearances, the R163W mutation heavily affects the zinc binding region, despite not being present in it.

Sod1 binding was weakened by the R163W mutation. R163W Ccs has an affinity for Sod1 at 237.3 ± 22.4 nM. This compares to our previously reported affinity of wild-type Ccs for Sod1 at 136.0 ± 11.0 nM. While still a strong association, it is approximately twice as weak as the association with wild-type Ccs. It was previously observed that Sod1 does not bind to R163W Ccs (16), however this assay was done with full-length R163W Ccs over several hours. We found that R163W Ccs rapidly degrades, even at 4°C, and the degradation prevents interaction with Sod1.

A novel copper binding site

R163W Ccs was found to bind copper with a similar affinity to wild-type Ccs. However, wild-type Ccs binds copper in a 1:1 ratio despite having two copper binding sites unless heavily overloaded in vitro. When loaded in a protein:copper ratio of 1:2 or 1:3, R163W Ccs was found to have 1.1-1.3 copper ions bound per monomer of protein, which indicates a mixed population binding either 1 or 2 copper ions. R163W Ccs has a copper affinity of $2.28 \pm 0.85 \times 10^{-19}$ M, showing no significant decrease from wild-type Ccs. Mutations made to the copper binding region in domain 1 or in domain 3 still resulted in more than 1 copper bound. Mutations to stop binding at both copper sites resulted in 1 copper bound to some monomers. Deletion of domain 1 and 3 still showed 18% of the monomers had copper bound. This indicates the presence of a new, aberrant copper site separate from the two putative sites on Ccs.

R163W mutation causes loss of function specific to human Ccs

Since R163W Ccs is able to bind both Sod1 and copper, it meets the minimal requirements for activation of Sod1. However, this mutation completely abolishes Sod1 activation (**Fig. 6.1 A**). A mutation was made in the homologous residue of yeast Ccs, L165W, and it was found to still have full activity (**Fig. 6.1 B**). Therefore, this mutation does not cause a general destabilization

that leads to lack of activity but interferes with some specific part of human Ccs necessary for Sod1 activation.

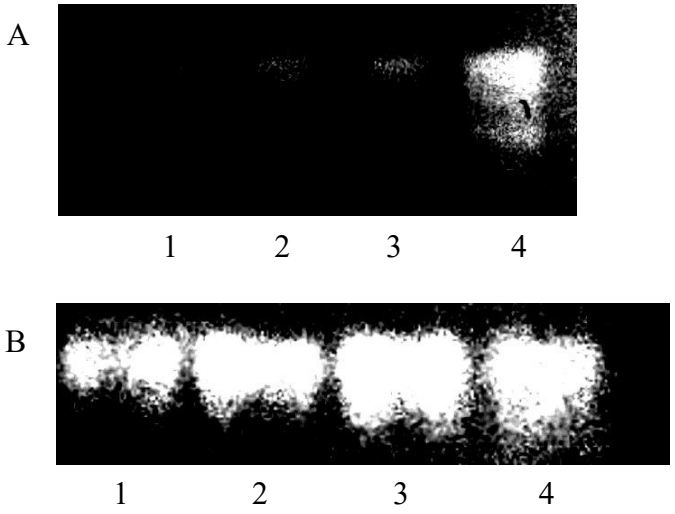

Fig 6.1. Activation of Sod1 by R163W Ccs and a homologous mutant. A) Activity assay of R163W Ccs showing an inability to activate Sod1. Lane 1: apo-Sod1, Lane 2: apo-Sod1 + apo-R163W Ccs, Lane 3: apo-Sod1 + Cu(I)-R163W Ccs, Lane 4: apo-Sod1 + Cu(I) Ccs. B) A homologous mutation was made in the functionally similar yeast Ccs. Lane 1: apo-Sod1, Lane 2: apo-Sod1 + apo-L165W, Lane 3: apo-Sod1 + Cu(I) L165W, Lane 4: apo-Sod1 + Cu(I) Ccs.

Loss of function not due to loss of zinc

A logical conclusion might be that the absence of zinc renders Ccs completely unable to activate Sod1, as this function has been obviously stopped by the R163W mutation. To test this, wild-type Ccs was stripped of zinc and an activation assay was performed on wild-type Sod1 that was previously loaded with zinc (**Fig. 6.2**). This assay was done in a buffer with 200 μM of the zinc chelator PAR to ensure that no free zinc was present and Ccs remained zinc-free. Ccs lacking zinc and Ccs with zinc bound were equally able to activate Sod1, showing that the absence of zinc alone is insufficient to abolish Sod1 activation by Ccs.

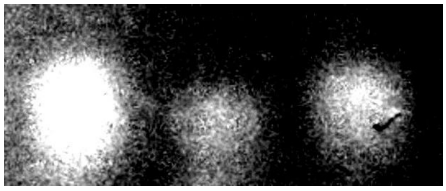

1 2 3

Fig 6.2. Activation of Sod1 with zinc-free Ccs. Lane 1: Zn-Sod1 + Cu(I) Zn-free Ccs, Lane 2: Zn-Sod1, Lane 3: Zn-Sod1 + Cu(I) Ccs with zinc. Activity of Zn-free Ccs shows up more strongly than Zn-loaded Ccs due to a bright spot present in the gel and these two results should be viewed as the same level of activity.

Rescue of degradation sensitivity with deletion of domain 3

Ccs is normally very stable, able to remain intact and active for days to weeks even at room temperature. In contrast, R163W Ccs begins degrading from the C-terminus within hours even when kept refrigerated. Deletion of domain 3 stabilizes this degradation, which suggests the exposure of some part of domain 3 that is normally protected.

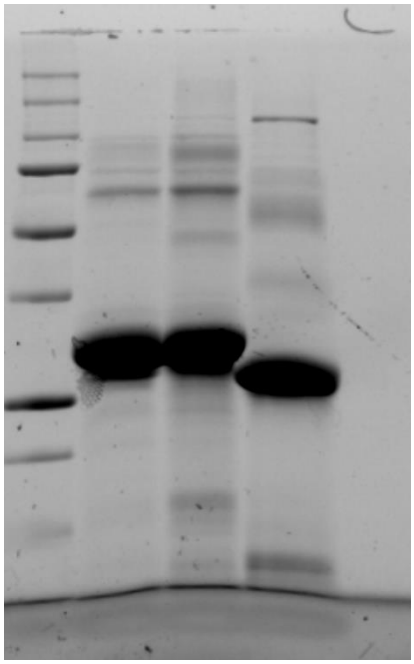

Figure 6.3. R163W Ccs has an increased rate of degradation, which is rescued by deleting domain 3. This is a 14% SDS-PAGE gel imaged using a stain-free technique. Lane 1: molecular weight marker, Lane 2: wild-type Ccs, Lane 3: R163W Ccs, Lane 4: D3D R163W Ccs. This gel was run after allowing all three protein samples to sit at room temperature for an hour.

Discussion

The R163W mutation to Ccs causes several changes to the overall function of the protein. The most apparent is the complete loss of zinc binding, in stark contrast to the extremely tight zinc binding in wild-type Ccs. (**Chapter 4**) Ccs binds zinc at four residues, none of which are affected directly by the R163W mutation. The complete loss of zinc binding immediately suggests a major disruption of domain 2.

Despite this, there is still a relatively tight interaction between Sod1 and R163W Ccs. The interface of Sod1 and Ccs encompasses a large portion of Ccs domain 2, so any major disruption

of domain 2 structure or charge would be expected to weaken Sod1 binding more than what is observed. This disagrees with the idea that domain 2 is disrupted.

The copper affinity of R163W Ccs is similar to wild-type, indicating that loss of copper is not likely to be a reason for the disease association. Instead, a new copper binding activity not present in wild-type Ccs and having nothing to do with the putative copper binding sites has appeared in domain 2. This domain has abundant cysteine and histidine residues, which are the most common binding partners for metals. One candidate may be mis-metallation in the zinc binding site, which has 3 histidines and may be positioned abnormally due to the mutation.

In addition to the loss of zinc binding, R163W Ccs has also lost the ability to activate Sod1 (**Figure 6.1**). There is no clear reason why activation of Sod1 is no longer possible, as Sod1 and copper can both be bound. A homologous mutation in yeast causes no issue in Sod1 activation, so the R163W mutation disrupts some function in human Ccs specifically. The disrupted function cannot be zinc binding alone, as this is not enough to stop Sod1 activation in wild-type Ccs. Indeed, it is very difficult to completely stop Sod1 activation. We have previously seen that multiple mutations must be made to the copper binding sites before activation will not proceed, despite the extreme necessity of copper for the maturation process. (**Chapter 4**) Therefore, some other part of Ccs must be affected besides the zinc binding region.

The increased sensitivity to degradation provides some hints to what the other affected region might be. R163W Ccs is much more degradation prone than wild-type Ccs unless domain 3 is deleted. Without domain 3, it behaves similarly to wild-type Ccs. Since the mutation is in domain 2, and affects domain 2's zinc binding function, one would expect that domain 2 would be

the destabilized region. Paradoxically, we see that domain 2 is stable, but domain 3 becomes unstable with this mutation.

This instability provides a clue why Sod1 activation is abolished in R163W Ccs. The ability of Sod1 to bind and the stability of domain 2 indicate that there is not a major structural change in this region. However, domain 3 has clearly been affected by the mutation, becoming much more unstable (**Figure 6.3**). This indicates a disruption of normal domain 3 interaction with the other two domains, which could explain the lack of Sod1 activation. Domain 3 is indicated to deliver copper to Sod1 and simultaneously form the disulfide bond, both required for Sod1 activation. This suggests a novel interaction between domain 3 and the rest of Ccs. Domain 3 is thought to be unstructured and open, however the increased sensitivity to degradation proves that some part of it must be protected in the wild-type.

References

1.J. M. McCord, I. Fridovich, Superoxide dismutase. An enzymic function for erythrocuprein (hemocuprein). J Biol Chem 244, 6049-6055 (1969).

2.D. Klug, J. Rabani, I. Fridovich, A direct demonstration of the catalytic action of superoxide dismutase through the use of pulse radiolysis. J Biol Chem 247, 4839-4842 (1972).

3.B. F. Shaw, J. S. Valentine, How do ALS-associated mutations in superoxide dismutase 1 promote aggregation of the protein? Trends Biochem Sci 32, 78-85 (2007).

4.M. M. Fetherolf, S. D. Boyd, D. D. Winkler, D. R. Winge, Oxygen-dependent activation of Cu,Zn-superoxide dismutase-1. Metallomics 9, 1047-1059 (2017).

5.S. D. Boyd et al., The yeast copper chaperone for copper-zinc superoxide dismutase (CCS1) is a multifunctional chaperone promoting all levels of SOD1 maturation. J Biol Chem 294, 1956-1966 (2019).

6.V. C. Culotta et al., The copper chaperone for superoxide dismutase. J Biol Chem 272, 23469-23472 (1997).

7.A. L. Lamb et al., Crystal structure of the copper chaperone for superoxide dismutase. Nat Struct Biol 6, 724-729 (1999).

8.E. R. Stadtman, Berlett, B. S., Fenton Chemistry: Amino Acid Oxidation. JBC 266, 17201-17211 (1991).

9.P. J. Schmidt, M. Ramos-Gomez, V. C. Culotta, A Gain of Superoxide Dismutase (SOD) Activity Obtained with CCS, the Copper Metallochaperone for SOD1. J. Biol. Chem 274, 36952-36956 (1999).

10.H. Kawamata, Manfredi, G., Import, Maturation, and Function of SOD1 and Its Copper Chaperone CCS in the Mitochondrial Intermembrane Space. Antioxid Redox Signal 13, 1375-1384 (2010).

11.M. Watanabe et al., Histological evidence of protein aggregation in mutant SOD1 transgenic mice and in amyotrophic lateral sclerosis neural tissues. Neurobiol Dis 8, 933-941 (2001).

12.M. C. Carroll et al., Mechanisms for activating Cu- and Zn-containing superoxide dismutase in the absence of the CCS Cu chaperone. Proc Natl Acad Sci U S A 101, 5964-5969 (2004).

13.M. Son et al., Overexpression of CCS in G93A-SOD1 mice leads to accelerated neurological deficits with severe mitochondrial pathology. Proc Natl Acad Sci U S A 104, 6072-6077 (2007).

14.K. Sugaya, I. Nakano, Prognostic role of "prion-like propagation" in SOD1-linked familial ALS: an alternative view. Front Cell Neurosci 8, 359 (2014).

15.P. Huppke et al., Molecular and biochemical characterization of a unique mutation in CCS, the human copper chaperone to superoxide dismutase. Hum Mutat 33, 1207-1215 (2012).

16.G. S. Wright, Antonyuk, S. V. and Hasnain, S. S., A faulty interaction between SOD1 and hCCS in neurodegenerative disease. Sci Rep 6, (2016).

17.M. M. Fetherolf et al., Copper-zinc superoxide dismutase is activated through a sulfenic acid intermediate at a copper ion entry site. J Biol Chem 292, 12025-12040 (2017).

BIOGRAPHICAL SKETCH

Born in Dallas, TX, Morgan Ullrich has had a life of academic success. Placed in an advanced program for gifted students from elementary school onward, she competed in several logic and debate competitions through high school. Graduating with academic honors, she continued on to college and graduated with a Bachelor's of Science in Biology and a Master's of Science in Molecular and Cellular Biology.

CURRICULUM VITAE

Morgan S. Ullrich

Education:
University of Texas at Dallas
Bachelor's of ScienceMajor: Biology Graduated: Fall 2014
University of Texas at Dallas
Master's of Science Major: Molecular and Cellular Biology Graduated: Fall 2016
University of Texas at Dallas
Doctor of Philosophy Major: Molecular and Cellular Biology Graduation: Fall 2020

Work Experience:

University of Texas at Dallas: Research Technician II
Full-time May 2016-June 2017
Duties: Preparation of stock solutions and buffers, pouring and running acrylamide and agarose gels, experimental design and execution, protein purification with a UNICORN system, cloning and mutagenesis of DNA constructs, biochemical analysis of protein characteristics, working with protein and metals in anaerobic conditions, transformation of DNA into yeast and bacterial strains for expression, etc.

Publications:

Boyd SD, Calvo JS, Liu L, Ullrich MS, Skopp A, Meloni G, Winkler DD. The yeast copper chaperone for copper-zinc superoxide dismutase (CCS1) is a multifunctional chaperone promoting all levels of SOD1 maturation. J Biol Chem. 2019 Feb 8;294(6):1956-1966. doi: 10.1074/jbc.RA118.005283. Epub 2018 Dec 10. PMID: 30530491; PMCID: PMC6369272.
Skopp A, Boyd SD, Ullrich MS, Liu L, Winkler DD. Copper-zinc superoxide dismutase (Sod1) activation terminates interaction between its copper chaperone (Ccs) and the cytosolic metal-binding domain of the copper importer Ctr1. Biometals. 2019 Aug;32(4):695-705. doi: 10.1007/s10534-019-00206-3. Epub 2019 Jul 10. PMID: 31292775; PMCID: PMC6647829.
Boyd SD, Ullrich MS, Calvo JS, Behnia F, Meloni G, Winkler DD. Mutations in Superoxide Dismutase 1 (Sod1) Linked to Familial Amyotrophic Lateral Sclerosis Can Disrupt High-Affinity Zinc-Binding Promoted by the Copper Chaperone for Sod1 (Ccs). Molecules. 2020 Feb 28;25(5):1086. doi: 10.3390/molecules25051086. PMID: 32121118; PMCID: PMC7179120.
Boyd SD, Ullrich MS, Skopp A, Winkler DD. Copper Sources for Sod1 Activation. Antioxidants (Basel). 2020 Jun 7;9(6):500. doi: 10.3390/antiox9060500. PMID: 32517371; PMCID: PMC7346115.